Crop Water Stress Under Climate Change Uncertainty: Global Policy and Regional Risk

by

Arthur Gueneau

Submitted to the Technology and Policy Program, Engineering Systems Division

in partial fulfillment of the requirements for the degree of

Master of Science in Technology and Policy

at the

MASSACHUSETTS INSTITUTE OF TECHNOLOGY

September 2012

Author ....
Technology and Policy Program, Engineering Systems Division
July 25, 2012

Certified by ....
C. Adam Schlosser
Principal Research Scientist, MIT Joint Program on the Science and Policy of Global Change
Thesis Supervisor

Certified by ....
Kenneth M. Strzepek
Research Scientist, MIT JPSPGC
Professor Emeritus of Civil, Environmental, and Architectural Engineering, University of Colorado at Boulder
Thesis Reader

Accepted by ....
Joel C. Clark
Professor of Materials Systems and Engineering Systems
Acting Director, Technology and Policy Program

Crop Water Stress Under Climate Change Uncertainty: Global Policy and Regional Risk

by

Arthur Gueneau

Submitted to the Technology and Policy Program, Engineering Systems Division
on July 25, 2012, in partial fulfillment of the
requirements for the degree of
Master of Science in Technology and Policy

Abstract

Fourty percent of all crops grown in the world today are grown using irrigation, and shifting precipitation patterns due to climate change are viewed as a major threat to food security. This thesis examines, in the framework of the MIT Integrated Global System Model, the potential impacts of climate change on crop water stress and the risk implications for policy makers due to underlying uncertainty in climate models. This thesis presents the Community Land Model - Agriculture module (CLM-AG) that models crop growth and water stress. It is a global generic crop model built in the framework of the Community Land Model and was evaluated for maize, cotton and spring wheat. A full climate model, the IGSM-CAM, was first used to force CLM-AG and show the regional disparity of the response to climate change. Some areas like the Midwest or Equatorial Africa benefit from the higher precipitations associated to climate change while others like Europe or Southern Africa see the irrigation need for crops increase. The effect of a mitigation policy appeared contrasted, as water-stress for some areas (including Europe and Africa) is increased if greenhouse gases emissions are limited while for other areas (Central Asia, United States) it is reduced. A second analysis was carried in Central Zambia using uncertainty ensembles. The ensembles demonstrate the notable extent of the uncertainty stemming from different climate sensitivities and different regional patterns in climate models. Crops are impacted differently but a consistent result is that climate mitigation policies reduce uncertainty in crop water stress, making it easier to plan for any anticipated future climate change.

Thesis Supervisor: C. Adam Schlosser
Title: Principal Research Scientist, MIT Joint Program on the Science and Policy of Global Change

Thesis Reader: Kenneth M. Strzepek
Title: Research Scientist, MIT JPSPGC
Professor Emeritus of Civil, Environmental, and Architectural Engineering, University of Colorado at Boulder

Acknowledgements

This thesis would not have been possible without the help of many people at MIT and beyond.

First and foremost I want to thank my supervisor C. Adam Schlosser for his continued and friendly support, his valuable insights and his patience with me. This thesis would not have existed without him.

I would also like to thank particularly Kenneth M. Strzepek for his encouragements, his great mentoring and his invaluable advice on this thesis.

This work would not have been possible without a great support from all the faculty, staff and students at the MIT Joint Program on the Science and Policy of Global Change. I owe special thanks go to Erwan Monier, Xiang Gao, Elodie Blanc, Yongxia Cai, and Jake Jacoby who all contributed in some way to this study. Chas Fant developed the CliCrop model that is the basis for CLM_AG and provided many valuable insights.

I also want to thank all my office mates at the Joint Program for their friendliness and their always challenging questions on my work. My thanks also go to my friends in Paris, Boston and beyond, especially the Polytechnique and TPP communities. Special thanks go to my Erie Street room-mates Paul, Fernando and Jan, for their support and all the good times spent together.

Last but not least, I want to thank my family, especially my parents and sister for sending me kind words of support from across the ocean and always believing in me. Finally, someone who will recognize herself deserves all my gratitude for her overall support, her amazingly precise reviews, her always pertinent questions and everything else.

The author also gratefully acknowledges financial support for this work provided by the MIT Joint Program on the Science and Policy of Global Change through a consortium of industrial sponsors and Federal grants. Development of the IGSM applied in this research was supported by the U.S. Department of Energy, Office of Science (DE-FG02-94ER61937); the U.S. Environmental Protection Agency, EPRI, and other U.S. government agencies and a consortium of 40 industrial and foundation sponsors. For a complete list see http://globalchange.mit.edu/sponsors/current.html.

Contents

List of Figures

List of Tables

List of Abbreviations and Acronyms

AOGCM Atmospheric and Oceanic Global Climate Model

AR4 IPCC Fourth Assessment Report

CAM Community Atmosphere Model

CCSM Community Climate System Model

CGE Computable General Equilibrium

CLM Community Land Model

CLM_AG Community Land Model - Agriculture module

CRU Climate Research Unit, University of East Anglia

DSSAT Decision Support System for Agrotechnology Transfer

EPIC Erosion-Productivity Impact Calculator

EPPA Emission Prediction and Policy Analysis

FAO Food and Agriculture Organization, Rome

GAEZ Global Agro-Ecological Zones

GDD Growing Degree Days

GDP Gross Domestic Product

GPCP Global Precipitation Climatology Project

HFD Hybridized Frequency Distribution

IGSM Integrated Global System Model

IIASA International Institute for Applied Systems Analysis, Vienna

L1S Level 1 Stabilization scenario

L2S Level 2 Stabilization scenario

LAI Leaf Area Index

MIT Massachusetts Institute of Technology, Cambridge, MA

NCAR National Center for Atmospheric Research, Boulder, CO

NCC NCEP/NCAR Corrected by CRU

NCEP National Centers for Environmental Prediction, Camp Springs, MD

PFT Plant functional Type

ppm parts per million

SRES Special Report Emission Scenarios

SST Sea-Surface Temperature

UCE Unconstrained Emissions Scenario

UNFCC United Nations Framework Convention on Climate Change

WBM Water Basin Module

WRS Water Resource system

Chapter 1

Introduction

1.1 Background

1.1.1 The Challenge of Feeding Nine Billion People on a Finite Planet

With the global population projected to reach nine billion by 2050 (UN, 2004) and economic growth transforming the lives of millions in developing countries, world food demand is expected to roughly double by 2050 (FAO, 2009). This includes a westernization of diets in lower-income countries, where energy-, land- and water-intensive meat demand is expected to increase significantly. Agriculture already uses 34% of ice-free land worldwide (Ramankutty *et al.*, 2008) and is responsible for 10 to 12% of direct global greenhouse gases emissions[1] (Smith *et al.*, 2007), including most of the global emissions of methane. Humans used about 54% of all attainable runoff in 1996 (Postel *et al.*, 1996). Of this amount, 87% is used for agriculture, mostly for irrigation purposes (Shiklomanov, 2000).

Despite its footprint on the environment, food production is essential for human subsistence. As shown in Figure 1-1, after declining through the last quarter of the twentieth century, largely due to the Green Revolution and an unusually mild climate (Ziska, 2011), food prices have started to rise again, and it is estimated that in 2011 six hundred million people in developing countries are still undernourished (FAO, 2011). The double concern

[1]This number would be higher if we were to take into account indirect emissions due to deforestation to claim new crop land or pastureland, which is much harder to quantify.

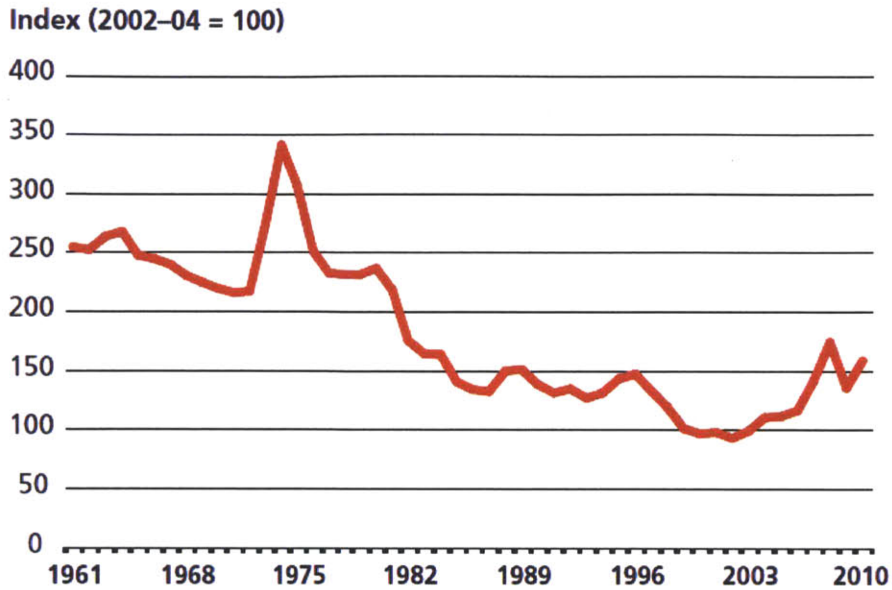

Figure 1-1: FAO Food Price Index, adjusted for inflation, 1961 - 2010, calculated using international prices for cereals, oilseeds, meats, and dairy and sugar products (FAO, 2011).

of environmental stress caused by agriculture and of the absolute necessity of producing enough food for humans makes feeding the planet sustainably one of the biggest challenges of the twenty-first century [2].

1.1.2 The Importance of Irrigation

In the broader context of food security, irrigation is an often overlooked but nevertheless important issue. Indeed, even if irrigated land composes only 20% of the cultivated area globally, it accounts for around 40% of the global food production (Döll, 2002). As is shown on the map of irrigated areas worldwide presented in Siebert *et al.* (2005) irrigation is crucial for food production in certain countries like Egypt, Pakistan or India. Any drop in irrigation capacity, whether from increased water demand from crops or decreased runoff in the streams would have dire consequences for these countries, especially at the time they need to ramp up their production capacity to meet the demands of a growing population. At the same time, the development of irrigation in some areas (mostly in Africa) could spur

[2]The interested reader can find a more extensive presentation of these issues in a TED talk given by Professor Jonathan Foley from University of Minnesota (Foley, 2010).

an agricultural revolution in these countries and increase crop yields, thus improving food security and being part of the answer to meeting food demand growth.

Irrigation is crucial to the agricultural policies of many countries but evaluating the relevance of irrigation projects becomes increasingly difficult as climate changes. Indeed, one of the major factors relevant to assess the potential success of such a project is the amount of water required by crops to grow healthily. However this irrigation need is highly dependent on temperature and on precipitation, and is likely to vary significantly under a changed climate.

Thus tools are needed to assess the potential impact of climate change and its surrounding uncertainty to help policy makers make informed decisions on irrigation projects and, more broadly, to assess the risks future climate change could pose on human food supplies. The potential impacts of climate change on irrigation need for crops and the uncertainties policy makers must take into account when dealing with these issues are the subject of this master's thesis.

1.2 Contributions

1.2.1 Main Questions and Approaches

The issues that have been outlined in the previous section give rise to many interesting questions. We will concentrate on the following issues:

- Which areas in the world could face the largest changes in irrigation need by the middle of the century? What would be the impact of mitigation policies on this outcome? Would agricultural production be better or worse off in a warmer world, from a water stress point of view?

- How can we efficiently characterize irrigation need uncertainty at the regional level? What are the relevant tools we can provide policy makers to help them make informed decisions on irrigation projects whose success are dependent on a potential change in climate? Do global climate policies have an impact on irrigation at the local level?

As it is impossible to rely on past observations to predict future irrigation need – given climate change and its impact on the planet – we must rely on models to answer these questions. For this work, a crop and irrigation model called the Community Land Model - Agriculture module (CLM-AG) has been developed. This model was designed to be a part of the MIT Integrated Global System Model (IGSM) framework (Prinn *et al.*, 1999; Sokolov *et al.*, 2005). This integrated approach ensures that all models parameters and results (from greenhouse gases emissions to irrigation need) are consistent with one another and do not result in physical impossibilities.

To answer the first question we use the results of a full 3-D climate model, the IGSM - Community Atmosphere Model (IGSM-CAM, Monier *et al.* (2012)) driven by the emissions scenarios from the MIT Emission Prediction and Policy Analysis (EPPA, Paltsev *et al.* (2005)) model. We then compare the average irrigation need modeled for the period 1980-2000 with what the model predict for the period 2040-2060. Two distinct scenarios were considered for the future runs: an unconstrained emissions scenario and a climate change mitigation scenario. This allows us to draw conclusions on the different regional impacts of climate change and on the potential impact of a mitigation policy on irrigation need.

To answer the second question, we focus on the Central Province of Zambia in South-Western Africa and take advantage of the IGSM functionality to run uncertainty scenarios. For each emissions scenario, the hybridization of a statistically representative ensemble of 400 IGSM 2-D model runs with AR4 kernels for regional impacts (Schlosser *et al.*, 2011) leads to a distribution of 6800 possible outcomes. We reduce this distribution to approximately 400 weighted outcomes using a Gaussian Quadrature reduction technique (Arndt, 1996). CLM-AG allows us to characterize the impact of these different scenarios on crop irrigation need and to build probability distribution of the evolution of crop water stress by 2050 in the Central Province of Zambia under the two emissions scenarios.

1.2.2 Outline

Chapter 2 reviews the existing literature on the impacts of climate change on agriculture, on the models that have been used to make these assessments, and on the underlying uncertainties.

Chapter 3 describes the crop and irrigation model called CLM-AG that was developed for this study. We also present in this chapter two different evaluations of CLM-AG. The first one compares CLM-AG to another crop model, the IIASA-FAO Global Agro-Ecological Zones (GAEZ, Fischer *et al.* (2012)). The second one compares a subset of the model for the United States to the water withdrawn for irrigation of maize as reported in the Farm and Ranch Irrigation Survey conducted by the US Department of Agriculture (USDA, 2008).

Chapter 4 shows the results of the global study using the IGSM-CAM forcing under two different scenarios: an unconstrained emissions scenario and a scenario where policies limit the concentration of carbon dioxide to 550 ppm by the end of the century. We then identify the impacts of these two policies on major growing areas of corn, wheat and cotton globally and conclude on some of the impacts of a mitigation policy on irrigation as well as on the regional patterns of change.

Chapter 5 then presents the results of the regional analysis carried out for the Central Province of Zambia. We analyze the distribution of the possible outcomes for irrigation need under two different scenarios and provide a few tools to evaluate them and interpret the results in a policy making framework.

We finally summarize the main findings of this work in Chapter 6 and discuss future research that the development of CLM-AG renders possible.

Chapter 2

Literature Review

This chapter reviews relevant literature in the field. Section 2.1 focuses on the effects of climate change on agriculture and crop production. Section 2.2 describes the different varieties of crop models that have been developed to study the impacts of climate change on agriculture. It assesses the strengths and weaknesses of each model and focuses particularly on irrigation models. Finally, Section 2.3 reviews the major uncertainties a modeler is faced with when developing an assessment tool for future agricultural production.

2.1 Impacts of Climate Change on Agriculture

The twentieth century has been characterized by a constant increase in agricultural production driven by the use of new varieties and the development of fertilizers (Figure 2-1). This has been widely referred as the Green Revolution. It has helped keep food prices at a historically low level. However, the Green Revolution occurred during a time of remarkable climate stability (Swanson *et al.*, 2009). Will agricultural production be able to continue rising in the coming years under a changing climate? As most of the existing science is compiled in chapter 8 of the working group II report for the International Panel on Climate Change (Smith *et al.*, 2007) we only review the main findings here and highlight what can be explored with CLM-AG.

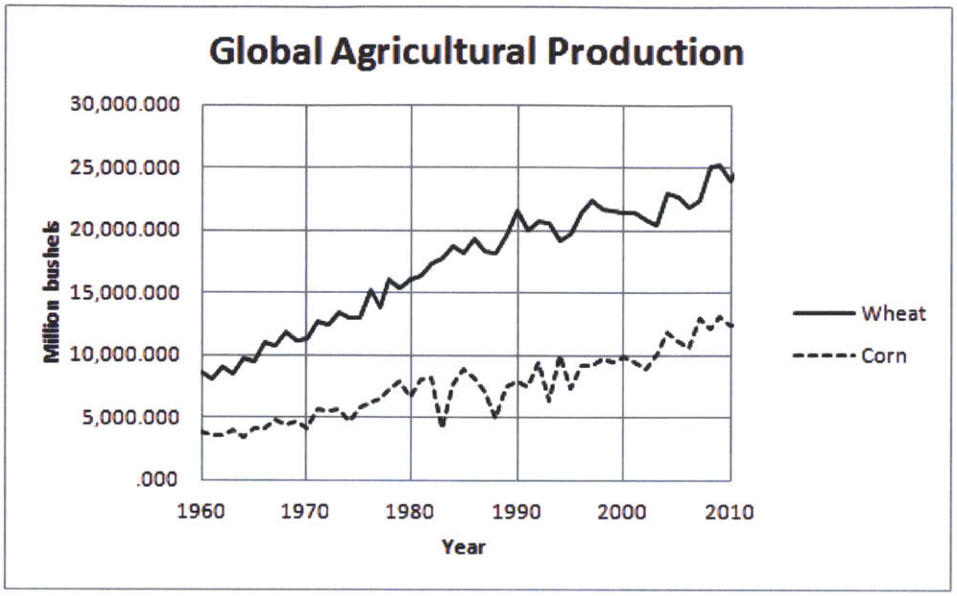

Figure 2-1: Increase in global agricultural production. Data source: USDA.

2.1.1 Direct Effects of Climate Change

Water

Crops require water to grow. Currently, irrigated land represents 20 percent of cultivated land but 40 percent of total agricultural production (Döll, 2002). The largest impact in the agricultural sector is likely to be felt in irrigation, as water supply becomes scarcer in some areas and more subject to extreme variations (Ziska, 2011). According to Döll (2002), two-thirds of current globally irrigated areas will need more water by 2070, due to a combination of higher temperatures and lower precipitation. At the same time, water supply – namely river runoff – is likely to decrease in some of these areas (Kundzewicz *et al.*, 2007, 2008). According to a study by Fischer *et al.* (2007), mitigation could reduce globally the impacts of climate change on annual agricultural water requirements by about 40 percent, or 125 to 160 billion m^3 compared with an unconstrained emissions scenario. However, this study relies on a rather simple crop model and we aim at improving the results regionally by considering a more complete description of the crop and soil hydrology processes.

Temperature

Crops are very sensitive to temperature. Ziska (2011) provides a table of optimal flowering and vegetative stage temperatures for the main US crops (Table 2.2 in the cited volume). Under climate change it is likely that temperature will frequently exceed the optimal range for crops, leading to reduced yields or a need to develop new hybrids. The main finding is that crop response to temperature is not linear, as shown in Schlenker and Roberts (2009). These non-linearities are not implemented in CLM-AG (discussed in Chapter 3) as new hybrids better adapted to a warmer climate may appear. Nevertheless, temperature indirectly affects the water requirement from the crop as a warmer weather means a higher evapotranspiration from the plant, which CLM-AG takes into account.

Extremes

Under any climate change (i.e. human or natural), extreme weather events are likely to become more frequent and/or more intense, for temperatures and precipitation alike (IPCC, 2012). The most impactive of extreme events to agriculture are droughts and floods, as well as heat waves. These extreme events can dramatically reduce crop yields when they occur during the most critical stages of crop growth and could impact overall agricultural production (Rosenzweig *et al.*, 2001; Smith *et al.*, 2007). As the intent of CLM-AG is to model irrigation, it does not model the direct impact of these events on crop physiology. It does, however, model the impact of a drought on irrigation demand and the associated yield reduction.

Change in Carbon Dioxide Concentration

Extensive studies have been conducted on the effect of increasing CO_2 concentrations on crop yields. Kimball *et al.* (1993) posits a yield increase of 30% under a doubled carbon dioxide concentration based on closed environment experimentations, but this rate is highly contested as the technique involves small volumes of air that may create micro-climatic effects (Ziska and Bunce, 2007). It is thus very uncertain that this result would hold in a natural environment. It is clear that more research in this area is required before providing a conclusive parameterization in this regard, thus this implementation of CLM-AG does not directly take carbon dioxide concentrations into account when modeling the plant physiology.

Nutritional Value

Rising levels of carbon dioxide in the atmosphere also impact the physiology of the plant through different mechanisms (more efficient nitrogen uptake, stomatal closure, etc.). Taub *et al.* (2008) estimate experimentally that crop nutritional value could decrease as much as 15% if the concentration of CO_2 in the atmosphere doubles. Loladze (2002) shows that rising carbon dioxide could also reduce the quantity of essential micronutrients in the plants, such as iron, iodine and zinc. These findings have strong implications for the quantity of food that needs to be grown to feed the planet; however, they do not impact directly crop water requirements and are not considered in this implementation of CLM-AG.

2.1.2 Indirect Effects of Climate Change Mitigation Strategies

Fertilizer Price

Synthetic fertilizers are overwhelmingly produced from natural gas. As of 2003, fertilizer production was consuming approximately 1.2% of the world's energy and was responsible for approximately 1.2% of total greenhouse gases emissions (Kongshaug and Jenssen, 2003). Hence any climate policy that prices directly or indirectly emissions (like a carbon tax or a cap-and-trade policy) will increase fertilizer price, decrease fertilizer use and therefore impact global agricultural production. Irrigation can potentially offset the amount of fertilizer needed to improve yields and is consequently an important tool for mitigating the impacts of such a climate policy.

Biofuels

Some politicians (see the US Energy Policy Act of 2005 and the EU Directive 2003/30/EC) and scientists (Demirbas, 2009) have championed replacing conventional fossil fuels with biofuels as a way to green the transportation sector. However, Melillo *et al.* (2009) showed that the introduction of biofuels created unintended consequences for agricultural production. By shifting some of the best land from agricultural production to fuel production (as biofuel prices as likely to be higher than food prices), it relegates food production to less fertile land. This would either reduce yields, require an intensification of the production through the use of more fertilizers, or require more irrigation because food production is displaced to marginal land. As a consequence, biofuels are generally seen as a threat to food security (Rosegrant *et al.*, 2008b; Boddiger, 2007). Though it is not the focus of this work, CLM-AG would allow us to explore in future works the impacts of such a displacement of food production on the irrigation need and on the water systems of countries.

2.2 Crop Models

Farm production is influenced by biophysical conditions (temperature, rainfall, soil, pests, etc.) and by the socio-economical context (population, lifestyle, income, water resources, etc.) Farmers respond to these external conditions through management decisions (crop choice, irrigation, fertilizer use, etc.) The variety of parameters that influence a crop and the high adaptivity of farmers makes modeling crops a very difficult task. Moreover, inputs range from the local (soil, precipitation) to the regional (water resources, subsidies) or even the global (carbon dioxide concentration, food prices), and all need to be taken into account if one wants to reliably model food production.

As a result this system is too complex to be studied in its entirety. First, experiments to study the impact of climate change on food production are not possible. Thus, research has to rely on models to analyze potential effects. Second, as one cannot model the system in its entirety, different models perform different types of assessments at different scales.

There are three general types of crop models: process-based models, statistical models and economic models. We describe all of them below, but focus more extensively on process-based crop models as CLM-AG falls into this category.

2.2.1 Process-Based Crop Models

Process-based crop models are usually deterministic. Any change in the model results is due to input data or parametrization. Most of these models consist of three modules: a soil module with water infiltration from precipitation or irrigation, a plant module to represent the growth and physiology of the plant, and a canopy air-space module to simulate evaporation and transpiration. They are usually based on a numerical integration over a rather short period of time that can range from hours to a month (Faivre *et al.*, 2009). These models are all data-intensive but they can capture non-linear responses to climate change (Challinor *et al.*, 2003).

DSSAT

The Decision Support System for Agrotechnology Transfer model (DSSAT, Jones *et al.* (2003)) was developed to provide farmers with a way to predict the response of their crops to different management options such as fertilizer use or irrigation. It is very detailed and has been developed for as many as twenty different crops. It focuses on fertilizer use and plant processes. In climate change studies it has been used to see how crop management might evolve under a changing climate (e.g. Rosenzweig *et al.* (1994)) or for local studies on specific crops (Guereña *et al.*, 2001; Brumbelow and Georgakakos, 2001)). Arguably the most detailed of crop models, it nevertheless requires a large amount of data. Further, its very detailed parametrization becomes problematic at a global scale as field data aggregation for inputs can lead to large errors.

EPIC

The Erosion-Productivity Impact Calculator (EPIC, Williams and Singh (1995)) is primarily a soil hydrology model. It was developed to track the impacts of erosion and soil productivity on crops. Stockle *et al.* (1992) modified the model by adding a carbon dioxide function for climate change assessments. It has been used since in a number of such climate assessments (Izaurralde *et al.*, 2003; Tan and Shibasaki, 2003; Easterling *et al.*, 1996). It is also a field-scale model that requires a number of local parameter inputs and therefore becomes parametric intensive on a global scale.

The FAO models: CROPWAT and AquaCrop

CROPWAT (Smith, 1992) is an empirical process-based crop model. In contrast to the preceding models it has the advantage of being generic and requiring very little input parameters for the plant or soil specifications. Conversely, this results in a somewhat larger uncertainty in the outputs. It has been used for local studies of the impact of climate change on irrigation resources (Rodríguez Díaz *et al.*, 2007; Rosenzweig *et al.*, 2004) or on rainfed agriculture (Moussa and Amadou, 2006).

AquaCrop (Steduto *et al.*, 2009; Raes *et al.*, 2009) is the evolution of CROPWAT. It is also a process-based model, focused on evaluating the irrigation need for crops. As it was developed and released only recently, and is parametrized for relatively few crops, only a few studies have used it (e.g. Chung (2010)). AquaCrop simulates crop growth over the season, and tracks a variety of different stresses to the crop (heat, water or nutrient shortage, soil salinity, etc.) and hydrological processes in the ground. As a result, it outputs a variety of indicators including yield and water deficit.

CLM-AG is directly inspired by these models as its purpose is to be a global irrigation model. However, only the water-deficit routines from AquaCrop were implemented as total yield is secondary to this study. It is, like CROPWAT and AquaCrop, a generic crop model and has been parametrized for corn, wheat and cotton, given the global agro-economic importance of these crops.

2.2.2 Agroclimatic Indices and Production Functions

Agroclimatic Indices

Agroclimatic indices are used to determine if a crop can be grown at a given place. They rely mostly on temperature, average rainfall and soil characteristics to compute the suitability of a given place for a given crop. Carter *et al.* (1996) at a local level or Fischer *et al.* (2005) at a global level use this method to assess the potential shift of agricultural land and crops under future climate scenarios. This method somewhat accounts for management practice adaptations and provides insights on climate impacts on crop localization; however it does not compute actual yields and irrigation needs, except when coupled with a process-based model (Fischer *et al.*, 2012).

Production Functions

Production function models are statistical models based on a regression of relevant factors that underly the yield of a crop. For example, these factors can include temperature, rainfall, sowing date and fertilizer use. They are mostly modeled after present-day systems and thus are a very unreliable estimate for future yields as regression coefficients are bound to change because of climate change and subsequent adaptations (Mearns *et al.*, 1997). However, Parry *et al.* (2004) at a global level or Iglesias *et al.* (2000) at a local level have combined such models with precise process-based model runs of DSSAT (see 2.2.1) to calibrate the regressions in the future.

2.2.3 Economic Models

Economic models do not predict the irrigation need of crops as they lack a physical basis. Aside from macroeconomic models that incorporate results from a process-based model (Parry *et al.* (2004) for example), the main economic approach to modeling the impacts of climate change on the farm is the Ricardian method. This method uses statistical production functions to compute not a yield but the value of the land or the farm revenue. These outputs are in turn used to analyze the economic effects of climate change as in Mendelsohn *et al.* (1994).

2.3 Uncertainty

As it is the rule for any model, crop models are uncertain in nature and do not exactly represent reality. This is an even bigger problem when it is run in the future as there is a wide uncertainty surrounding climate models. The three major sources of uncertainty in the water stress predicted by any process-based crop model are the uncertainty in greenhouse gases emissions, the uncertainty in the temperature and precipitation outputs from the climate model and the uncertainty in the computed crop water need from the crop model itself.

2.3.1 Economic Uncertainty

The largest input uncertainty in climate models comes from the uncertainty in greenhouse gases emissions (Stott and Kettleborough, 2002; Webster *et al.*, 2002). Indeed these emissions depend largely on the future state of the economy and on the production techniques that will be chosen, as well as on eventual mitigation policies. One way to quantify the evolution of these emissions in the future is to use a Computable General Equilibrium (CGE) model. One such model is the MIT Emission Prediction and Policy Analysis (EPPA) model (Paltsev *et al.*, 2005). In contrast to the IPCC Special Report Emission Scenarios (SRES, Nakicenovic *et al.* (2000)), using a CGE model ensures that emissions and economic growth are consistent with each other. However, as summarized in Abler *et al.* (1999), there is wide uncertainty associated with CGE models outputs, even given a particular growth course, as most economic elasticities are highly uncertain. Webster *et al.* (2008) provide a technique to quantify some of these uncertainties in the EPPA model.

2.3.2 Climate Uncertainty

Climate model uncertainties are well recognized and documented (Deser *et al.*, 2012; Randall *et al.*, 2007). Three parameters summarize most of this climate models internal uncertainty: climate sensitivity, ocean uptake rate and aerosol forcing effect[1]. The uncertainty surrounding these parameters explains most of the prediction differences between climate models in terms of temperature increase.

One way to recognize this uncertainty is to create several runs of a given climate model while varying these parameters. Forest *et al.* (1999) describes a technique to select a phys-

[1]The climate sensitivity can be defined as the ratio of temperature change to radiative forcing change in an equilibrium state, the ocean heat uptake rate is the amount of carbon absorbed by the oceans and the aerosol forcing is the impact of aerosols and clouds on the radiative forcing of the atmosphere. More complete definitions can be found in Sokolov *et al.* (2009).

ically possible subset of these parameters given the climate observations during the twentieth century. This is the approach that is used in the MIT Integrated Global System Model (Sokolov *et al.*, 2005, 2009) to represent the underlying climate uncertainty.

Besides the uncertainty on the level of the climate response to an increased concentration of greenhouse gases, there is a large disagreement between the different climate models in terms of regional impacts of climate change. For example, some models predict that precipitation could increase by 20% in the North-East United States while others predict that they could decrease by 20% (Christensen *et al.*, 2007). Schlosser *et al.* (2011) describe a technique to take this regional uncertainty into account and describe a multi-model ensemble of climate forcings. We discuss this technique at length in Chapter 5.

2.3.3 Crop Models Uncertainty

Finally, there is a very high uncertainty associated with crop models themselves as crop growth depends on a large number of parameters (Monod *et al.*, 2006). Different types of models face different issues.

A detailed model like DSSAT represents crops very precisely but in return require extensive input data. This data is usually not available at the global scale, and aggregation issues will arise.

On the contrary, a generic crop model like CLM-AG or AquaCrop does not simulate all the processes involved in crop growth. It is thus likely to be imprecise at the field level. However, at a global scale the model representation becomes more palatable as it does not require much data.

Although these uncertainties have an impact on the absolute water deficit the crop is facing, we argue later in this work that only differences in irrigation need from 2050 to the present are useful to policy makers. Indeed global model outputs need to be downscaled at a local level to generate relevant data for decision maker. This process requires changes in irrigation need (or water stress) and not the absolute values. Following the community, we contend that differences are much more reliable as they identify the impact of one factor only (here climate change).

Chapter 3

The CLM-AG model

In this chapter we describe the CLM-AG model. The chapter first explains the reasons for developing the model and the specifications the MIT Integrated Global System Model required it to have. Then we describe its structure and algorithms. Finally we present two different evaluations of the model on a historic run with past climate data.

3.1 A Process-Based Model for Global Change Studies

3.1.1 The IGSM Framework

The CLM-AG model has been developed with the potential to become a component the MIT Integrated Global System Model (Prinn *et al.*, 1999) that would be used for water and food studies under global change. In the context of an integrated global assessment, a crop water stress and irrigation demand model must meet certain specifications that differ from other crop models (yield prediction or irrigation planning at the field scale require different specifications for example). First the model needs to output a monthly irrigation demand (later used in the Water Basin Model in the IGSM framework) and a rainfed yield factor (that quantifies the effects of water stress on crop yields, and that is used in calculating the agricultural output). Second, as the model has to be global, it must be able to run on large grid cells and to be as computationally efficient as possible. Finally, as it is difficult to predict how crop characteristics will change in the future, this model needs to be a generic crop model with a minimal set of inputs.

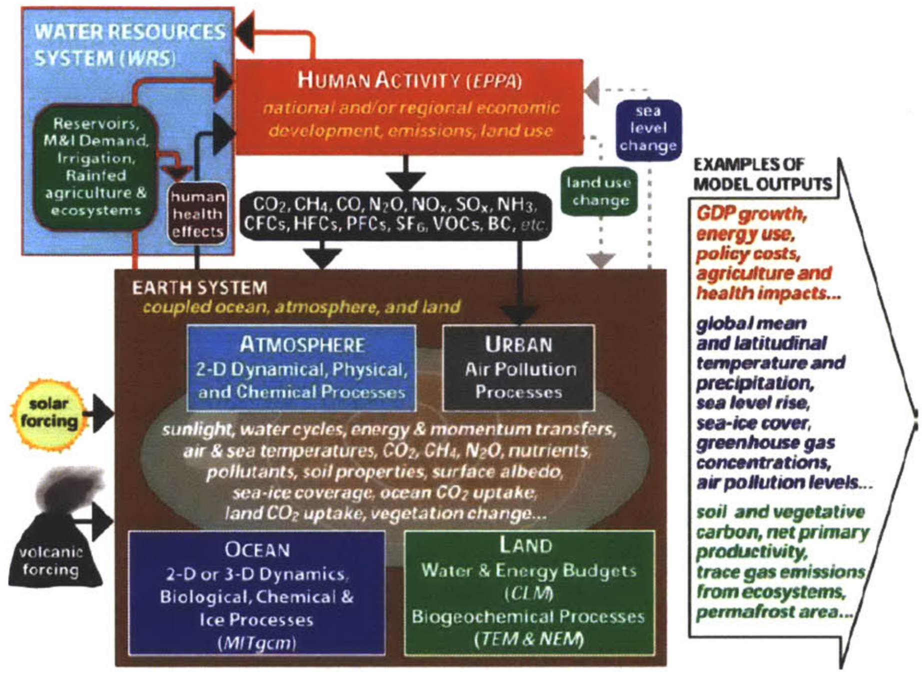

Figure 3-1: The IGSM Framework.

Figure 3-1 describes the MIT Integrated Global System Model (IGSM) framework, with a particular highlight on the Water Resource System (WRS, Strzepek *et al.* (2010)). Using emission predictions and economic outputs from the MIT Emission Prediction and Policy Analysis (EPPA) model (Paltsev *et al.*, 2005) and earth system modeling predictions from the IGSM (Sokolov *et al.*, 2005), the Water Basin Module (WBM) describes climate impacts on water demand as described in Figure 3-2. Previously, the hydrology part (runoff) would come from the Community Land Model (CLM, Bonan *et al.* (2002)) and the agriculture part from CliCrop (Fant *et al.*, 2012). These two distinct parts may create an inconsistency in the framework. Indeed, CLM and CliCrop did not have the same soil water calculation algorithms, leading to inconsistencies in their respective water balance when putting the results together in WBM. CLM-AG solves this issue by integrating the two models with a single soil water module. It also integrates advances in crop modeling that were not simulated or simulated differently in CliCrop.

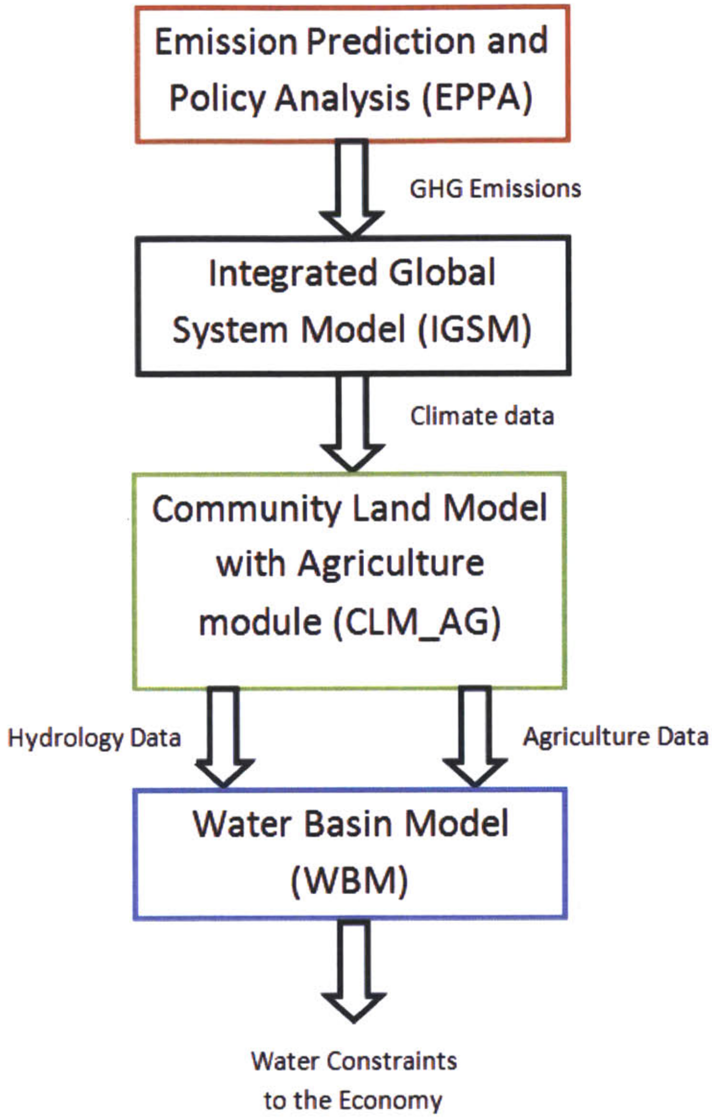

Figure 3-2: The WRS framework.

3.1.2 Philosophy of the Model and Inspiration

CLM-AG was originally intended to be a simple implementation of CliCrop in the very flexible Community Land Model (CLM v3.5, Oleson *et al.* (2004) and Oleson *et al.* (2008))[1]. However, it evolved to include advances in modeling and a better understanding of management options for agriculture.

[1]The MIT Joint Program on the Science and Policy of Global Change currently uses the version 3.5 of CLM for most of its land studies.

As an evolution of CliCrop, CLM-AG relies on the same principles; the irrigation and yield reduction routines are taken from CROPWAT (Smith, 1992). However, the physiology of the crop needed to be more precise than the one in CROPWAT as CLM runs on an hourly time-scale (CROPWAT is monthly). CLM-AG thus relies primarily on AquaCrop physiology routines to drive plant growth (Raes *et al.*, 2009). Meanwhile the soil hydrology remains unchanged from the original CLM model.

3.2 Description of the Model

We describe here only the agriculture and irrigation routines created during the course of this work. The interested reader will find a precise description of the other CLM routines in the CLM 3.0 technical description (Oleson *et al.*, 2004) and the subsequent improvements of CLM 3.5 in the CLM 3.5 description (Oleson *et al.*, 2008).

3.2.1 Structure in CLM

The CLM structure is a nested subgrid hierarchy under the unit of the gridcell. Climate inputs are given at the gridcell unit. Each gridcell is composed of multiple landunits, soil columns and Plant Functional Types (PFTs). Soil properties are defined at the landunit level. The energy and water balances are made at the column level. Of primary concern for agriculture, soil hydrology routines operate at this level. Finally, plant dynamics are simulated at the PFT level with both biophysical and biochemical routines.

Figure 3-3 shows the changes from the usual CLM structure made in CLM-AG. Cropland is now a separate landunit with each crop being a distinct column. Separating crops in different columns (and not only PFTs) prevents them from competing for the same water resources present in the ground: two distinct fields are completely independent when it comes to the water content in the soil.

The scheme is entirely flexible and one can add new crops as needed. Currently, only maize, spring wheat and cotton are implemented in the framework as they are among the two most important food crops and cash crop, respectively. It is also important to note that besides the plant physiology, all other CLM routines (hydrology, energy and water

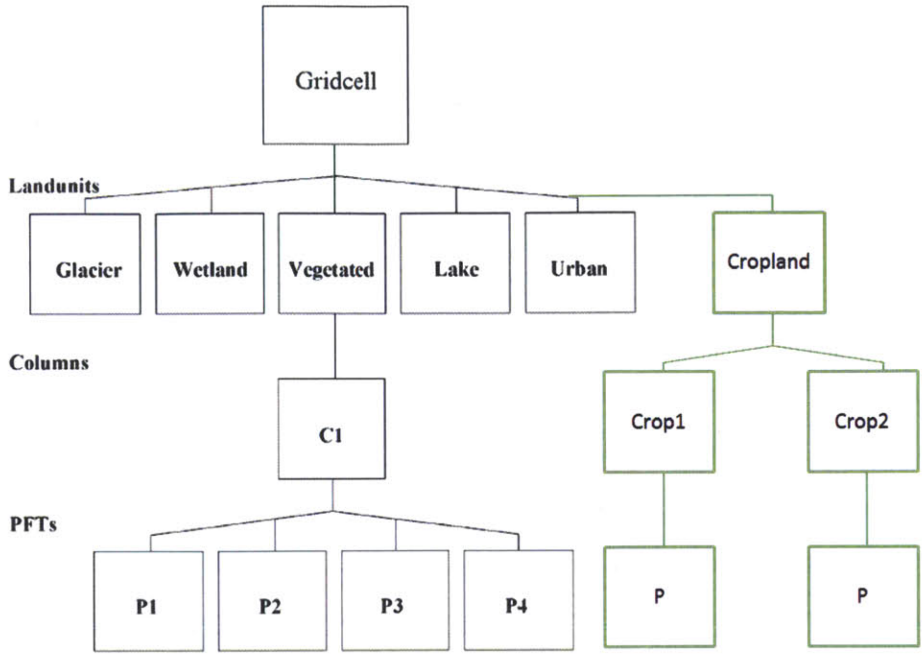

Figure 3-3: The CLM-AG structure. Changes to the usual CLM structure are represented in green. (Adapted from Oleson *et al.* (2004).)

balance, snow cover, etc.) apply to crop landunits as they apply to natural PFTs. This ensures consistency between the different landunits.

3.2.2 Crop Physiology

CLM-AG adds new plant types to CLM. The physiology of these news plants (the crops) differs from the other plants physiology as simulated in CLM. In the standard CLM, root extension is fixed and plant height and Leaf Area Index (LAI) are interpolated from monthly input data. This is a good approximation for natural plants but is too imprecise to calculate crop water stresses. To generate an accurate representation of the irrigation demand, we indeed need a better representation of the crop itself. The representation implemented in CLM-AG is largely based on the physiology routines of AquaCrop (Raes *et al.*, 2009).

CLM-AG being a generic crop model, all crop parameters appearing below, except mentioned otherwise, are crop dependent and do not vary geographically. The values of these parameters for maize, spring wheat and cotton are detailed in Appendix A.

Growing Degree Days

The planting date and the length of the growing season are prescribed by an input data file and held constant for this study. In CLM-AG the growth of a crop is not measured in days but in growing degree days (GDD) that are defined for each day as follow:

$$GDD = \frac{T_{min} + T_{max}}{2} - T_{base}$$

where GDD is the accumulated growing degree days for the day, T_{min} and T_{max} are respectively the minimum and maximum temperatures (with minimum and maximum threshold values being the crop parameters T_{base} and T_{upper}) for the day and the crop parameter T_{base} is the base temperature for the crop (all temperatures in Kelvin).

We also define for each crop and each gridcell a GDD ratio as the ratio between the length of the growing season in a particular gridcell and a standard length of the growing season. This is to account for the fact that farmers in colder climates will plant faster-growing crops than in warm climates[2] . This standard length is defined arbitrarily as it is but a reference point and has no impact on the final result. The GDD ratio is calculated as follow:

$$gddratio = \frac{gr\_length(lat, lon)}{gr\_length\_std}$$

where $gddratio$ is the unitless growing length ratio, $gr\_length(lat, lon)$ is the growing length of the gridcell (in GDD) and gr_length_std is the arbitrary standard value of the length of the growing season for this crop (in GDD).

Crop Cover

Figure 3-4 presents the AquaCrop physiology implemented into CLM-AG. The crop cover is the basis for calculating the physiology of the plant and varies with the number of growing degree days elapsed since the planting date. The crop cover is defined as the proportion of the ground covered by the crop canopy at a given time. There are four distinct stages in

[2]A longer growing season usually improves the yield but can create a weather risk (freezing, drought, etc.) in some areas.

the growing season:

- Initial stage: the seed is in the ground and the roots grow until the emergence of the plant.
- Vegetative stage: the plant grows and develop its leaves until it reaches full canopy cover.
- Yield formation: the plant is at full canopy cover. This is when flowering happens and fruits begin to appear.
- Senescence: the canopy cover diminishes as the plant ages and the fruits finish growing until they are harvested.

We describe below how CLM-AG simulates these different stages in chronological order.

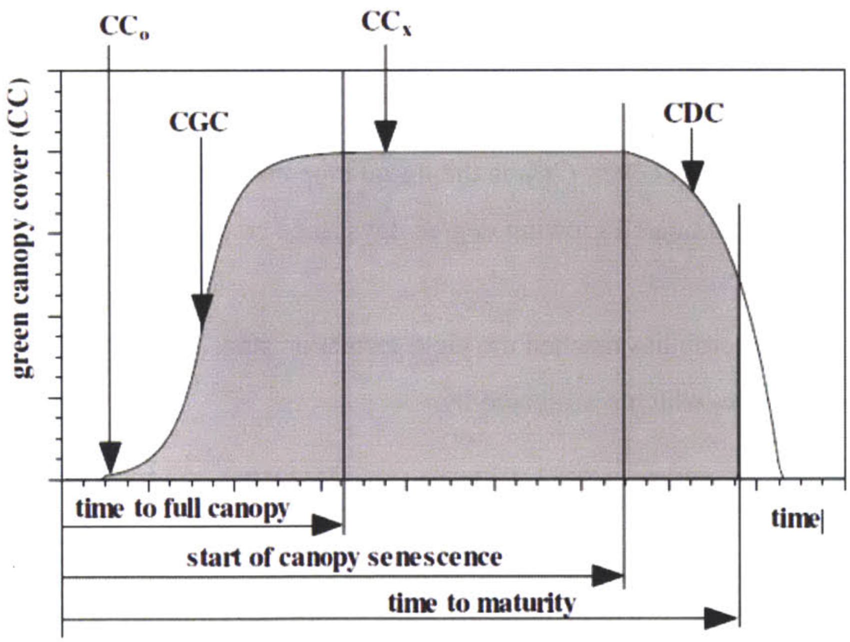

Figure 3-4: CLM-AG crop physiology is a transcription of the AquaCrop model (Raes *et al.*, 2010).

After planting the seed stays in the ground until emergence time that is prescribed by:

$$gdd > t\_em \cdot gddratio$$

where gdd is the accumulated[3] growing degree days since planting and the time to emergence t_em is a crop parameter (in GDD).

Upon emergence, the initial crop cover of the crop is defined by the crop parameter CC_0 and the crop enters the vegetative state.

Then, until it reaches a crop cover of 0.5 (or 50%), the crop grows exponentially at the end of every day:

$$CC = CC_0 \cdot \exp\left(\frac{gdd}{gddratio} \cdot CGC\right)$$

where CC is the crop cover, CC_0 is the initial crop cover, gdd is the accumulated growing degree days since emergence (in GDD) and CGC is a crop parameter.

After reaching this threshold of $CC = 0.5$, the growth rate of the crop decreases until it reaches 98% of the maximal crop cover value CC_x (which is a crop parameter):

$$CC = CC_x - 0.25 \cdot \frac{CC_x^2}{CC_0} \cdot \exp\left(-\frac{gdd}{gddratio} \cdot CGC\right)$$

where CC is the crop cover, CC_0 is the initial crop cover, CC_x is the maximum crop cover, gdd is the accumulated growing degree days since emergence (in GDD) and CGC is a crop parameter.

At this point the crop has reached the yield formation stage and the crop cover stays at CC_x until senescence, which is triggered by:

$$gdd > t\_sen \cdot gddratio$$

where gdd is the accumulated growing degree-days since emergence and the time to senescence t_sen is a standard crop parameter (in GDD).

The crop then starts to decay during the senescence stage according to the equation:

$$CC = CC_x \left(1 - 0.05 \cdot \exp\left(\frac{CDC}{CC_x} \frac{gdd}{gddratio} - 1\right)\right)$$

[3]Growing degree days are accumulated by adding every day to the previous day total the corresponding number of growing degree days.

where CC is the crop cover, CC_x is the maximum crop cover, gdd is the accumulated growing degree days since the beginning of senescence (in GDD) and CDC is a crop parameter.

Finally the crop is harvested when the crop reaches maturity as follows:

$$gdd > t\_mat \cdot gddratio$$

where gdd is the accumulated growing degree days since the beginning of senescence and the time to maturity t_mat is a standard crop parameter (in GDD).

CC is subsequently held at zero until the beginning of the next growing season the following year.

Crop Coefficient, Crop Height and Root Growth

The basal crop coefficient Kcb expresses how much evapotranspiration comes from the crop as compared with a well-watered reference grass (a precise definition of which can be found in Allen *et al.* (1998)).

As in AquaCrop, before the canopy reaches the maximum canopy cover Kcb can be calculated as:

$$Kcb = \left(1.72 \cdot CC - CC^2 + 0.3 \cdot CC^3\right) \cdot Kcb_x$$

where Kcb is the basal crop coefficient, CC is the crop cover and Kcb_x is a crop parameter representing the maximum basal crop coefficient.

Once the crop has reached maximal canopy cover, and after a five day time lag, the crop canopy ages and Kcb is expressed as:

$$Kcb = Kcb_x - (t - 5) \cdot f_{age} \cdot CC_x$$

where t is the number of days since maximum canopy cover, the crop parameter CC_x is the maximal canopy cover and f_{age} is a crop parameter.

Finally when senescence starts and the canopy starts to decay the previous expression of Kcb is corrected by the ratio $\frac{CC}{CC_x}$ as follows:

$$Kcb = \frac{CC}{CC_x} \cdot (Kcb_x - (t-5) \cdot f_{age} \cdot CC_x)$$

The height of the canopy is calculated following AquaCrop by:

$$h = h_x \cdot \frac{CC}{CC_x}$$

where h is the height of the canopy, h_x is a crop parameter representing the maximum height of the canopy, CC is the crop cover and CC_x is the maximum crop cover. The crop height does not decrease after senescence starts but stays at maximum height until harvesting, even after the crop cover declines.

Roots grow by a fixed amount on a daily basis as soon as the crop is planted and until maximum depth is reached. Initial root depth (rt_{ini}), daily root growth (rt_{gr}) and maximum root depth (rt_{max}) are crop parameters. The root fraction in a given layer of soil (per unit of volume) is then calculated at the end of every day using the same routine CLM uses for other plants (see Oleson *et al.* (2004)).

Leaf Area Index

The Leaf Area Index (LAI) is defined as the area of leaf per area of ground and represents the density of the canopy. It differs from crop cover in the sense that it takes into account multiple layers of leaves. CLM needs the Leaf Area Index as a crucial parameter to calculate the energy and water balances in the crop. We follow here the observations and parametrization of LAI by Vina (2004) that shows that the crop cover is an exponential function of the LAI.

We thus estimate the LAI based on the crop cover as:

$$LAI = LAI_x \cdot \frac{log(1 - CC)}{log(1 - CC_x)}$$

where LAI and LAI_x are respectively the current and maximum LAI of the plant (LAI_x is a crop parameter) and CC and CC_x are respectively the current and maximal crop cover.

3.2.3 Biogeophysics and Hydrology

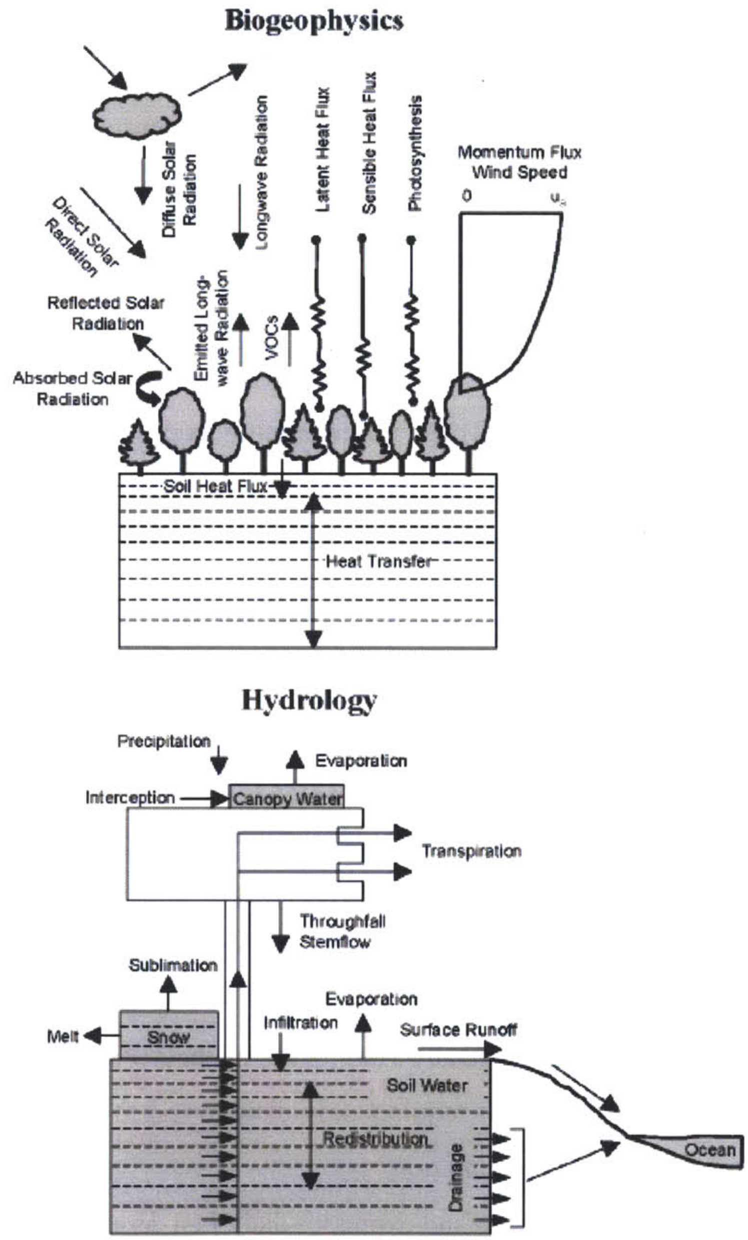

Figure 3-5: The biophysical and hydrological processes simulated in the Community Land Model (Oleson *et al.*, 2004).

Figure 3-5 presents the biogeophysical and hydrological processes simulated in CLM 3.5. CLM-AG uses these same routines for crop columns to preserve consistency.

It is interesting to note that CLM has ten different soil layers among which water flows. This implies for crops that even if it does not rain they may still absorb required moisture from deeper soil layers. Accurate simulation of the snow pack is also crucial in some areas. On the American Great Plains for example most of the water crops need come from snow melt on the field at the beginning of the season. The interested reader will find a more extensive description of the biogeophysical and hydrological routines in the CLM technical description (Oleson *et al.*, 2004).

3.2.4 Irrigation Need and Yield Reduction

Following CROPWAT (Smith, 1992), the water deficit is calculated in CLM-AG as the difference between potential and actual evapotranspiration of the crop. Actual evapotranspiration is easily drawn from existing CLM variables, however we need to define a measure of the potential evapotranspiration.

Potential Evapotranspiration

There are several methods to calculate evapotranspiration in the literature; they differ in precision and complexity. The historic and most trusted method is the Penman-Monteith equation (Monteith, 1965; Allen *et al.*, 1998). However, this formula is data-intensive as it requires precise measures of humidity and wind. To address this issue, many methods have been developed to estimate potential evapotranspiration (PET) with less data requirements. One such method is the Modified Daily Hargreaves method (Farmer *et al.*, 2011) developed at the MIT Joint Program. It requires only daily average, maximum and minimum temperatures as well as daily precipitation.

CLM-AG follows this approach and expresses daily PET as:

$$PET = 0.0019 \cdot 0.035 \cdot Ra \cdot (T_m + 21.0584) \cdot ((T_x - T_n) - 0.0874 * P)^{0.6278}$$

where PET is the daily PET (in mm/day), Ra is the incoming solar radiation (in W/m2), T_m, T_x, T_n are respectively the average, maximum and minimum temperature (in °C) and P is the precipitations (in mm/day).

Actual Evapotranspiration and Evapotranspiration Demand

The Actual Evaporation is calculated from the CLM routines of canopy fluxes and plant biochemistry using Monin-Obukov similarity theory and a Newton-Raphson iteration to solve for energy and water vapor fluxes (Oleson *et al.*, 2004). We define the actual evapotranspiration of the crop as:

$$ET_A = Qevap_{veg} + Qevap_{soil}$$

where ET_A is the actual evapotranspiration (in mm/day), $Qevap_{veg}$ and $Qevap_{soil}$ are the evaporation (and transpiration) of the plant and the soil, respectively.

The evapotranspiration demand is then calculated following AquaCrop methodology (Raes *et al.*, 2010) as:

$$ET_D = (Kcb + Ke) \cdot PET$$

where ET_D is the evapotranspiration demand (in mm/day), Kcb is the basal crop coefficient calculated as described in the previous section and Ke is the soil evaporation coefficient.

The soil evaporation coefficient Ke depends on the crop cover CC and is calculated as in AquaCrop by:

$$Ke = \left(1 - \left(1.72 \cdot CC - CC^2 + 0.3 \cdot CC^3\right)\right) \cdot Ke_x$$

where the maximum evaporation coefficient Ke_x is a model parameter (constant for all crops and locations) taken equal to 1.1 as in AquaCrop.

To account for reduced evaporation due to dead canopy cover during senescence, the previous Ke is multiplied during the senescence stage by $(1 - f_{CC} \cdot CC_x)$ where f_{CC} is a crop parameter.

Irrigation Demand

The irrigation demand is the difference between potential and actual evapotranspiration. For a given month, the irrigation demand is expressed as:

$$IRR = \Sigma_{days}(ET_D - ET_A)$$

Yield Factor

The yield factor expresses the percentage of the yield of a crop lost due to water stress as compared with that of an irrigated crop with the same inputs (fertilizer, soil, etc.) The yield factor is defined in CROPWAT (Smith, 1992) and we employ this same method in CLM-AG.

The yield factor is defined as:

$$YF = 1 - \prod_s \left(Ky_s \left(1 - \frac{ET_A^s}{ET_D^s} \right) \right)$$

where the yield coefficient Ky_s is a crop parameter dependent on the growing stage s, ETD_s and ETA_s are the total demanded and total actual evapotranspiration for the growing stage s (in mm) respectively.

The four growing stages are the same as those defined in Section 3.2.2:

- Initial Stage: from planting to 10% of the crop cover.
- Vegetative Stage: from 10% of the crop cover to full crop cover.
- Yield Formation: from full crop cover until senescence. It is the stage where crops are the most sensitive to water stress with Ky_3 often greater than one.
- Senescence: from the start of senescence to harvesting.

3.3 Model Evaluation: Historic Runs

To evaluate the model, we run it with observed weather from the late twentieth century and current crop datasets. As observations of irrigation demand at the aggregate scale are unavailable, we evaluate the model by comparing it to an existing modeled dataset: the IIASA-FAO Global Agro-Ecological Zones (GAEZ) dataset (Fischer *et al.*, 2012). CLM-AG is run for corn, spring wheat and cotton for this comparison.

For a second evaluation, we concentrate on the United States and use the 2008 USDA Farm and Ranch Irrigation Survey (FRIS, USDA (2008)) for corn crops. After computing a measure of the irrigation efficiency, we compare it to usually accepted values for this parameter.

3.3.1 Input Data and Method for the Evaluation

Crop Data

The crop parameters used in this study are drawn from multiple sources that include CROPWAT, AquaCrop and several other publications. These values and their sources for maize, spring wheat and cotton can be found in Appendix A.

The crop calendar (planting date and length of the growing season) is drawn from the GAEZ dataset. It is important to note that the planting date identified in GAEZ is modeled as the one that results in the highest yield for the year and is not based on observation or survey. However, as in the real world, rainfed crop planting dates can differ significantly from irrigated planting dates. We use crop calendars that are reflective of irrigated maize and cotton and rainfed wheat for this study.

Weather Data

We use the National Centers for Environmental Prediction/National Center for Atmospheric Research Corrected by Climate Research Unit (NCC, Ngo-Duc *et al.* (2005)) as a weather forcing data for CLM-AG. NCC is a six-hourly weather dataset with temperature, rainfall, snowfall, wind, pressure, specific humidity, longwave and shortwave incident radiation at a resolution of 1x1 degrees. It is built by taking the six-hourly NCEP/NCAR reanalysis runs and correcting the monthly means with CRU observations. To reduce the processing time of CLM, we run it at a 2x2.5 degrees resolution instead of 1x1[4].

[4] Another reason for running at 2x2.5 degrees is that it is the standard IGSM resolution used in most other MIT Joint Program studies.

Evaluation Model Runs

We run the model from 1975 to 2000 and calculate the average irrigation need on the 1980-1999 period (the first five years being considered as a spin-up time for the soil hydrology in CLM before it reaches an equilibrium state).

3.3.2 Results and Comparison with GAEZ

The GAEZ Dataset

The IIASA-FAO Global Agro-Ecological Zones (GAEZ) dataset (Fischer *et al.*, 2012) is a dataset constituted as the output of a global agriculture and soil model. It has a resolution of five by five minutes of arc. GAEZ includes numerous data for a wide variety of crops. It distinguishes irrigated and rainfed crops, the input level (low, intermediate or high)[5], and the year (the model uses the CRU global historic weather dataset).

For this particular study, we look at the water deficit (in mm) for the three selected crops (irrigated maize, irrigated cotton and rainfed spring wheat) under an intermediate input scenario averaged over the years 1961-1990.

Results for Maize

This section only shows the results for maize as the results for spring wheat and cotton are highly similar. These other results can be found in Appendix B.

[5] A low input level is associated with a traditional subsistence agriculture. An intermediate input level is associated with a subsistence and partially market-oriented agriculture with some mechanization. High input level relates to industrial agriculture. It is useful to note that the input level does not change the planting date or the length of the growing season in GAEZ, but only the yield.

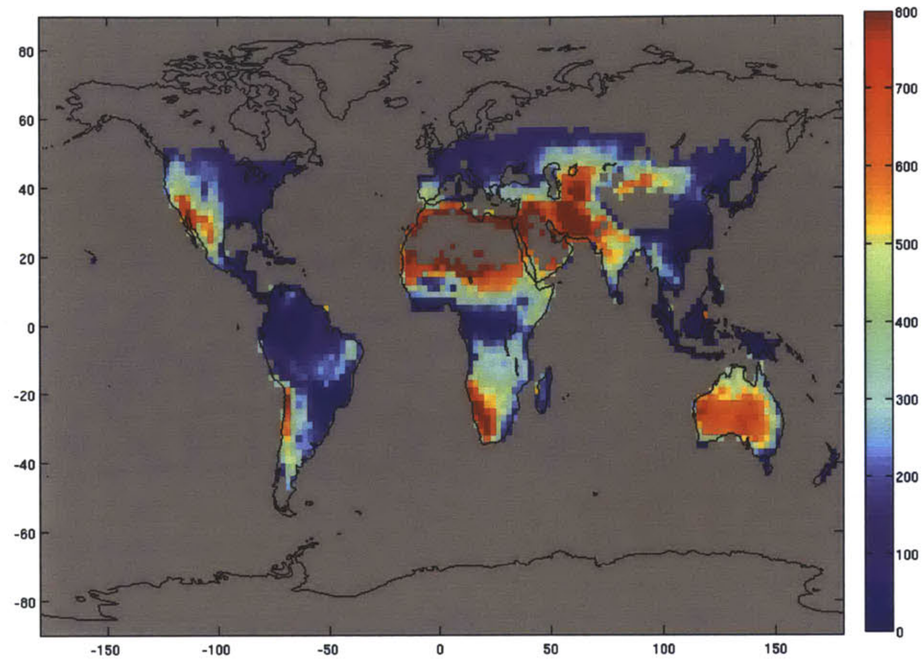

Figure 3-6: CLM-AG water deficit (in mm) for irrigated maize - NCC dataset, 1980-1999 average.

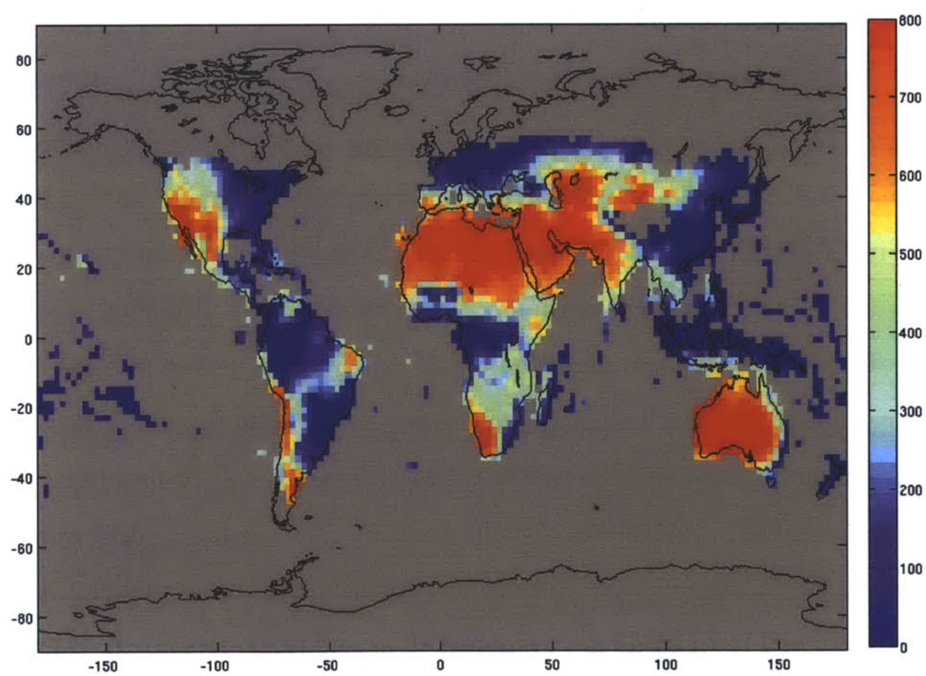

Figure 3-7: GAEZ water deficit (in mm) for irrigated maize - CRU dataset, 1961-1990 average.

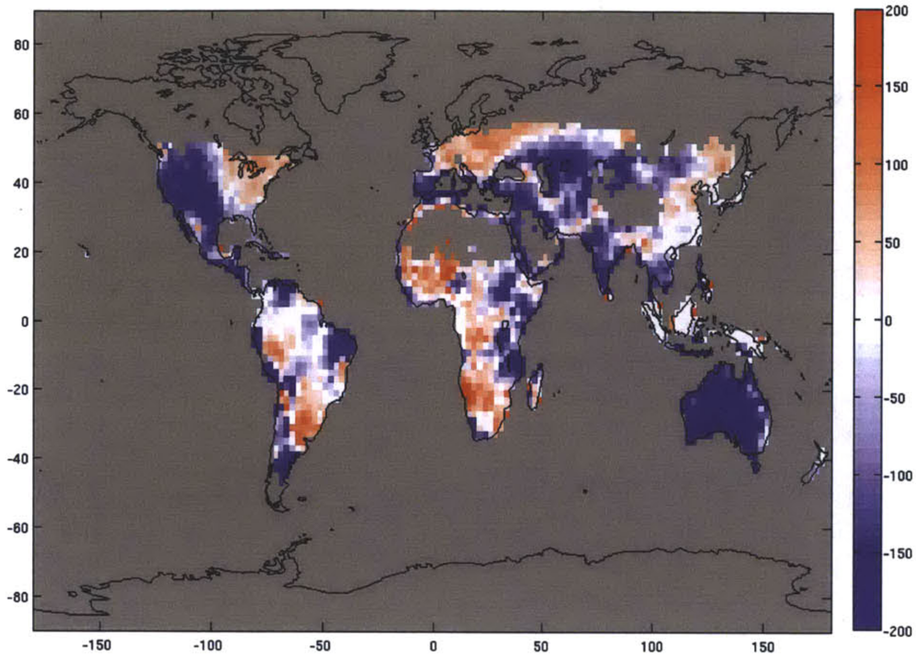

Figure 3-8: Difference in water deficit estimates between CLM-AG and GAEZ (in mm) for irrigated maize – same specifications as the previous figures.

Analysis

CLM-AG and GAEZ define the same patterns in terms of irrigation need for maize in the world (Figures 3-6 through 3-8). Wet zones more suitable for agriculture appear at the same place in CLM-AG and GAEZ, while drier zones (with a higher irrigation need) also match between the two models. As Figure 3-8 shows, the only difference resides in the magnitude. CLM-AG is quite wetter than GAEZ in dry areas (Western USA, Australia, Mediterranean Basin, etc.) and slightly drier in wet areas (Eastern USA, Central Europe, Northern Argentina, etc.). This difference may be explained by a difference in the treatment of the soil in the models. CLM-AG benefits from the full ten-layer CLM model, while GAEZ relies only on a "bucket layer" soil that evaporates more quickly under a dry climate; the deep layers of soil in CLM do not evaporate so as rain percolates down, water remains available in the ground longer for the crop to use. Appendix B presents similar results for rainfed spring wheat and irrigated cotton. It is worth noting that CLM-AG is globally slightly drier than GAEZ for rainfed spring wheat, which may be explained by differences in crop parametrization between the models.

Despite these few differences and considering the uncertainty in both models, CLM-AG represents the irrigation need accurately enough for studies in the global framework we have developed.

3.3.3 Evaluation for the USA with FRIS

Every five years the United States Department of Agriculture - National Agricultural Statistics Service (USDA-NASS) conducts the Agriculture Census as mandated by law. For a few selected farms in the country (around 10 percent of the total number of farms) the census includes an extra survey on irrigation. The Farm and Ranch Irrigation Survey (FRIS) is usually released a year after the census. The latest available version is the 2008 FRIS with 2007 data (USDA, 2008). From the results of the survey, FRIS reports the amount of water withdrawn by farmers per acre of land irrigated and per crop aggregated at the State level.

Results

To carry out this analysis, we aggregate CLM-AG results at the State level and calculate the implied irrigation efficiency (defined as the irrigation demand from CLM-AG divided by the amount of water withdrawn by the farmers as reported in FRIS). Table 3.1 presents the results for the states where irrigated maize covers more than fifty thousand acres of land.

Analysis

The average efficiency (weighted by the cultivated surface) is 51.4% according to this study[6]. Pimentel *et al.* (1997) reports an average irrigation efficiency of 50% for the United States so CLM-AG is an accurate measure of irrigation need on this measure.

Individual numbers vary significantly from a state to another. There are several explanations for this fact, some explaining why different states have different efficiencies, some being modeling shortfalls.

[6]Nebraska and Kansas alone make for more than three quarter of the surface irrigated.

State (sorted by acreage)	Irrigation efficiency modeled
Nebraska	50.3%
Kansas	44.1%
Texas	62.2%
Colorado	46.9%
Missouri	45.0%
Illinois	67.5%
California	67.4%
Arkansas	65.4%
Michigan	69.0%
Minnesota	54.9%
Indiana	74.6%
South Dakota	59.9%
Mississippi	36.9%
Louisiana	21.9%
Georgia	48.8%
Oklahoma	42.5%
Wisconsin	42.3%
Iowa	72.1%
Washington	36.4%
North Dakota	59.9%
Idaho	32.9%

Table 3.1: Irrigation Efficiency for Maize in the United States drawn from CLM-AG results and FRIS data.

First, states where water is scarce (Texas, California) tend to have a higher irrigation efficiency thanks to highly efficient irrigation systems while wetter states (like Missouri or Washington) are not as efficient.

Second, we do not take into account in CLM-AG water needs for other uses than crop irrigation itself like freezing prevention or salt leaching[7]. These can make a significant difference in the total irrigation need in certain states.

Third, FRIS data is likely to contain systematic biases and/or errors as it is a survey of farmers and not field observations. FRIS itself warns that farmers in drier areas keep better accounting of the water they use as the price they pay for it is higher.

However, the biggest discrepancies may come from the spatial aggregation of the data. Irrigation can vary notably from location to location within a state (or even within a 2 x

[7]Use of irrigation for salt leaching probably explains the very low number obtained for Louisiana.

2.5 degree grid cell) and any one farm will likely have a different approach to irrigation from the next one. This study also aggregates water demand at a state level. This raises two issues. First, precipitation and hence water deficit can vary significantly inside the state borders (this is particularly a concern in a state like California). Second, farms may not be homogeneously spread in the state and concentrate on a specific area where there is a specific climate (for example in Colorado, farms are situated on the Eastern part of the State that faces a drier climate than the Western mountainous areas).

Going forward, we contend that CLM-AG is far too imprecise to be used in a current situation setting to do water planning at a regional scale[8]. Nevertheless, it adds value by correctly approximating the irrigation need and determining the large-scale patterns. Moreover, despite being imperfect at the local level, it will be able to measure the relative impacts of climate variations on irrigation needs. After this evaluation, CLM-AG can be confidently used to provide insights on the impact of future climate on water stress for agriculture.

[8]We would recommend using a model like DSSAT instead.

Chapter 4

Irrigation in 2050 - A Global Perspective in an Integrated Framework

In this chapter we run CLM-AG under a full 3D climate model – the IGSM-CAM – under two different policy scenarios. We investigate the impact of an Unconstrained Emissions scenario on the irrigation demand for maize and cotton and on the rainfed yield for spring wheat by 2050. We also run a mitigation scenario that limits concentrations of "greenhouse gases" by the end of this century to 660 ppm CO_2 equivalent[1] to assess the impact of potential mitigation policies.

4.1 Datasets

4.1.1 Climate Data

The climate data for these runs are taken from the IGSM-CAM model (Monier *et al.*, 2012). The Community Atmosphere Model (CAM) is a climate model developed by the National Center for atmospheric Research (NCAR). The IGSM-CAM version developed at the MIT Joint Program on the Science and Policy of Global Change is composed of two main modules (among others that also consider ocean and urban airshed processes) –

[1]This is the total quantity of greenhouse gases that would be equivalent to having 660 ppm of carbon dioxide in the atmosphere but no other greenhouse gas. This is roughly equivalent to a concentration of 550 ppm of CO_2 in a standard emission scenario.

an atmosphere module and a land module – that interact. Two different sets of data are required for these runs:

- Greenhouse Gases Forcing: CAM requires as a forcing a time series of the concentration of the main greenhouse gases. Two policy scenarios are run in EPPA to generate emissions scenarios, which then provide inputs into the IGSM to create the corresponding greenhouse gases concentration forcing sets. The first one is an Unconstrained Emissions scenario (UCE) where no specific policy is put in place to address climate change. The second one is a so called Level 2 stabilization scenario (L2S) where emissions are limited globally to stay below a concentration of greenhouse gases in the atmosphere equivalent to 660 ppm CO_2 by the end of the century (2100)[2].

- Ocean Forcing: CAM is constrained by the Sea-Surface Temperature (SST) anomalies from the IGSM 2.3 (2-D atmosphere and full 3-D ocean model) added to a climatological annual cycle taken from an observed dataset (Hurrell *et al.*, 2008).

The IGSM-CAM is run for the period 1950-2050 at a resolution of 2 degrees of latitude by 2.5 degrees of longitude using median climate sensitivity, rate of ocean uptake and aerosol forcing as described in Sokolov and Monier (2011). The output is an hourly dataset of surface temperature, precipitations, radiation, humidity, wind and surface pressure. This is the input needed to run CLM-AG.

4.1.2 Crop Data

The crop data inputs are the same as those described in Section 3.3.1. The crop parameters, drawn from various sources, can be found in Appendix A. The planting dates and length of the growing cycles are drawn from the Global Agro-Ecological Zones project (GAEZ, Fischer *et al.* (2012)).

There is no crop management adaptation to climate change beyond a reduction of the length of the growing season due to the rise in temperature under climate change as the

[2]More details on the construction of the L2S scenario can be found in Webster *et al.* (2012).

growing season length is prescribed in Growing-Degree Days and not in days in CLM-AG. Though there are very good reasons to believe that farmers will adapt to climate change (see for example Smit and Skinner (2002) or Easterling *et al.* (2007)), quantifying the effect of these adaptation strategies is far from trivial and falls outside of the scope of this work. The results of this chapter should thus be interpreted as the impacts of climate change on irrigation need *in the absence of adaptation* and *under one particular climate model.* We discuss further the implication of these limitations in Section 4.3.

4.2 Results

4.2.1 Evaluation of CAM versus NCC

Figure 4-1 presents the results of a historic run of CLM-AG with IGSM-CAM forcing. Pictured is the irrigation need for maize averaged over the years 1990-1999. The relative location of wet and dry areas are the same as the ones obtained using NCC forcing data, or using the IIASA dataset (see Chapter 3, Figures 3-6 and 3-7). One of the main differences is that Africa and Asia feature a lower irrigation need using CAM forcing while North America appears drier than under NCC. To confirm this observation we plot the absolute (Figure 4-2) and relative (Figure 4-3) differences in irrigation demand for maize between NCC and CAM forcing.

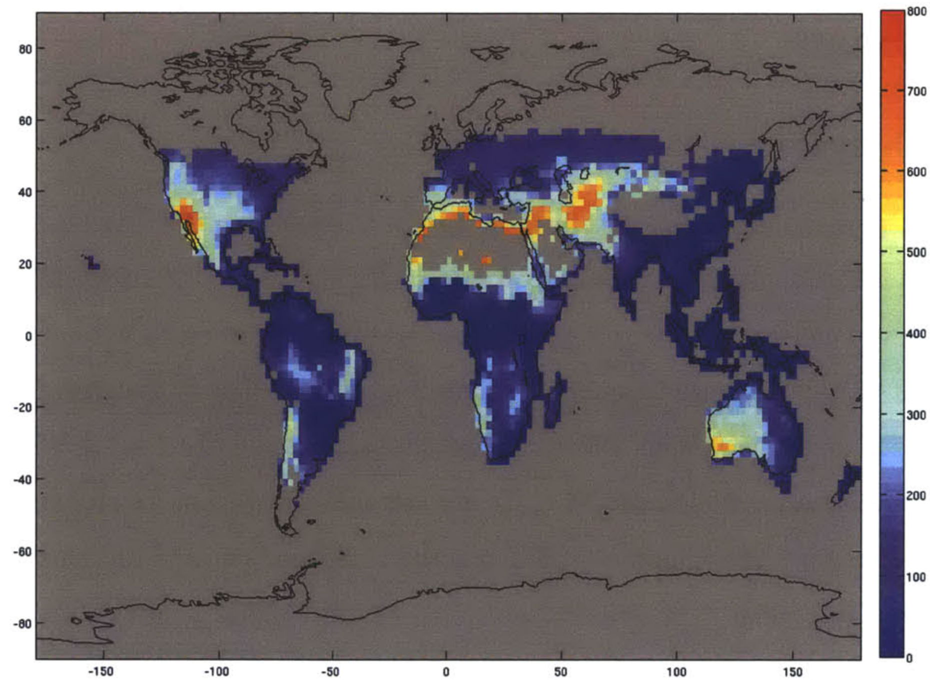

Figure 4-1: CLM-AG water deficit (in mm) for irrigated maize – IGSM-CAM run, 1990-1999 average.

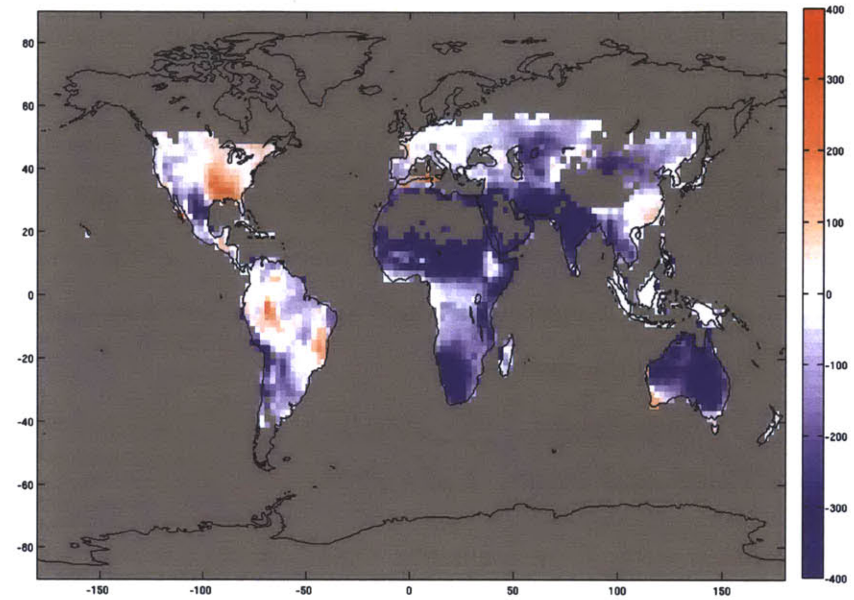

Figure 4-2: CLM-AG water deficit (in mm) for irrigated maize – absolute difference between the IGSM-CAM run and the NCC run (a positive number indicates that IGSM-CAM is drier than NCC), 1990-1999 average.

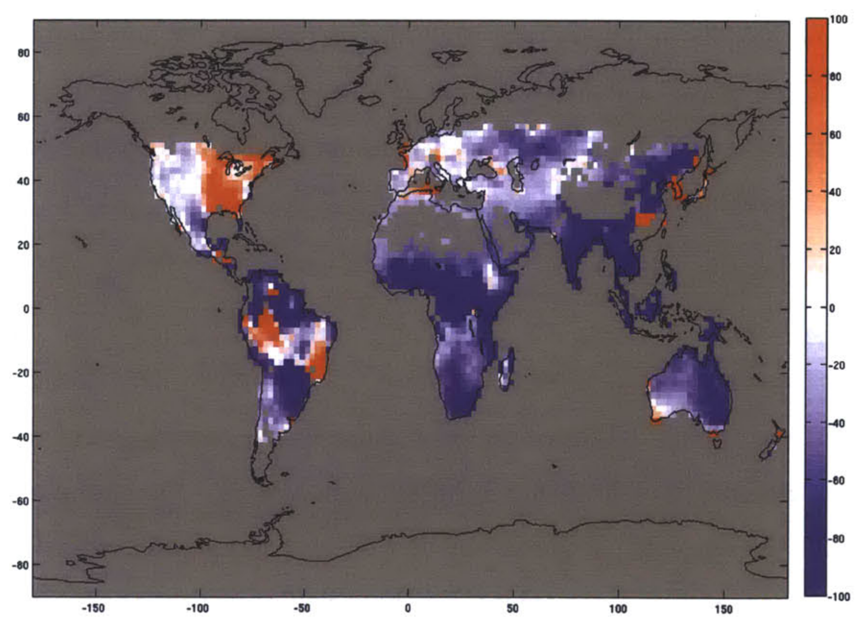

Figure 4-3: CLM-AG water deficit for irrigated maize – relative difference (in percent) between the IGSM-CAM run and the NCC run (a positive percentage indicates that IGSM-CAM is drier than NCC), 1990-1999 average.

CAM appears to be wetter than the historic average as recorded by NCC in the Southern hemisphere. These results were expected as the NCAR Community Climate System Model (CCSM) model – whose atmosphere is modelled by CAM – overestimates precipitation rates (Hack *et al.*, 2006). Once again we warn against interpreting the absolute results of a climate model and contend that only variations and trends relative to a model's climatology (between future and historic runs) are relevant to capture some of the dynamics in play. Consequently the next section presents absolute and relative variations of future versus historic runs instead of absolute numbers.

4.2.2 Future Runs and Impacts of Policy

There are two common methods for evaluating impacts of climate change: "differences" and "ratios". Using "differences" means the relevant number used for results interpretation is the difference between the future and the historic run in absolute terms (mm for irrigation need, for example); using "ratios" means the relevant number is the percentage change between future and historic values. The two methods stem from the need to downscale imprecise global models to the regional scale that is relevant for policy making. Both techniques have advantages and disadvantages and there is no commonly accepted method to distinguish which one is unequivocally more insightful. We thus present both absolute change and relative change.

Maize

The next two pages successively present the change in irrigation need between future (2040 - 2050) and historic (1990 - 2000) values for irrigated maize under first an Unconstrained Emissions scenario and second a Level 2 Stabilization scenario. On both pages, the first figure represents the absolute change in mm and the second figure the relative change in percent. For this second figure, the values have been limited to a range of -50% to +50%. Indeed very large values of relative change can occur where the irrigation need is extremely close to zero in historic runs.

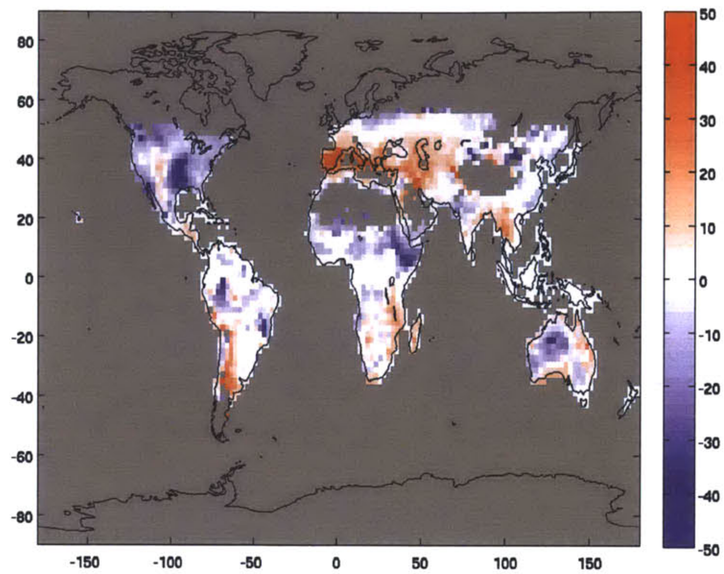

Figure 4-4: CLM-AG water deficit for irrigated maize – absolute difference (in mm) between the 2040-2049 Unconstrained Emissions scenario average and the 1990-1999 average.

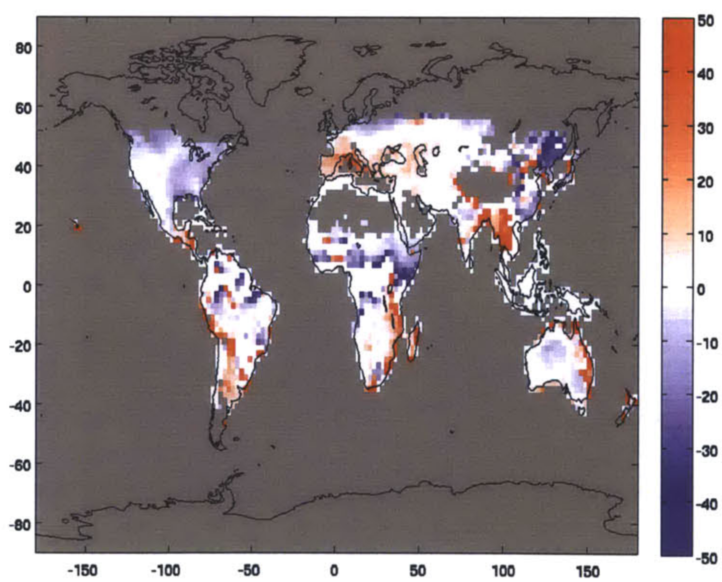

Figure 4-5: CLM-AG water deficit for irrigated maize – relative difference (in percent) between the 2040-2049 Unconstrained Emissions scenario average and the 1990-1999 average.

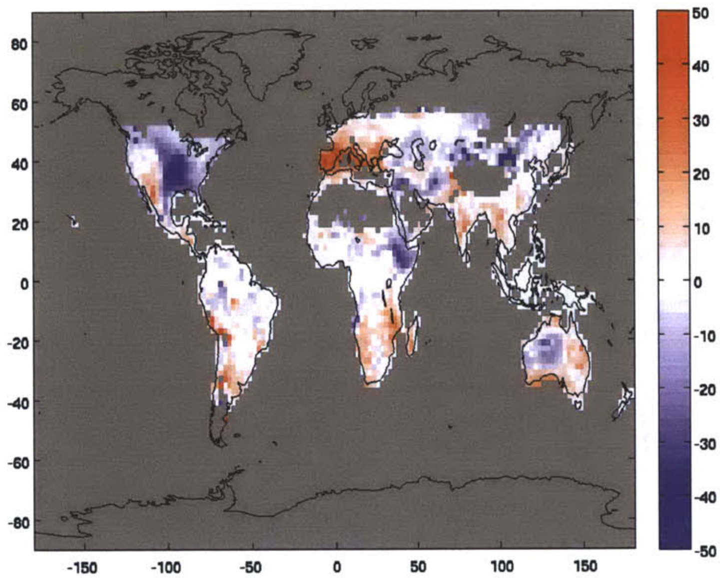

Figure 4-6: CLM-AG water deficit for irrigated maize – absolute difference (in mm) between the 2040-2049 Level 2 Stabilization scenario average and the 1990-1999 average.

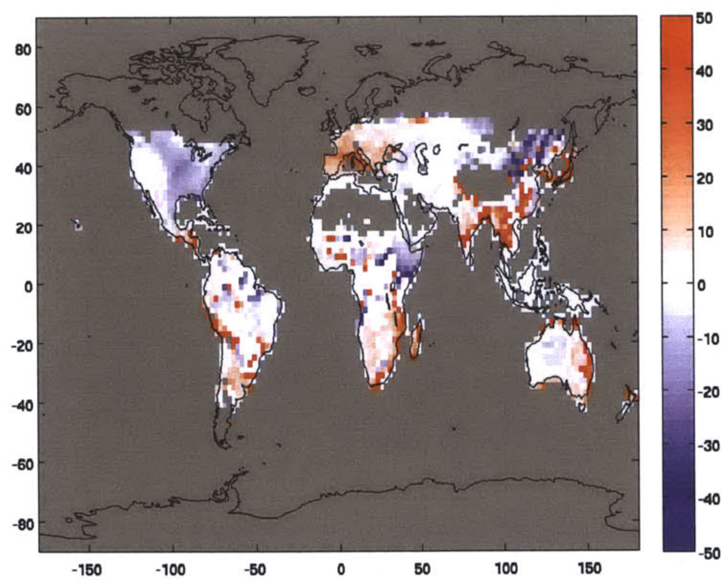

Figure 4-7: CLM-AG water deficit for irrigated maize – relative difference (in percent) between the 2040-2049 Level 2 Stabilization scenario average and the 1990-1999 average.

To analyse these results we concentrate on the largest maize producing areas globally. The largest irrigated producing areas are from West to East: the Western US Corn Belt, Western and Central Europe, the Nile and Zambezi Valleys, Northern Pakistan and North-Eastern China. Other important areas where maize is irrigated exist but are less dependent on irrigation to achieve a reasonable yield and are thus less likely to be impacted by climate change. Tables 4.1 and 4.2 summarize what can be drawn from the maps above for these areas.

Area	Observed Change
U.S. Corn Belt	20 to 30% decrease
Europe	5 to 15% increase
Nile Delta	Increase of about 5%
Zambezi Valley	5 to 20% increase depending on the area
Northern Pakistan	Nearly no change
N.E. China	Nearly no change

Table 4.1: Changes in irrigation need between 2050 and 2000 under an UCE scenario for the major corn producing regions with irrigation.

Area	Observed Change
U.S. Corn Belt	Sharp decrease of 30 to 50%
Europe	Large increase of 15 to 25%
Nile Delta	5 to 10% increase
Zambezi Valley	10 to 25% increase depending on the area
Northern Pakistan	Increase of about 15%
N.E. China	Nearly no change

Table 4.2: Changes in irrigation need between 2050 and 2000 under a L2S scenario for the major corn producing regions with irrigation.

A first observation is that the US Corn Belt appears to be a beneficiary of climate change as modeled by CAM, while other areas see their irrigation need increase, especially sharply for Europe and the Zambezi River Valley. A second interesting observation is that the changes seem to be more important under a L2S scenario than under the UCE scenario which is quite counter-intuitive. To get a clearer view on the impact of the L2S policy compared to the UCE scenario we plot on the next page the difference between the two scenarios for maize irrigation need.

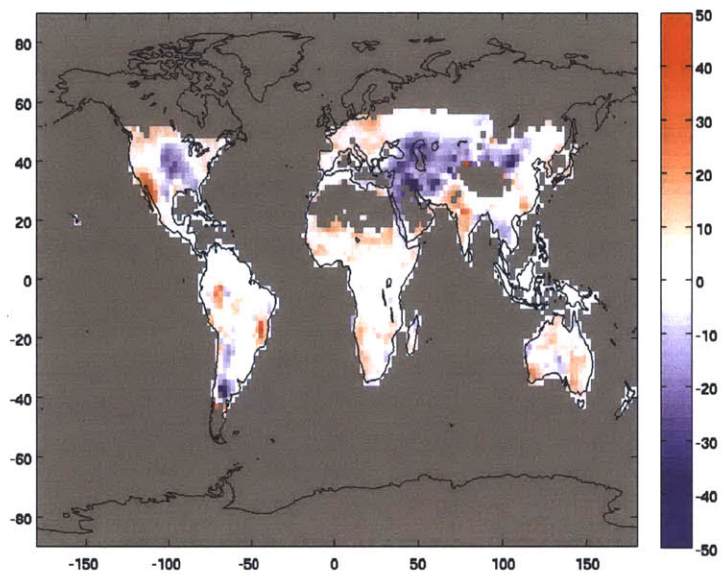

Figure 4-8: CLM-AG water deficit for irrigated maize - absolute difference (in mm) between the 2040-2049 Level 2 Stabilization scenario average and the 2040-2049 Unconstrained Emission scenario average.

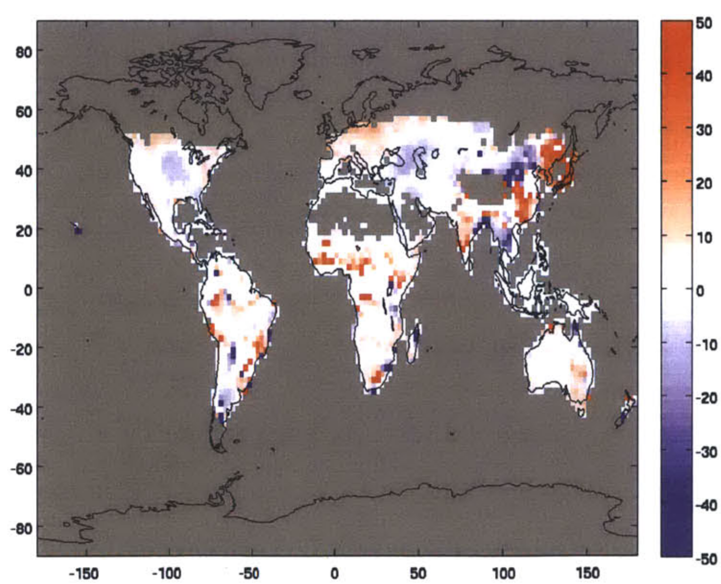

Figure 4-9: CLM-AG water deficit for irrigated maize - relative difference (in percent) between the 2040-2049 Level 2 Stabilization scenario average and the 2040-2049 Unconstrained Emission scenario average.

As summarized in Table 4.3 putting in place a L2S policy that would limit global greenhouse gases emissions to 660 ppm CO_2 equivalent actually increases the impact of climate change for key corn producing regions. The change benefits the U.S. Corn Belt where the stabilization policy makes the climate wetter – and thus further decreases irrigation need – while in Europe, the Zambezi Valley or Northern Pakistan irrigation needs increase further. A more thorough analysis of CAM results shows that these increases root in the fact that precipitations increases in a UCE scenario for these regions (or decrease less compared with the historic average in the case of Europe) which reduces irrigation need despite increased temperature. Another item of note is that warmer climate results in faster crop growth, which in turn decreases total growing season water demand in CLM-AG.

Area	Difference between the two scenarios
U.S. Corn Belt	10 to 20% decrease
Europe	Increase of about 10%
Nile Delta	Increase of about 5%
Zambezi Valley	Increase of about 5%
Northern Pakistan	Increase of about 10 to 15%
N.E. China	Nearly no change

Table 4.3: Changes in irrigation need in 2050 between a L2S and a UCE scenario for the major corn producing regions where irrigation is present.

Spring Wheat

Spring wheat is rarely an irrigated crop. More relevant than irrigation need is the impact of water stress on the yield of spring wheat. As explained in Chapter 3, CLM-AG computes a water-stress yield factor as the amount by which the yield of the rainfed crop is reduced because of water stress, independently of other production factors. The major producing areas of spring wheat are the Northern American Great Plains, the Black Sea area (Ukraine and Turkey), the Ganges Valley, Central-Eastern China and Southwestern Australia.

We only present here the relative yield factor change – and not the absolute change – as it represents directly a relative yield change for the crop.

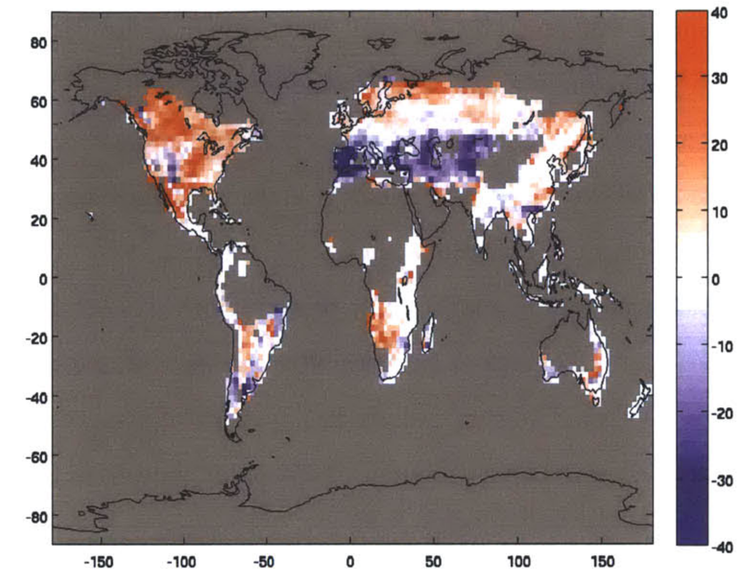

Figure 4-10: CLM-AG yield factor for rainfed spring wheat – relative difference (in percent) between the 2040-2049 Unconstrained Emissions scenario average and the 1990-1999 average yields.

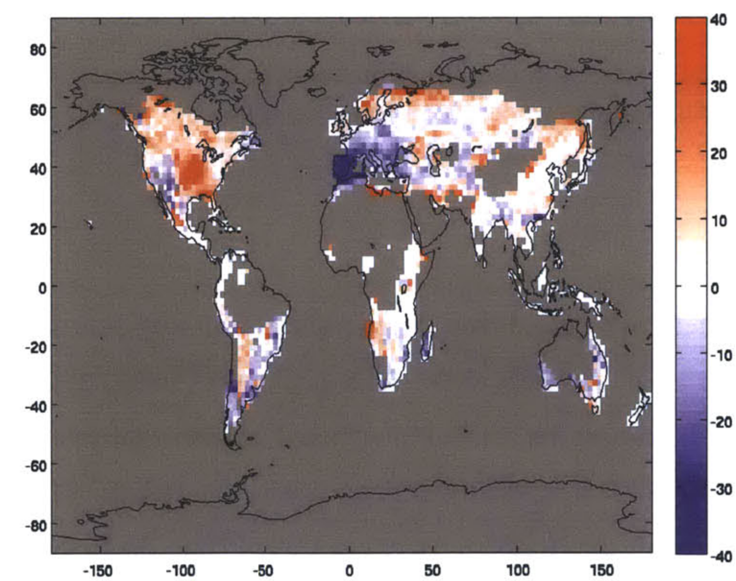

Figure 4-11: CLM-AG yield factor for rainfed spring wheat – relative difference (in percent) between the 2040-2049 Level 2 Stabilization scenario average and the 1990-1999 average yields.

The following tables (Tables 4.4 and 4.5) present the results for the major spring wheat producing regions as it appears on the maps above. North America becomes wetter, which is reflected in a rise of rainfed spring wheat yield. Ukraine and Turkey both see decreases of rainfed yield under climate change. Neither the Ganges Valley nor China see any major change as these areas are not water-stressed – the rainfed factor as calculated by CLM-AG is 1, meaning that the crop can produce at a full non water stressed yield – and it does not change in our simulations. Southwestern Australia, like Europe, see its rainfed spring wheat yield diminish.

Area	Observed Change
Northern Great Plains	Increase of about 20 to 30%
Ukraine	No change
Turkey	15 to 25% decrease
Ganges Valley	No change
China	No change
SW Australia	Decrease of about 10%

Table 4.4: Changes in rainfed yield between 2050 and 2000 under an UCE scenario for the major regions producing spring wheat.

Area	Observed Change
Northern Great Plains	5 to 15% increase
Ukraine	Decrease of about 10%
Turkey	10 to 20% decrease
Ganges Valley	No change
China	No change
SW Australia	Decrease of about 10%

Table 4.5: Changes in rainfed yield between 2050 and 2000 under a L2S scenario for the major regions producing spring wheat.

To better show the implications of putting in place a Level 2 Stabilization policy, we map the relative yield difference between the UCE and L2S scenarios in 2050.

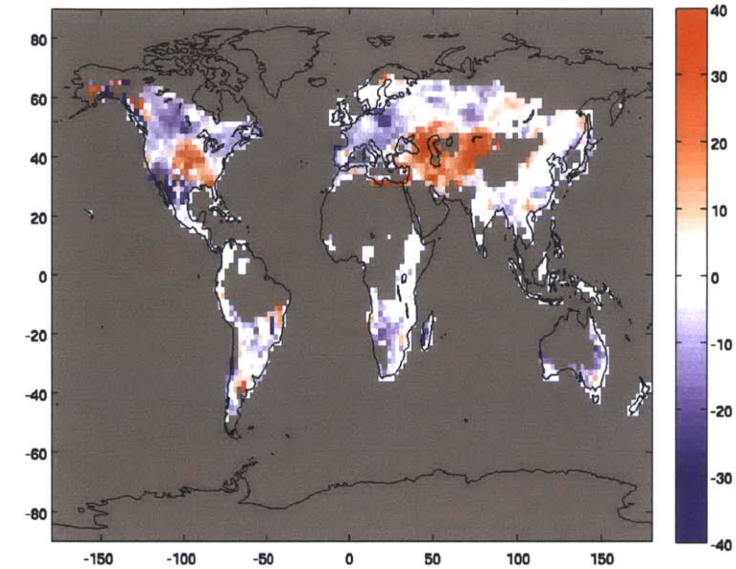

Figure 4-12: CLM-AG yield factor for rainfed spring wheat – relative difference (in percent) between the 2040-2049 Level 2 Stabilization scenario average yields and the Unconstrained Emissions scenario average yields.

Once again, because the climate becomes globally wetter in IGSM-CAM under a UCE scenario than a L2S scenario, putting in place a Level 2 Stabilization policy globally decreases the rainfed yield of spring wheat. Only Turkey sees a positive impact of mitigating climate change in terms of spring wheat yield.

Area	Observed Change
Northern Great Plains	5 to 15% decrease
Ukraine	5 to 10% decrease
Turkey	5 to 10% increase
Ganges Valley	No change
China	No change
SW Australia	Nearly no change

Table 4.6: Changes in rainfed yield between 2050 and 2000 under a L2S scenario for the major regions producing spring wheat.

Cotton

Cotton is one of the principal cash crops in the world and some economies rely on it heavily to balance exports and imports. For some nations it contributes up to 5 percent of GDP. Consequentially, any change in the price of cotton has high repercussions in such different countries as Nigeria, Zimbabwe, Pakistan, India or Turkmenistan (see Baffles (2004)). Even if not all these countries irrigate cotton, irrigation need changes in other regions can have dire impacts on the commodity price.

Of the main cotton producing areas in the world, irrigation plays a major role in California Central Valley, Northern Texas, the Mississippi Valley, Georgia, Greece, Southern Turkey, the Nile Valley, Central Asia (Turkmenistan, Uzbekistan, Tajikistan and Kyrgyzstan), the Indus Zalley and Eastern China.

On the next two pages we successively present the change in irrigation need (or water deficit) for irrigated cotton under first an Unconstrained Emissions scenario and second a Level 2 Stabilization scenario. On both pages, the first figure represents the absolute change in mm and the second figure the relative change in percent. For this second figure, the values have been limited to a range of -50% to +50%. Indeed very large values of relative change occur only on wet areas where the irrigation need is very close to zero. In some areas like California or Central Asia, the absolute change is more significant than the relative change as the irrigation need is already high (more than 500 mm per year).

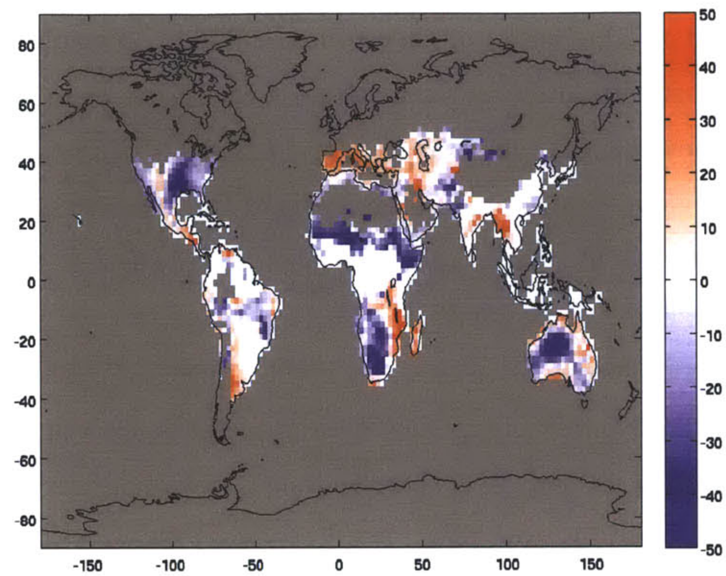

Figure 4-13: CLM-AG water deficit for irrigated cotton – absolute difference (in mm) between the 2040-2049 Unconstrained Emission scenario average and the 1990-1999 average.

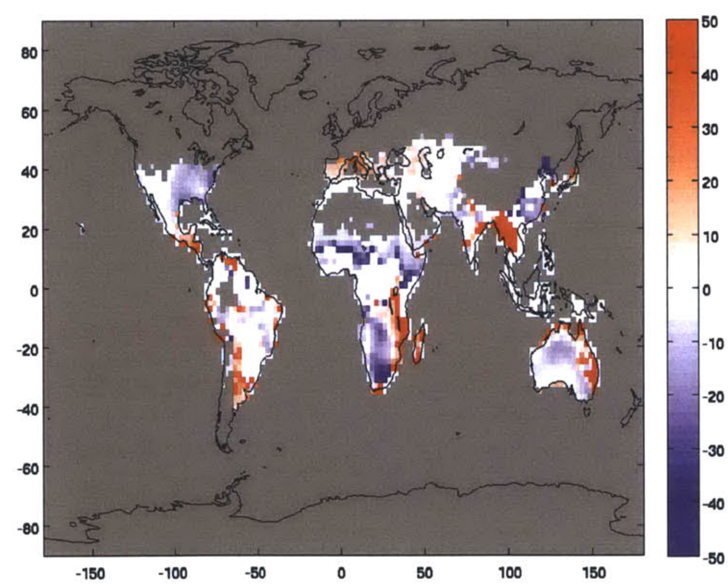

Figure 4-14: CLM-AG water deficit for irrigated cotton – relative difference (in percent) between the 2040-2049 Unconstrained Emission scenario average and the 1990-1999 average.

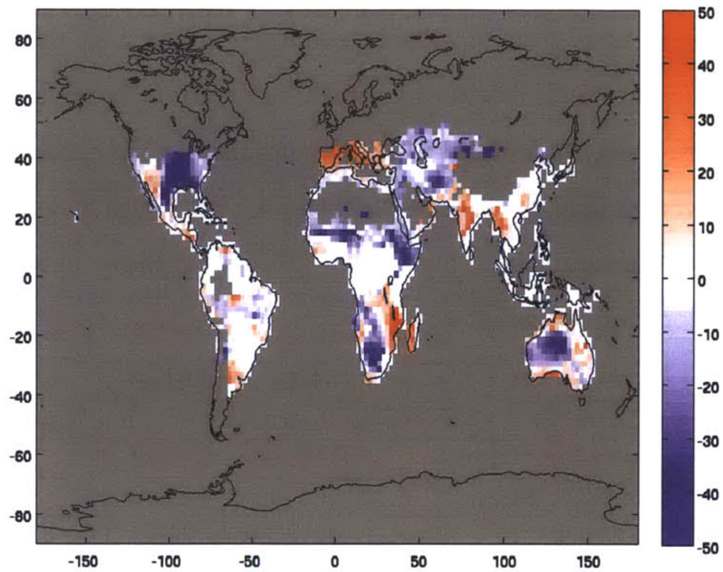

Figure 4-15: CLM-AG water deficit for irrigated cotton – absolute difference (in mm) between the 2040-2049 Level 2 Stabilization scenario average and the 1990-1999 average.

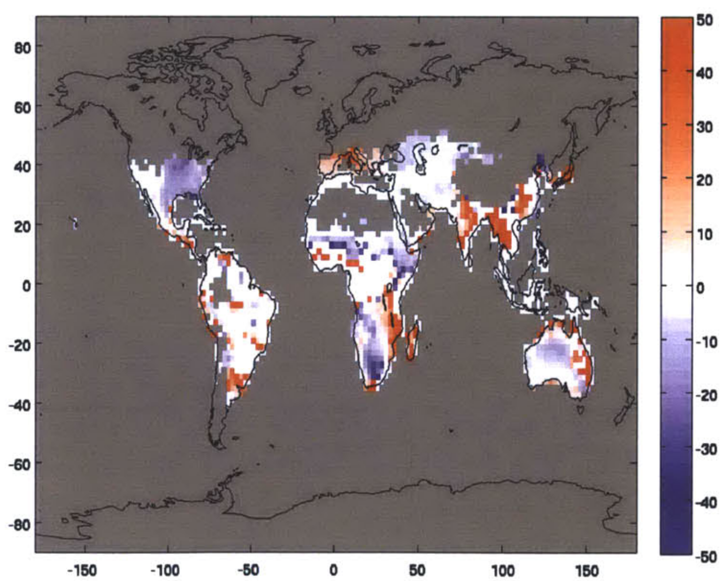

Figure 4-16: CLM-AG water deficit for irrigated cotton – relative difference (in percent) between the 2040-2049 Level 2 Stabilization scenario average and the 1990-1999 average.

Overall, the irrigation change patterns for cotton mirror those of maize. Slight differences exist in some areas as growing seasons can differ between the two crops. Although the relative change is lower than for corn, the absolute change is not as cotton is usually grown in drier areas. Even if a decrease of 20 mm of water need in California appears small compared to the average irrigation need of 500 to 700 mm, it still makes a significant difference for stressed water resources. The Tables 4.7 and 4.8 below summarize the changes for each of the major growing areas.

Area	Observed Change
California	Slight decrease of 10 to 20 mm
Texas and Mississippi	Decrease of about 10%
Georgia (US)	Decrease of about 5%
Greece	Increase of about 5%
Turkey	Increase of about 5%
Nile Valley	Decrease of about 5%
Central Asia	Very slight decrease of 5 to 10 mm
Indus Valley	5 to 10% decrease
Eastern China	No change

Table 4.7: Irrigation need changes between 2050 and 2000 under a UCE scenario for the major cotton producing regions where irrigation is present.

Area	Observed Change
California	Slight decrease of 5 to 10 mm
Texas and Mississippi	Decrease of about 15%
Georgia (US)	Decrease of about 15%
Greece	Increase of about 5%
Turkey	Decrease of about 5%
Nile Valley	No change
Central Asia	Decrease of 20 to 30 mm
Indus Valley	Increase of about 5%
Eastern China	No change

Table 4.8: Irrigation need changes between 2050 and 2000 under a L2S scenario for the major cotton producing regions where irrigation is present.

To better show the effects of implementing a Level 2 Stabilization policy, we map the absolute and relative differences between irrigation under the UCE and L2S scenarios in 2050.

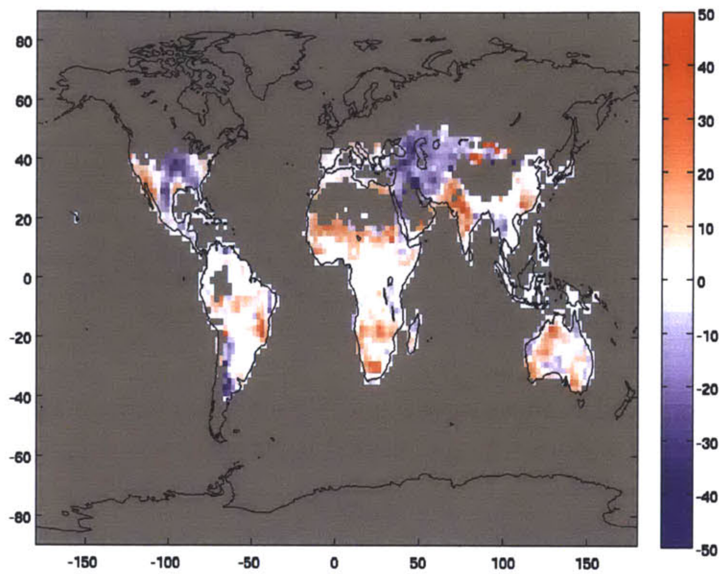

Figure 4-17: CLM-AG water deficit for irrigated cotton – absolute difference (in mm) between the 2040-2049 Level 2 Stabilization scenario average and the 2040-2049 Unconstrained Emission scenario average.

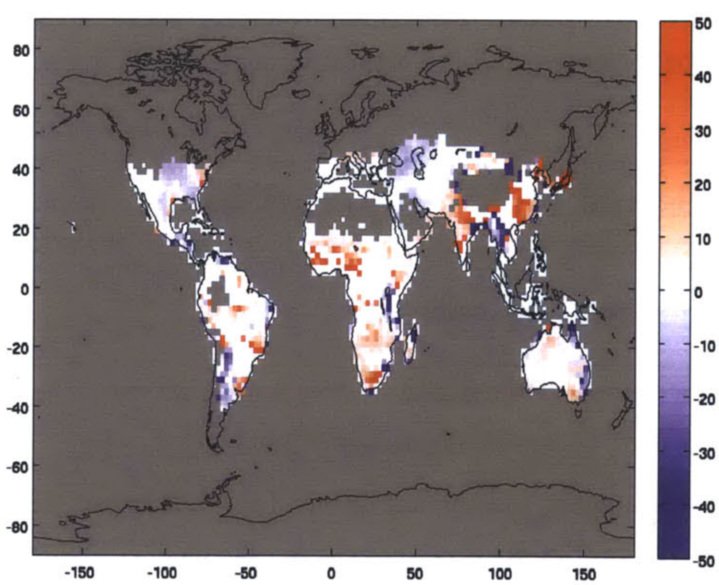

Figure 4-18: CLM-AG water deficit for irrigated cotton – relative difference (in percent) between the 2040-2049 Level 2 Stabilization scenario average and the 2040-2049 Unconstrained Emission scenario average.

Area	Observed Change
California	Increase of about 10 mm
Texas and Mississippi	Decrease of about 5%
Georgia (US)	Decrease of about 10%
Greece	No change
Turkey	Decrease of about 5 to 10%
Nile Valley	5% increase
Central Asia	20 to 25 mm decrease
Indus Valley	5 to 10% increase
Eastern China	No change

Table 4.9: Irrigation need changes between 2050 and 2000 under a L2S scenario for the major cotton producing regions where irrigation is present.

Here again, the picture differs from region to region and mitigating climate change does not always have a positive impact on cotton water deficit. Besides Turkey and Central Asia where an actual mitigation of negative effects of climate change happens (in the case of Turkey even reversing from an increase to a decrease in irrigation need) and the South-Eastern US where a mitigation strategy brings a larger decrease in water deficit than in an Unconstrained Emissions scenario, the other areas see an increase in water deficit under a Level 2 Stabilization scenario compared with an Unconstrained Emissions scenario.

4.3 Analysis and Policy Implications

4.3.1 Main Findings and Analysis

Independently from the crop-by-crop area-by-area results, we review here general findings from the IGSM-CAM CLM-AG study presented above.

First, the analysis suggests that climate change has a real impact on irrigation need of vital crops. Some of these changes may contradict the common intuition that irrigation demand increases in a warmer climate, as climate change appears beneficial to some areas, at least from a crop water-stress point of view.

Second, these changes are not global but vary significantly among regions. On the one hand, North America and Sub-Saharan Africa see their water deficit decrease under climate change. On the other hand, Europe and Southern Africa become drier and water needs increase.

Third, implementing a mitigation policy (such as a global limitation of greenhouse gases to 660 ppm CO_2 equivalent in this case) may create unintended effects. If such a policy effectively mitigates the harmful effects of climate change in some areas (most notably Central Asia), it reinforces water stress impacts overall. Indeed precipitation increase is globally larger under an Unconstrained Emissions scenario than under a mitigation scenario. One notable area profiting from climate change is the U.S. Midwest where a larger increase of precipitations under the L2S scenario results in a dramatically decreased irrigation need.

Fourth, there are some notable differences between crops. While the model shows rainfed spring wheat crops barely affected by climate change in the Zambezi Valley, irrigated cotton or maize – grown at a different time of the year – see their irrigation need increase significantly.

4.3.2 Limitations of the Study

As outlined in the chapter introduction, this study shows the impacts of climate change on irrigation need or rainfed yield *in the absence of adaptation* and *under one particular climate model*. The rest of this section explores these two main limitations of this study.

Adaptation

As outlined in Smit and Skinner (2002), farmers have many adaptations techniques available to reduce the impact of climate change on crop production. The most relevant for mitigating the impacts of climate change on irrigation (or taking profit of it in the case of a better climate for crops) are changing the timing of planting and harvesting, changing the crop varietal planted on-farm or even changing the crop grown in an area itself[3]. For example, during the exceptional drought of the 2000s, Australia's Murray River Valley shifted irrigation water from paddy rice culture towards orchards and grapes, preserving

[3]Cassava for example requires less water than maize and could be a replacement for drought stricken areas.

the economic output of the area despite historically low precipitations. Hence, the major cultivated areas identified in the analysis above could become secondary growing areas for the considered commodity. On the other hand as warming makes more land suitable for agriculture (especially in the northernmost latitudes), new growing areas could emerge where it was unthinkable before.

Despite these general observations, adaptation is difficult to predict accurately as it relies partly on management practices and farming decisions as well as on macroeconomic factors such as commodity prices and national GDP. As a consequence, even if modeled predictions of irrigation need for a specific crop were perfectly accurate, forecasting the exact repartition of the crops grown and their characteristics in 2050 is not possible.

The analysis we carry out in this chapter (as well as in the next one) is an analysis of agriculture *as is*. It describes the impacts of climate change on the current agricultural system and subsequent effects should this system stay static. If it does not predict the future, it gives valuable insights on potential new stresses and their effects on agriculture.

Modeling

The climate model itself is a substantial uncertainty in this study. All climate models predict an atmospheric warming if greenhouse gases concentrations rise, however there is little agreement in impacts on precipitation (Randall *et al.*, 2007). Figure 4-19 from the IPCC Fourth Assessment Report (AR4) shows how models do compare[4]. White represents places where less than two thirds of the models agree on *the sign of* precipitation change. Notable areas where disagreements exist include Southern Africa in winter and Northern America and Central Asia in summer. On the other hand, stippled areas show where more than 90% of the model agree. A notable example is a sharp drying of the Mediterranean area.

As the models exhibit large differences in future precipitation, there is a wide uncertainty on the measures of water-stress presented in this chapter. There is little agreement on methods to reduce this uncertainty in regional precipitation patterns and there is no telling whether IGSM-CAM is closer to what would be a true prediction than other models.

Further, we are using for this study a median climate sensitivity parameters but, as

[4]There are a total of 19 models in this AR4 comparison.

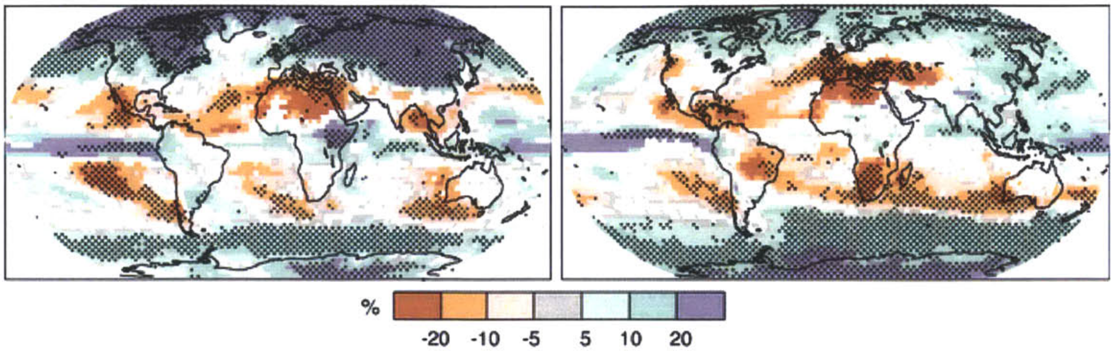

Figure 4-19: Relative changes in precipitation (in percent) for the period 2090-2099, relative to 1980-1999. Values are multi-model averages based on the SRES A1B scenario for December to February (left) and June to August (right). White areas are where less than 66% of the models agree in the sign of the change and stippled areas are where more than 90% of the models agree in the sign of the change. Figure 3-3 in IPCC (2007).

described in Forest *et al.* (2002) there is a wide uncertainty in these parameters. There is no certainty that the median case is the one that will occur in the future.

To address some of these modeling limitations,the next chapter presents a technique based on a statistical sampling of both parameters uncertainty (based on Sokolov *et al.* (2009)) and climate model regional uncertainty (based on Schlosser *et al.* (2011)) to quantify regional irrigation need uncertainty stemming from climate models uncertainty.

Chapter 5

Climate Change Uncertainty: a Regional Study in the Zambezi River Valley

This chapter describes a technique to reveal climate change uncertainty and its impact on irrigation. Using the IGSM framework we derive a distribution of the expected impact of two policy scenarios – an Unconstrained Emissions scenario and a Level 1 Stabilization scenario – on climate change in Central Zambia and the subsequent impact on irrigation need and crop production. We finally discuss the underlying uncertainty, what it implies for policy making and how to best use this new tool.

5.1 Motivation and Model

5.1.1 Central Zambia in the Zambezi River Valley

The Central Province is one of the most important agricultural provinces in Zambia. The area is characterized by a strong rainy season during the summer months between October and March when the Inter-Tropical Convergence Zone moves over Southern Africa from North to South. Heavy precipitation is followed by dry weather during the winter months. The dry season provides a substantial decrease in soil moisture compared with the rainy season. Zambian agriculture features both irrigated and rainfed crops. Some crops are grown during winter (dry season), others during summer (rainy season). This study features irrigated maize, as it is the most important crop for the country (see Banda (2011)) and irrigated cotton, an important cash crop. To compare rainy season and dry season dynamics, the study also considers rainfed spring wheat[1].

Figure 5-1 shows a map of the Zambezi River Valley and highlights the area chosen for this study.

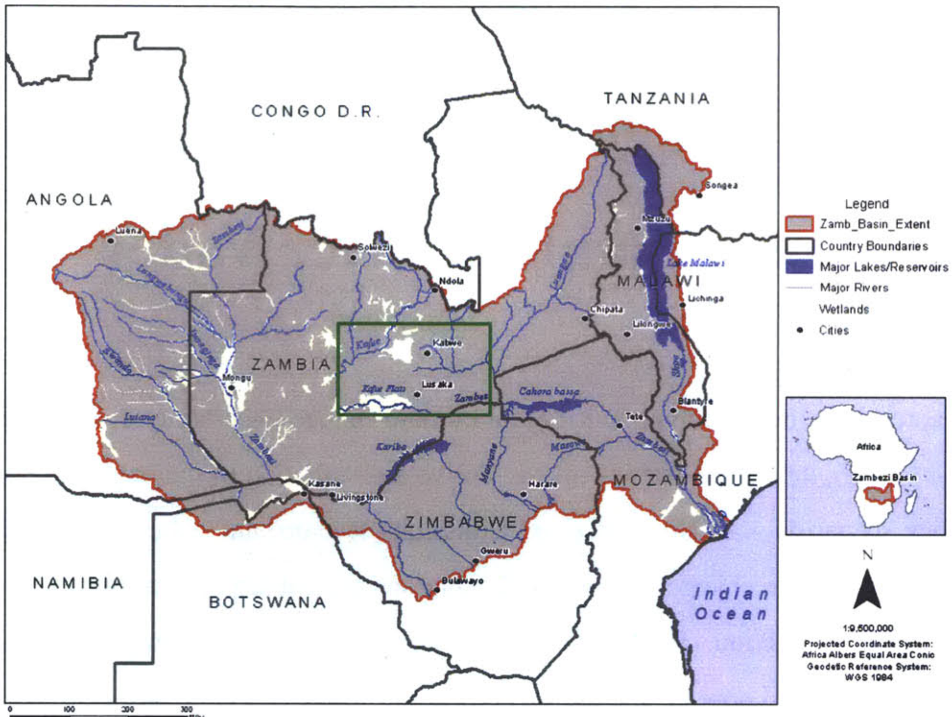

Figure 5-1: Map of the Zambezi River Valley. This study examines the area contoured in green, approximately covering Zambia's Central Province.

5.1.2 Climate Data and Uncertainty Quantification

As outlined in previous chapters, different climate models lead to varying results for change in precipitation. Furthermore, the uncertainty in climate sensitivity and other key parameters can lead to varying results in temperature and precipitation change for any single model. To take into account these two types of uncertainties, Schlosser *et al.* (2011) combined the MIT IGSM framework with a Hybridized Frequency Distribution (HFD) approach. This approach is presented in this section.

[1]Contrary to maize and cotton, wheat is planted in late February and grows mostly during the dry season.

IGSM-EPPA ensemble run

As described in Forest *et al.* (2002) and Sokolov *et al.* (2009), it is difficult to estimate key climate parameters (climate sensitivity (S), rate of ocean heat uptake (K_v) and aerosol forcing (F_{aer}) from historic records. At best one can generate an estimation of a probability distribution of these parameters: Figure 5-2 represents, for example, the probability space of the marginal probability distribution of the climate sensitivity and of the rate of ocean heat uptake, holding the aerosol forcing constant as a constant. An ensemble of (S, K_v, F_{aer}) vectors sampling this distribution is built using these probabilities. The exact process used to carry out this sampling is explained in further detail in Sokolov *et al.* (2009). The sample chosen is a 400 ensemble of these three parameters consistent with historic records (the red dots in Figure 5-2 represent the S and K_v values in the ensemble).

To investigate the impact of climate policies on crop water stress, two scenarios on the Emission Prediction and Policy Analysis (EPPA, Paltsev *et al.* (2005)) model have been run: one Unconstrained Emissions (UCE) scenario and a Level 1 Stabilization (L1S) scenario that limits greenhouse gases concentration to 550 ppm CO_2 equivalent by the end of the century[2]. The emissions of the different gases obtained in EPPA are then used as an input into the IGSM 2-D model (Sokolov *et al.*, 2005) which is run with each of the 400 (S, K_v, F_{aer}) parametrizations for these two scenarios globally.

Hybrid Frequency Distribution

After these steps a 400-member ensemble of zonal averages of monthly changes in temperature, precipitations, pressure, humidity and wind (at a four degree of latitude resolution) was produced for each scenario. The IGSM is a 2-D model in altitude and latitude but this study requires regional results in longitude as well. A method to downscale the zonal results to local results (on a two by two degrees grid) is to project these changes to a 3-D grid using available outputs from the AR4 AOGCMs (Atmospheric and Oceanic Global Climate Models). Technique and validation are explained in detail in Schlosser *et al.* (2011); but a brief summary follows below.

[2]This is the most stringent proposed climate policy and the one that limits global warming to 2 degrees from pre-industrial levels under the average of the IPCC AR4 models.

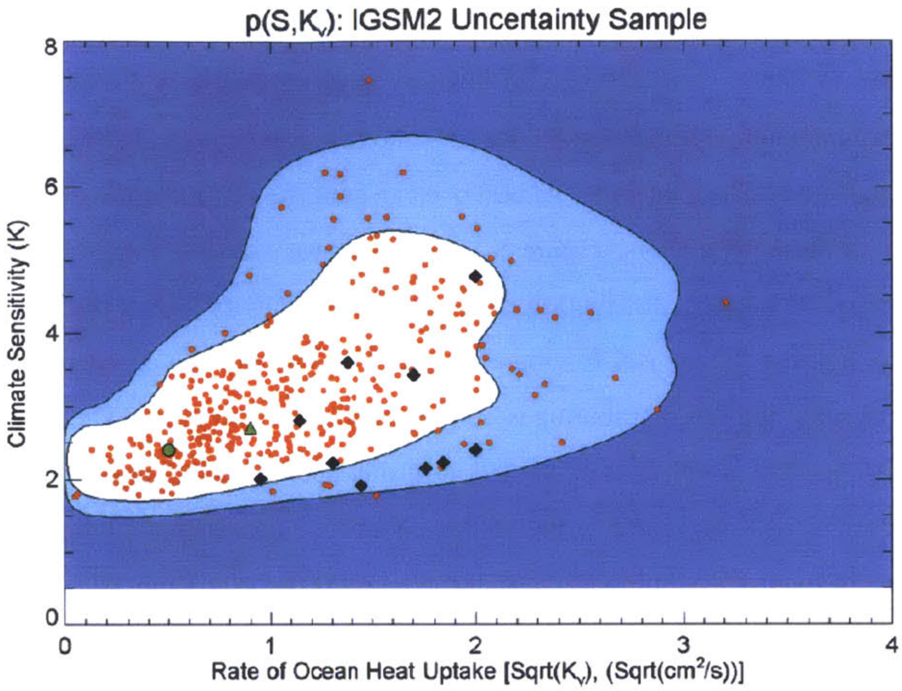

Figure 5-2: Probability space of the climate sensitivity (K) and ocean heat uptake (K_v). The shading and thick contours denote rejection regions for significance levels of 10% and 1%, respectively. Green circle and triangle indicate the mode and the median of the distribution, respectively. Black diamonds indicate values of the parameters of the MIT IGSM climate model needed to represent the behavior of different AR4 GCM models. Red dots represent a 400 hundred ensemble obtained by a Bayesian estimate. *Reproduced form Sokolov et al. (2009) with the permission of the MIT Joint Program on the Science and Policy of Global Change.*

Figure 5-3 describes the technique. For each of the two values of interest (average temperature and total precipitation) the IGSM produces a monthly average value for the latitude band $\overline{V_y}$. To obtain the gridcell value of latitude-longitude coordinate this value is multiplied by a coefficient $C_{V,m,x,y}$ depending on the variable V, the month m, the latitude y and the longitude x such that:

$$V_{x,y} = C_{V,m,x,y} \cdot \overline{V_y}$$

where $V_{x,y}$ is the variable of interest in the gridcell (x,y), $C_{V,m,x,y}$ is the transformation coefficient and $\overline{V_y}$ is the zonal average of the variable of interest over the latitude band y.

The approach postulates that the local change in relevant climate parameters (tempera-

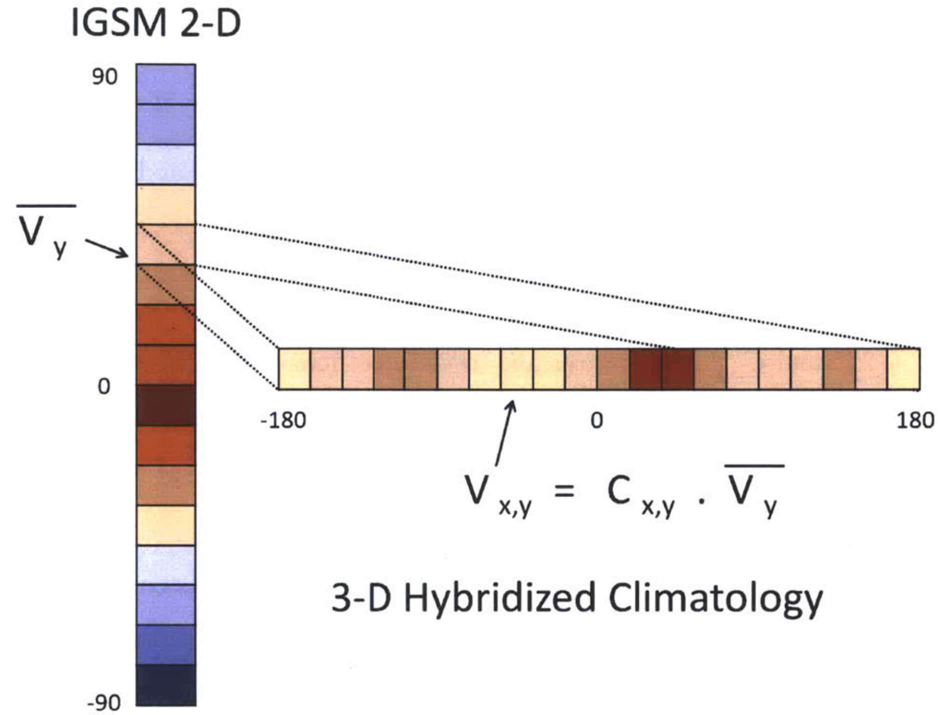

Figure 5-3: Schematic of the hybridization technique described in Schlosser *et al.* (2011).

ture and precipitation) can be associated with anthropogenic global change in temperature. The $C_{V,m,x,y}$ coefficients were calculated using a first-order Taylor expansion:

$$C_{V,m,x,y}(\Delta T_{Global}) = C^{hist}_{V,m,x,y} + \frac{dC_{V,m,x,y}}{dT_{Global}} \cdot \Delta T_{Global}$$

where T_{Global} is the average monthly global temperature, ΔT_{Global} its variation from the historic value and the other variables are defined as follows:

The historic coefficients $C^{hist}_{V,m,x,y}$ were calculated using the Climate Research Unit dataset (CRU, New *et al.* (1999)) for temperature and the Global Precipitation Climatology Project (GPCP, Adler *et al.* (2003)) for precipitations. For temperature for example, the historic coefficient for the month m is[3]:

$$C^{hist}_{T,m,x,y} = \frac{T^{CRU}_{x,y}(m)}{\overline{T^{CRU}_{y}(m)}}$$

For precipitation, it is:

[3]For this study, the values of $T^{CRU}_{x,y}(m)$ are averages for the given month over the years 2000 - 2010

$$C^{hist}_{P,x,y} = \frac{P^{GPCP}_{x,y}}{\overline{P^{GPCP}_{y}}}$$

The climate shift coefficient $\frac{dC_{V,x,y}}{dT_{Global}}$ is defined for each AOGCM and each variable as:

$$\frac{dC_{V,x,y}}{dT_{Global}} = \frac{C^{2075}_{V,x,y} - C^{hist}_{V,x,y}}{T^{2075}_{Global} - T^{hist}_{Global}}$$

where $C^{2075}_{x,y}$ and $C^{hist}_{x,y}$ are the average model coefficients for 2070 - 2080 and 2000 - 2010 respectively and T^{2075}_{Global} and T^{hist}_{Global} are the average temperatures of the model for 2070 - 2080 and 2000 - 2010 respectively. Thus ΔT_{Global} of the IGSM is calculated using a 2000 - 2010 base.

This technique was used to create, for each of the 17 AR4 models considered and each of the 400 runs of the IGSM ensemble described in the previous section, a monthly ΔT and ΔP. This constitutes a total of 6800 runs for each scenario. As using all of these cases in CLM-AG would be too time-consuming, a method has been developed to reduce the set while preserving the observed distribution.

Gaussian Quadrature

The challenge of preserving the distribution of irrigation need is that the final distribution cannot be observed. The goal is thus to select relevant variables whose distributions need to be conserved. A Gaussian Quadrature method was used to sample the distribution (Arndt, 1996; Arndt *et al.*, 2006). This method supposes that substantial information inherent in the distribution of climate outcomes can be summarized in a limited number of variables.

We use the specific dataset developed in Arndt *et al.* (2012) for a study of the Zambezi River Basin under climate change. This dataset has been developed to preserve the distributions of six distinct variables over two areas (Western and Eastern Zambezi). The six variable are:

- Maximum monthly precipitation in 2050
- Maximum monthly change in temperature in 2030
- Maximum monthly change in temperature in 2050

- Climate Moisture Index[4] in 2030

- Climate Moisture Index in 2050

- Standard deviation of the change in seasonal precipitation in 2050

This selection of variable allows the new distribution to conserve the moments (mean, variance and skewness) of the significant variables for irrigation in particular. Subsection 5.2.1 presents the temperature and rain distributions for the two scenarios (UCE and L1S) after the Gaussian Quadrature sampling.

Generation of Hourly Data

After the reduction of the ensemble using the Gaussian Quadrature, the UCE and L1S sets were each populated with approximately 400 climatologies for the Zambezi River Valley, with monthly temperature and precipitation variations from the historic climate (1990-2000). However CLM-AG requires hourly data to run.

The NCEP/NCAR corrected by CRU dataset (NCC, Ngo-Duc *et al.* (2005)) is the basis for this temporal downscaling. We use historical NCC data for all variables but temperature and precipitations (arguably the most important to agriculture). Bootstrapping is not a relevant option here as it could lead to large physical impossibilities[5] so historical time series are reproduced. To account for temperature change in the future, the time series is modified as:

$$T^{CLM}_{2040+y}(t) = T^{NCC}_{1980+y}(t) + \Delta T^{IGSM}(month)$$

where $T^{CLM}_{2040+y}(t)$ is the temperature created for CLM-AG in year $2040+y$ and at instant t, $T^{NCC}_{1980+y}(t)$ is the historic temperature from NCC in year $1980 + y$ and at instant t and $\Delta T^{IGSM}(month)$ is the monthly temperature difference calculated by the IGSM for the month and year t belongs to.

[4]The Climate Moisture Index is defined in Willmott and Feddema (1992) and measures the climate aridity of an area. It is calculated as a function of the ratio of precipitation to potential evapotranspiration. CMI ranges from -1 to +1, where -1 is very dry and +1 is very humid.

[5]Weather parameters are somewhat correlated with each other (rain and temperature for example) and temporally (a large jump in temperature or humidity in six hours is very improbable).

Precipitation change form the historic average[6] is outputed by the IGSM as a monthly total, but it has to be distributed during the month. However it would not make sense to distribute it over all time steps. Therefore, it is distributed proportionally to the intensity of the events in the historic NCC month. Mathematically:

$$P^{CLM}_{2040+y}(t) = P^{NCC}_{1980+y}(t) + \frac{\Delta P^{IGSM}(month)}{\sum_{month} P^{NCC}_{1980+y}(t)}$$

where $P^{CLM}_{2040+y}(t)$ is the precipitation (in mm) created for CLM-AG in year $2040 + y$ and at instant t, $P^{NCC}_{1980+y}(t)$ is the historic precipitation (in mm) from NCC in year $1980 + y$ and at instant t and $\Delta P^{IGSM}(month)$ is the precipitation (in mm) calculated by the IGSM for the month and year t belongs to.

Two 400-climates ensembles of regional temperature and precipitations that preserve the moments of the distributions of relevant outcome variables of the 6800-climates IGSM-HFD ensembles are built using this method (one for a UCE and one for a L1S scenario).

5.1.3 Crop Data

The crop data used in this study is the same as in previous chapters (see Section 3.3.1 and 4.1.2). In Zambia, according to GAEZ (Fischer *et al.*, 2012), both maize and cotton are planted in late July to be grown and harvested during the early rainy season while spring wheat is planted in late February at the end of the rainy season and grows on moisture accumulated in the soil. As spring wheat planted in February is harvested before the end of June and maize planted in July is harvested before the end of December, these two crops can be planted in a rotation on the same field. Cotton has a longer growing season and is harvested at the end of January or beginning of February.

5.2 Results

This section presents the results of the analysis for central Zambia. It first shows the evolution of temperature and precipitation by 2050, then it shows the change over time of

[6]This historic average is calculated over 2000 - 2010.

irrigation need for maize and cotton, and finally the yield for rainfed spring wheat.

5.2.1 Distribution of Temperatures and Precipitations

For temperature and precipitation, we plot on the same graph the distribution of the change in decadal average by 2040-2050 for the two scenarios (UCE in blue and L1S in green) as well as the historic variability (in red). The historic variability distributions are built by considering all realizations of either temperature or precipitation differences to the average over the years 1961-2000, each year being one point in the distribution.

Temperature Change

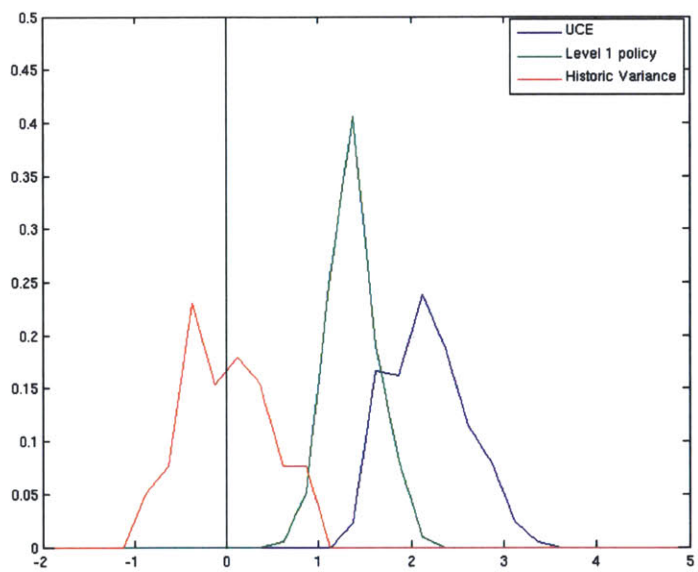

Figure 5-4: Probability function of the distribution of annual average temperature change (in degrees C) in the Central Province of Zambia. The zero line represents the historic average, while the red line represents the historic variability over 1960-2000. The blue and green lines represent, respectively, the UCE and L1S distributions of the change of the average irrigation need by 2040-2060 from 1960-2000 using the Gaussian Quadrature sample of the IGSM climate ensembles.

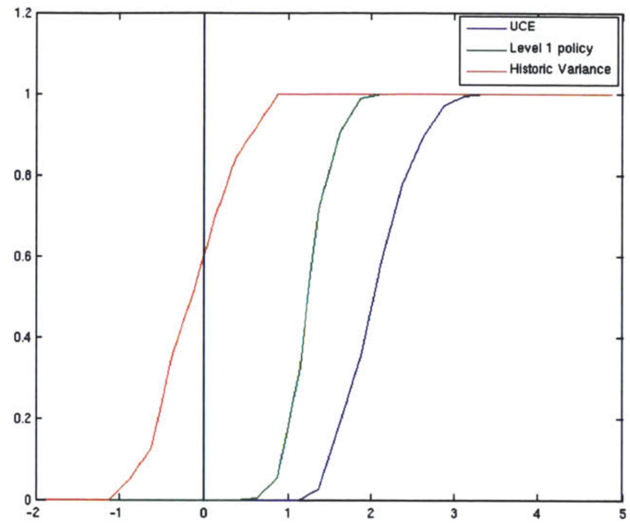

Figure 5-5: Cumulative probability function of the distribution of annual average temperature change (in degrees C) in the Central Province of Zambia. The zero line represents the historic average, while the red line represents the historic variability over 1960-2000. The blue and green lines represent, respectively, the UCE and L1S distributions of the change of the average irrigation need by 2040-2060 from 1960-2000 using the Gaussian Quadrature sample of the IGSM climate ensembles.

Temperature change is the most recognizable and best accepted signal of climate change. The Central Province of Zambia undergoes an average temperature rise of 1.3 degrees Celsius under a L1S scenario and of 2.3 degrees Celcius under a UCE scenario by 2050 across the hybridized frequency distribution of potential future climates as simulated by the IGSM. This is a very significant change as the decadal *average temperature* is very likely to exceed the warmest year on record from 1960-2000 in both scenarios (90% chance under a L1S scenario and 100% chance under the UCE scenario). Almost certainly, more than half of the years in the 2040-2050 decade will see a higher average temperature than the historic record between 1960 and 2000. Under a UCE scenario, the average temperature could be as high as three degrees Celsius warmer than what it was in 1960-2000. This change is likely to have significant direct impacts on human activities in itself. However, these are not the focus of this work.

Precipitation Change

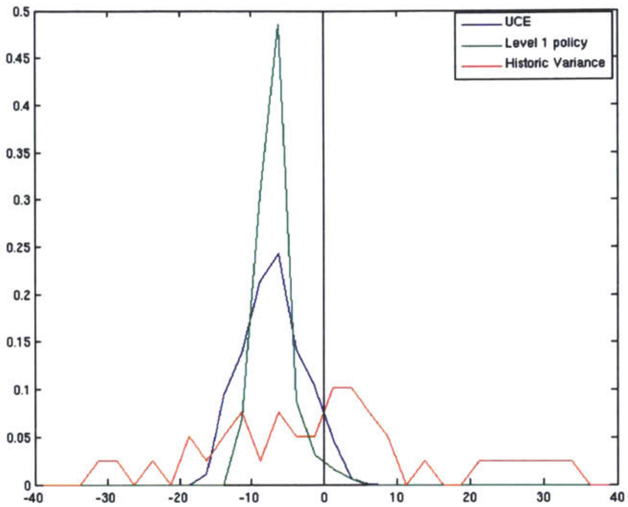

Figure 5-6: Probability function of the distribution of annual precipitation change (in percent) in the Central Province of Zambia. The zero line represents the historic average, while the red line represents the historic variability over 1960-2000. The blue and green lines represent, respectively, the UCE and L1S distributions of the change of the average irrigation need by 2040-2060 from 1960-2000 using the Gaussian Quadrature sample of the IGSM climate ensembles.

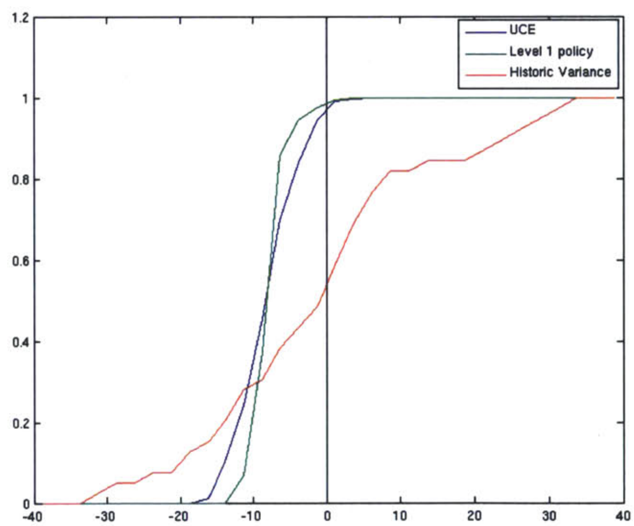

Figure 5-7: Cumulative probability function of the distribution of annual precipitation change (in percent) in the Central Province of Zambia. The zero line represents the historic average, while the red line represents the historic variability over 1960-2000. The blue and green lines represent, respectively, the UCE and L1S distributions of the change of the average irrigation need by 2040-2060 from 1960-2000 using the Gaussian Quadrature sample of the IGSM climate ensembles.

The average historic precipitation rate for central Zambia is 975 mm per year. Both the UCE and L1S scenarios lead to an average decrease in rainfall by about 7%. However, the distributions vary. If under a L1S scenario, 90% of the distribution of potential change is between 5 and 10% decrease, the distribution for the UCE is more spread out with a greater chance of both a larger than 10% decrease in precipitation and a greater chance of a smaller than 5% change. 40% of the runs show indeed an decrease of more than 10% and 20% of the runs show a decrease of less than 5% in precipitations.

This average change has consequences for extreme events. Indeed in the past, the ten-year drought meant that the country would get 20% less water than on an average year. If climate change decreases this average precipitation value by 7% (which is approximately the mean of the distribution for both scenarios), what was previously the one-in-ten-year drought will mechanically happen more often. If we suppose that every year sees a diminution of 7% of its precipitation, the distribution of the variability around the average total precipitation stays the same but it is shifted towards a dryer climate. What used to be the ten-year drought occurs now every three years on average. This is a notable change and we explain more in detail in Section 5.3.2 below what it means for public perception and policy making.

Notwithstanding exceptional events, rain falls during the rainy season (from October to March). To get a more precise picture we plot in Figures 5-8 and 5-9 the distributions of simulated precipitation change over the early rainy season (October - November - December) and over the late rainy season (January - February - March) respectively. Historically, the early rainy season saw an average of 377 mm of rain and the late rainy season an average of 588 mm.

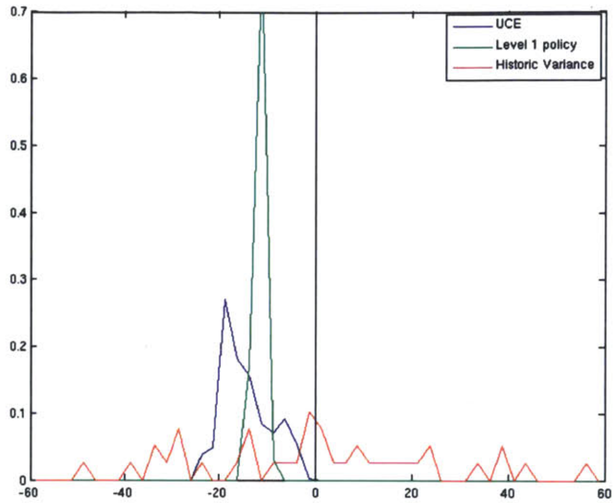

Figure 5-8: Probability function of the distribution of early rainy season (October - November - December) precipitation change (in percent) in the Central Province of Zambia. The zero line represents the historic average, while the red line represents the historic variability over 1960-2000. The blue and green lines represent, respectively, the UCE and L1S distributions of the change of the average irrigation need by 2040-2060 from 1960-2000 using the Gaussian Quadrature sample of the IGSM climate ensembles.

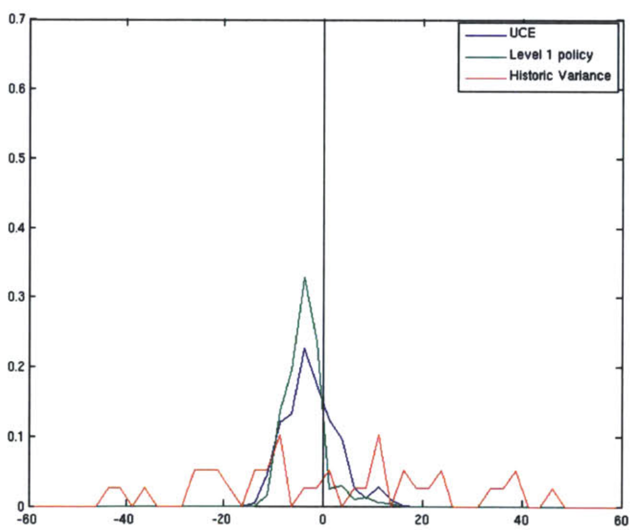

Figure 5-9: Probability function of the distribution of late rainy season (January - February - March) precipitation change (in percent) in the Central Province of Zambia. The zero line represents the historic average, while the red line represents the historic variability over 1960-2000. The blue and green lines represent, respectively, the UCE and L1S distributions of the change of the average irrigation need by 2040-2060 from 1960-2000 using the Gaussian Quadrature sample of the IGSM climate ensembles.

While the historic variability in precipitation was approximately the same for both halves of the rainy season, the impact of climate change is markedly different. On the one hand in the early rainy season, the ten-year average total rainfall decreases by 14.5% for the UCE and by 12% for the L1S scenario, which constitutes a very large decrease compared with the historic variability. On the other hand, the total rainfall in January-February-March decreases by only 2.3 and 3.9% for UCE and L1S, respectively (with a very significant probability of a precipitation increase under the UCE scenario). Consequently, patterns of change in water stress are likely to be different for early season crops (like maize and cotton) compared with late season crops (like spring wheat).

5.2.2 Irrigation Need for Maize

We present here the results of the uncertainty run for irrigated maize. In Zambia, maize is planted at the end of July and has a growing season of about four and a half months. Figures 5-10 and 5-11 below present the probability distribution and the cumulative probability distribution, respectively, of the average irrigation need change by the middle of the century. The historic variability, being much larger than the expected change, is not plotted on the following figures.

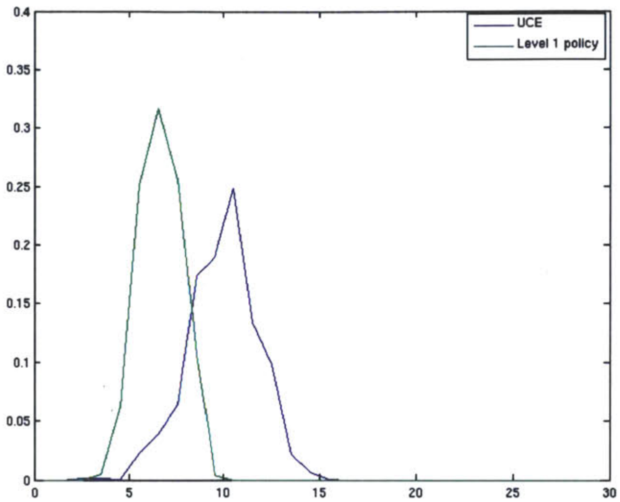

Figure 5-10: Probability function of the distribution of irrigation need change (in percent) in the Central Province of Zambia for maize. The zero line represents the historic average. The blue and green lines represent, respectively ,the UCE and L1S distributions of the change of the average irrigation need by 2040-2060 from 1960-2000 as calculated by CLM-AG using the Gaussian Quadrature sample of the IGSM climate ensembles.

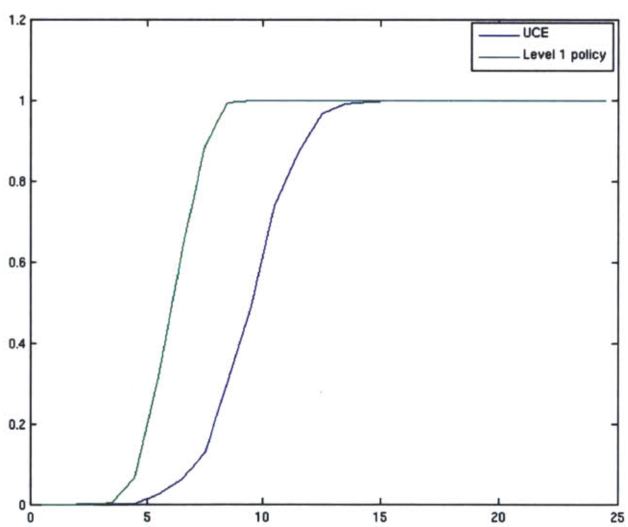

Figure 5-11: Cumulative probability function of the distribution of irrigation need change (in percent) in the Central Province of Zambia for maize. The zero line represents the historic average. The blue and green lines represent, respectively ,the UCE and L1S distributions of the change of the average irrigation need by 2040-2060 from 1960-2000 as calculated by CLM-AG using the Gaussian Quadrature sample of the IGSM climate ensembles.

There is a clear increase in the irrigation need for maize under both scenarios. The distribution for the UCE scenario presents an average 9.9 % increase and the L1S scenario an average 6.6% increase. The spread of the distribution is larger for the UCE scenario than L1S scenario with values up to a 15% increase in water deficit.

Further analysis of the historic run shows that the historic ten-year drought leads to an increased irrigation need of 20% compared to an average year. Using the historic variability distribution (not pictured here), it is possible to deduce how often this statistical ten-year drought would occur under a changed climate (still considering that the distribution of the year-to-year variability does not change). This is done by shifting the historic variability distribution by the average change calculated, and observing the new statistical probability of the value of the one-in-ten-year historic drought.

Under an average UCE scenario – which would increase the average irrigation need by 9.9% – this statistical ten-year drought would now occur every three years, notwithstanding the fact that extreme droughts would also become more intense as the average irrigation need increases. Under an average L1S scenario (featuring an irrigation need increase of 6.6%), the ten-year drought would now statistically occur every five years. Other values in the distribution would lead to a difference in the future frequency of the historic ten-year drought, with dramatic effects if the worst outcomes are realized.

5.2.3 Water-Stress Yield Reduction for Wheat

We present here the results of the uncertainty runs for rainfed spring wheat. In central Zambia, wheat is planted at the end of February and has a growing season of about three months. Figures 5-12 and 5-13 below present the probability distribution and the cumulative probability distribution, respectively, of the average change in yield by the middle of the century. The yield change we refer to here is only due to water stress change under climate change. It does not incorporate any management change or adaptation policies. The historic variability, being much larger than the expected change, is not plotted on the following figures.

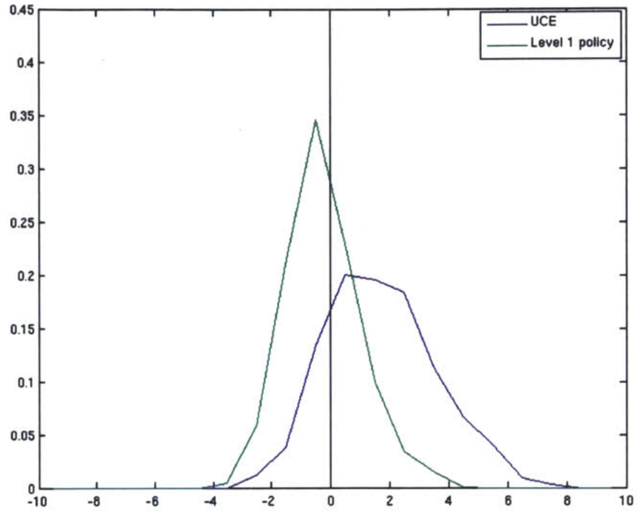

Figure 5-12: Cumulative probability function of the distribution of yield change (in percent) due to water-stress in the Central Province of Zambia for wheat. The zero line represents the historic average, while the red line represents the historic variability over 1960-2000. The blue and green lines represent, respectively, the UCE and L1S distributions of the average yield change due to water-stress by 2040-2060 from 1960-2000 as calculated by CLM-AG using a Gaussian Quadrature sample of the IGSM ensembles.

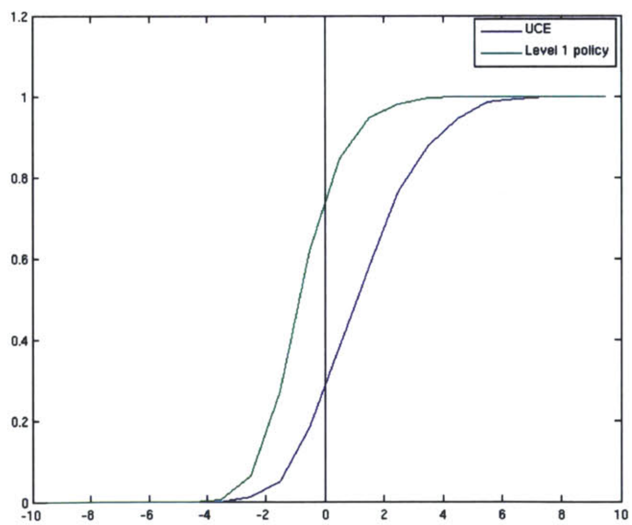

Figure 5-13: Cumulative probability function of the distribution of yield change (in percent) due to water-stress in the Central Province of Zambia for wheat. The zero line represents the historic average, while the red line represents the historic variability over 1960-2000. The blue and green lines represent, respectively, the UCE and L1S distributions of the average yield change due to water-stress by 2040-2060 from 1960-2000 as calculated by CLM-AG using a Gaussian Quadrature sample of the IGSM ensembles.

The results for wheat are notably different from those for maize. Under a UCE scenario, the average change on wheat yield as taken from the distribution shows an increase of 1.7% in yield, while the L1S average scenario presents an average yield decrease of 0.2%. These positive results are likely due to the fact that changes in precipitation are smaller for the late rainy season – when spring wheat starts to be grown – than for the early rainy season – when maize is grown.

In fact, if one considers only the average change in crop yields one could think that climate change has no significant impact on spring wheat yield in central Zambia. However, the actual outcome of climate change could lead to more significant impacts. Under a UCE scenario for example, some possible future climates forecast average yield increases of up to 8%, a considerable amount.

It is also interesting to note that, even as the worst outcome is the same for both scenarios (a decrease in yield of about 4%), the best outcome for the UCE scenario is substantially better than for the L1S scenario, making more climate change somewhat beneficial, on average, for spring wheat harvests.

5.2.4 Irrigation Need for Cotton

We present here the results of the uncertainty run for irrigated cotton. Cotton is planted at the end of July and has a growing season of about six months. Figures 5-14 and 5-15 show the probability distribution and the cumulative probability distribution, respectively, of the average change in irrigation need by the middle of the century.

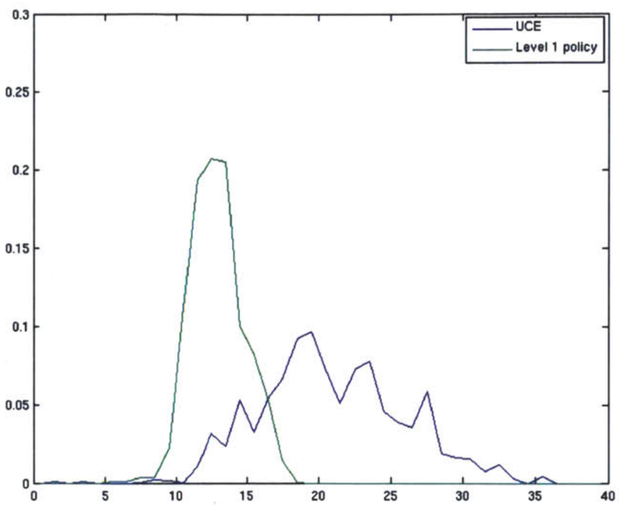

Figure 5-14: Probability function of the distribution of irrigation need change (in percent) in the Central Province of Zambia for cotton. The zero line represents the historic average, while the red line represents the historic variability over 1960-2000. The blue and green lines represent, respectively, the UCE and L1S distributions of the change of the average irrigation need by 2040-2060 from 1960-2000 as calculated by CLM-AG using the Gaussian Quadrature sample of the IGSM climate ensembles.

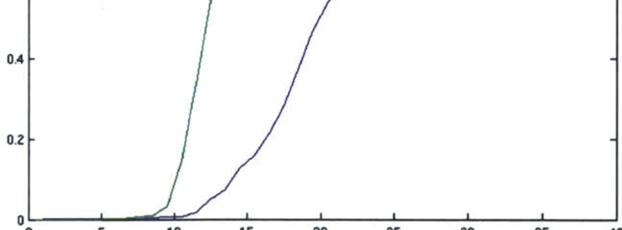

Figure 5-15: Cumulative probability function of the distribution of irrigation need change (in percent) in the Central Province of Zambia for cotton. The zero line represents the historic average, while the red line represents the historic variability over 1960-2000. The blue and green lines represent, respectively, the UCE and L1S distributions of the change of the average irrigation need by 2040-2060 from 1960-2000 as calculated by CLM-AG using the Gaussian Quadrature sample of the IGSM climate ensembles.

The averages of the two distributions show an increase in irrigation need for cotton of 21% and 13% for UCE and L1S scenarios, respectively. This is a salient increase. For the UCE scenario for example, an increase of 21% corresponds to a historic one-in-five-year dry year becoming the average year for irrigation need of cotton. For cotton, the L1S policy reduces significantly the risks of an extreme outcome as the worst case scenario presents a 15% increase in irrigation need, which is smaller than the 21% increase under the median UCE scenario. It is also interesting to note that the UCE distribution is extremely wide for cotton.

5.3 Analysis and Policy Recommendations

5.3.1 Use of Probability Distributions in a Policy-Making Environment

The distributions presented in the previous section can inform decision makers not only on the magnitude of climate change impacts, but also on the underlying uncertainty of these predictions. This section examines what information is relevant and how the distributions can be used in a policy making context.

Relevant Criteria for Decision Making

For a decision maker, the following criteria should be considered when using a model for future irrigation projects:

- Relevance of the prediction: The outcome of the model is as precise as possible and gives the number(s) that is (are) useful to make the right decision. For example simply giving the average change in irrigation need would not be completely relevant, as it does not communicate the wide uncertainty surrounding it. This uncertainty may have important implications in the policy making process.

- Ease to communicate results with the decision maker and public: Decision makers are busy people and want models that are easy to understand. If the result is too complicated a decision maker may overlook it by lack of time to understand it. Moreover, any decision may be scrutinized and if a model has been used in the decision-making process it may have to be explained to the public. A policy maker will always favor a model that is simple to understand and to explain for these reasons.

- Risk prevention: The model is accurate at identifying potential harmful outcomes. It allows the decision maker to plan for the worst and best case scenarios. This is particularly important for irrigation projects: if the source of the water – a lake, for example – runs dry, the consequences for the area could be dramatic in terms of food production.

- Time to carry out the analysis of the scenarios after the assessment: As irrigation projects are usually of a long span, the shorter the analysis, the better for the decision-maker. Indeed delays in planning are common and reducing the length of any step, here the model analysis, is a huge advantage and reduces the cost of the planning phase.

The 400-run ensemble distributions presented in the previous section satisfy easily two of these four criteria. They are relevant as they present all the information needed, and is accurate for risk prevention as it identifies the best and worst case scenarios. However, probability distributions are not easy concepts and it would take time for a decision maker to understand all the implications, let alone the general public.

Furthermore, using the full ensemble could considerably slow the analysis process. Indeed when making decisions about the economic relevance of an investment, for example, one would use the irrigation need as a parameter to a complex economic model. Using four hundred values and running this new model for each possibility would be time consuming. As a consequence, if the ensemble distribution provides relevant information, it can be seen as providing too much information to the decision maker. Thus it is interesting to create a tool that would convey the most relevant information to the decision maker.

Box Diagrams

A good way to communicate simply the underlying uncertainty in future climate change while retaining relevant information is to use box diagrams. These allow decision makers to have a quick and clear view of the median, the 50% confidence interval, and the extreme values of the distribution. While some information is lost and the graph is not as precise as a 400-run ensemble probability distribution, it is much easier to describe and explain. In addition it still emphasizes the high-risk scenarios (contrary to a simple average value). Finally it provides only five values to describe the distribution, which reduces the subsequent analysis time: the best and worst case scenarios, the median scenario, and the upper and lower bounds of the 50% confidence interval. Box diagrams thus answer the four key concerns of a decision maker as outlined above, providing simple and relevant information.

Figures 5-16 and 5-17 represent the box diagrams obtained for the irrigation need change by mid-century for maize and cotton, respectively, in Central Zambia, while Figure 5-18 represents the change in average yield of wheat due to water stress over the same period. These are the box diagrams associated with the distributions presented in the previous section.

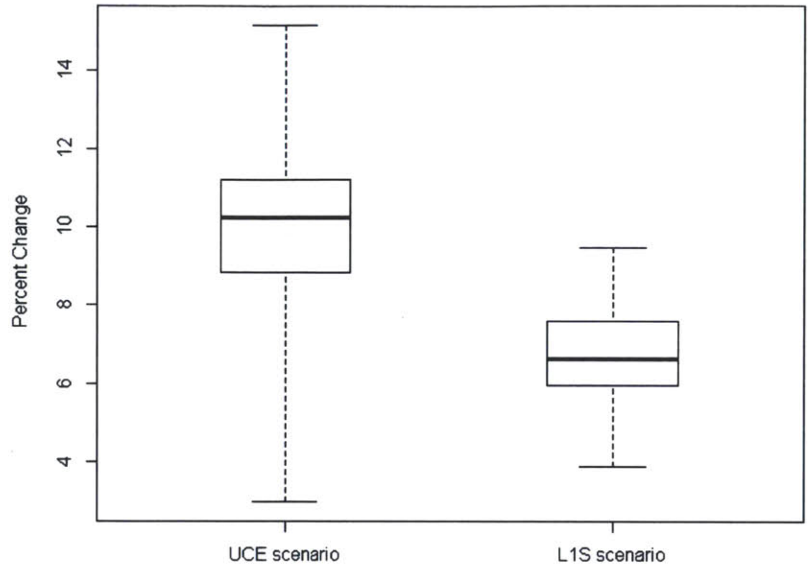

Figure 5-16: Box diagram of the distribution of the change in average irrigation need for maize in the Central Province of Zambia (in percent) between 2040 - 2060 and 1960 - 2000. The central box represents the median 50% of the distribution. The thick line represents the median of the distribution.

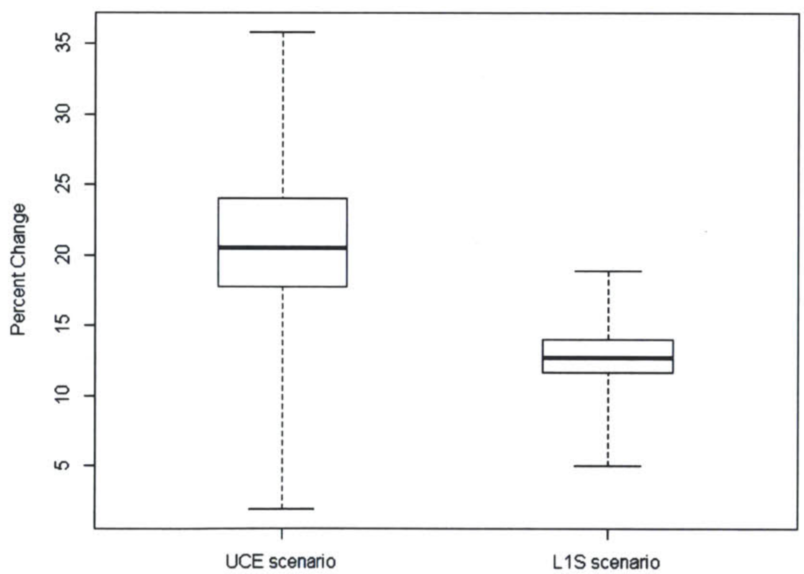

Figure 5-17: Box diagram of the distribution of the change in average irrigation need for cotton in the Central Province of Zambia (in percent) between 2040 - 2060 and 1960 - 2000. The central box represents the median 50% of the distribution. The thick line represents the median of the distribution.

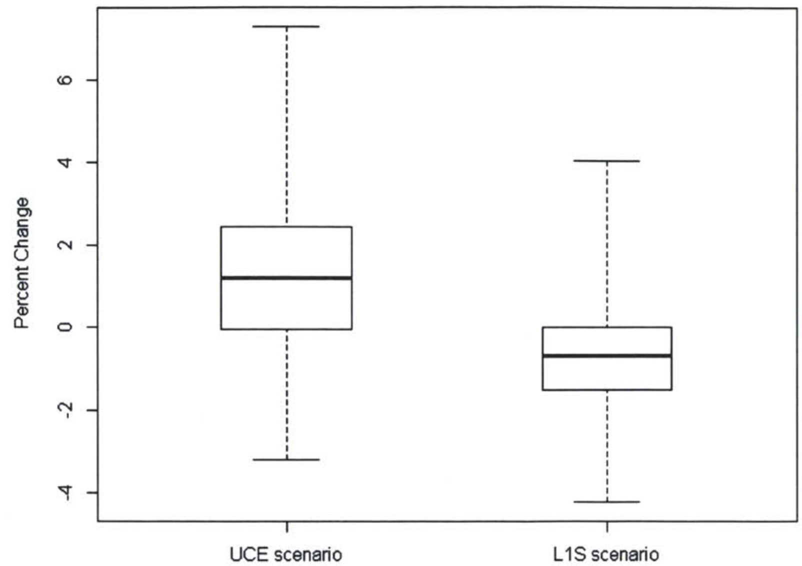

Figure 5-18: Box diagram of the distribution of the change in average yield for wheat in the Central Province of Zambia (in percent) between 2040 - 2060 and 1960 - 2000 due to water stress. The central box represents the median 50% of the distribution. The thick line represents the median of the distribution.

5.3.2 Policy Implications

Impact of Mitigation Policies on the Distribution of Outcomes

Using both the probability function distributions from Section 5.2 and the box diagrams in Section 5.3.1, some conclusions can be drawn on the impact of mitigation policies on crop water stress in the Central Province of Zambia.

For cotton and maize, all scenarios under both an Unconstrained Emissions policy or a Level 1 Stabilization policy lead to an increase in irrigation need. However, the impact of a L1S climate mitigation policy is generally positive for the Central Province of Zambia (compared with an Unconstrained Emissions scenario). First, mitigating climate change reduces the median irrigation need in the distribution of possible climates for both maize (from 10.5% to 6.5%) and cotton (from 21% to 13%). The improvement is notable in both cases as the 50% confidence intervals of the UCE and L1S scenarios do not overlap for both crops. Second, the mitigation policy markedly reduces the probabilities of extreme irrigation need outcomes for both maize and cotton. Indeed it makes the best case scenario slightly worse, but decreases considerably the harmful effects associated with the worst case scenario. For both crops, the worst case scenario under a L1S policy is indeed better than the median case for a UCE scenario for irrigation need.

Spring wheat, on the other hand, fares on average slightly better under a UCE scenario than under a L1S scenario. For example yields could increase as much as 8% under unconstrained future emissions compared to a maximum of 5% under a strict mitigation policy, the median of the distributions being at +1% and -1%, respectively. The difference is however not unequivocal as the 50% confidence intervals for UCE and L1S overlap. Notwithstanding extreme outcomes in the distributions, impacts of climate change – due to water stress – on spring wheat yields for central Zambia are minor.

However, uncertainty remains dominant under both scenarios and policy makers have to adapt their processes accordingly. In practice, this means that flexibility and robustness are key to any project whose success is highly dependent on future climate. Even if planners use the average (or median) outcome of the distribution as a basis for their projects, they should study the impact of the most extreme results in the distribution and develop contingency options to flexibly adapt to all possible outcomes. Best practice policies would try to maximize the return of the project in the 50% confidence interval, while planning contingency options for the best and worst case scenarios identified in the box diagrams.

Nevertheless, planning flexibility options for extreme outcomes is usually costly. This is why reducing uncertainty is critical for decision makers. The analysis of CLM-AG results shows for all three crops that a mitigation policy reduces the spread of the distribution of possible outcomes and prevents the possibility of more extreme outcomes. Mitigation thus reduces the uncertainty and allows for easier and cheaper planning of the future for project developers.

Historic Variability and Policy Making

Comparing potential climate change to historic variability is important as it determines both the public perception of climate change and the relative severity of the impact on human systems. Indeed even if the variation in the average temperature is mathematically significant, it will neither capture the attention of the public, nor have a significant impact on the decision making process if it stays well within the natural year to year weather variability. Decision making on irrigation systems or water systems is for example very dependent on climate change. These systems are usually planned to be resilient to all but the most extreme years on record (somewhere between ninety and ninety-nine years out of one hundred on record). Climate change thus becomes an extremely significant factor for these projects and requires major adaptation work (both in the planning and the operating phases) if the induced change increases the frequency of extreme events. For example, if the hundred-year drought now occurs every ten years in the future (becoming in fact a ten-year drought) adaptation becomes crucial. On the contrary, if the year to year variability does not change significantly[7] and the average climate change is limited compared with the natural variability, the likely impact on policy making would be minimal.

In Zambia, this is extremely important to take into account. Indeed for maize, the increase in irrigation need under the median UCE scenario is of approximately 10% for the average year, while the standard variation is 15%. This suggests that climate change consequences will be perceived as large by the public and decision makers alike, as what used to be extremely dry weather becomes more usual. The average irrigation need rises to reach, on average, values that were associated with bad years. The situation for cotton is similar, with the average increase in irrigation need for the median UCE scenario being two thirds of the standard deviation of the historic distribution.

For spring wheat on the other hand, the median scenarios present close to zero change. Even the best and worst scenarios present average changes of 4%, while the standard deviation of the historic distribution is 13%. Notwithstanding eventual changes in the distribution of extreme events, climate change is likely to have little impact on policy making as the system planned based on historic events, would be resilient to these comparatively small changes.

5.3.3 Limitations and Use of the Model

As explained in Section 2.3, there are many uncertainties surrounding such an analysis of impacts of climate change on agriculture. This study of the Central Province in Zambian

[7]This is probably an erroneous assumption as most studies predict an increase in the frequency of extreme events (IPCC, 2012). It is however still debated and not the subject of this work.

addresses the issue of quantifying the uncertainty in impacts due to the uncertainty in climate models. However it does not address fully either the emission uncertainty associated with predicting greenhouse gases emissions (besides using two different scenarios) or the uncertainty directly associated with the imperfection of the crop model. Moreover, this analysis spans only a portion of what can be called the "known unknowns", or the uncertainties that are well-identified and quantifiable.

Concerning the greenhouse gases emissions uncertainty, the scenarios used in this study reflect the two extreme future scenarios. Many policies other than a Level 1 Stabilization have been proposed but all credible ones lead to higher emissions than the L1S scenario[8]. This study could be repeated with other mitigation scenarios – or other emission patterns for the Unconstrained Emission scenario – but extreme or mean values are unlikely to be far outside the bounds delimited by the two scenarios run here. Consequently, even if these scenarios may not happen, a policy maker could use them to bound her predictions of climate change.

Concerning the crop model uncertainty, CLM-AG is very generic and thus may not take into account details of crop management or the specific crop varieties planted in Zambia. This could be partly solved by adapting the invariant CLM-AG crop parameters to the area studied, though this could render the model less relevant for the rest of the world. In any case, CLM-AG remains too imprecise to produce results at the individual field level. For this reason, it is mostly intended to, first, isolate the climate change impact on water stress and, second, provide a general measure of the associated uncertainty.

Used together with a precise field model like DSSAT for calculating historic values in a specific location, or historic observations if they exist, CLM-AG can provide a range of possible water stress outcomes given a specific emissions scenario. This range can then be used to determine the design of irrigation projects or other water projects, while fully recognizing the uncertainty in the key parameter that is water stress.

[8]The L1S scenario limits the concentration of carbon dioxide in the atmosphere to 450 ppm, which is predicted to result in a temperature increase of two degrees by the end of the century compared to pre-industrial average (on average over the IPCC models). This level is the one deemed "safe" by the United Nations Framework Convention on Climate Change (UNFCC) Conference of Parties and so it is highly unlikely any policy will try to achieve a lower target.

Chapter 6

Conclusion

6.1 Key Findings and Policy Implications

CLM-AG is a global generic crop model developed for water stress studies under climate change. Parametrized for three different crops at the time – maize, spring wheat and cotton – it can be extended to different crops and used in a variety of studies. For this work, two studies have been carried out: a global study with forcing from a single climate model and a regional uncertainty study in central Zambia. The main results of these studies are summarized below.

6.1.1 Global Findings

Evaluation of the Model

Chapter 3 shows that at a global level CLM-AG reveals the expected patterns of wet and dry zones for irrigation need. The comparison to the Global Agro-Ecosystem Zones dataset (GAEZ, Fischer *et al.* (2012)) shows that CLM-AG, forced with a historic dataset reproduces the salient patterns of water stress at a global level for the type of studies it was designed for.

Further evaluation was carried at the United States level. Using the irrigation observations contained in the Farm and Ranch Irrigation Survey (FRIS, USDA (2008)) and the crop irrigation needs as calculated by CLM-AG, a theoretical irrigation efficiency table was constructed. This irrigation efficiency was aggregated by state and the results are presented in Table 3.1. These results are extremely close to what would be expected given the different irrigation systems efficiencies over the United States. Overall, the average irrigation efficiency for maize in the United States is estimated at 51.4% using CLM-AG. This is consistent with the approximate value of 50% reported by Pimentel *et al.* (1997).

IGSM-CAM Global Runs

CLM-AG was then run under a future climate to assess the impact of climate change on irrigation need and water stress on crops. The climate forcing was created with a 3-D model developed at the MIT Joint Program on the Science and Policy of Global Change, the MIT IGSM-CAM (Monier *et al.*, 2012).

Results of these runs confirm that climate change has a significant impact on irrigation need and water stress. However, these impacts are not global but vary widely on a regional basis. Under the IGSM-CAM, for example, North America and Sub-Saharan Africa see decreasing water deficits while Western Europe and Southern Africa become drier. Counter intuitively, some crops in some areas actually benefit from climate change as precipitation increases. This is notably true for corn crops in the U.S. Midwest, where irrigation need decreases dramatically under future climate as simulated by the IGSM-CAM.

Different crops experience different water stress changes by 2050. For example, in some countries maize and spring wheat are not planted at the same time. As climate change affects the weather differently in different seasons, a given area could see water stress for maize increase, but water stress for wheat decrease. Though it is unusual, this is notably true for the Zambezi River Basin under the IGSM-CAM.

Finally, a global climate change mitigation policy may have unintended consequences for agriculture. Even if such a policy effectively mitigates the harmful effects of climate change for crops in Central Asia or increases the beneficial effects in the U.S. Midwest (reducing the irrigation need for maize for example), it is not necessarily the case in other areas of the world. Indeed, as precipitation decreases, most areas experience significant drying under a mitigation scenario (Level 2 Stabilization in this study) compared with an Unconstrained Emissions scenario. Consequently, these areas see a higher irrigation need and water stress in 2050 under a future with a mitigation policy than under a future lacking a specific climate policy. This phenomenon is particularly strong for Europe and Africa. However, it is important to note that these results are based on modeling out to 2050, and could change by the end of the century and that they represent the climate as predicted by only one climate model.

6.1.2 Findings in Central Zambia

The second study carried out in this work builds on the uncertainty capacities of the IGSM (Sokolov *et al.*, 2009) associated with the Hybridized Frequency Distribution approach (Schlosser *et al.*, 2011). Using this approach, coupled with a Gaussian Quadrature sampling technique, a distribution of 400 representative potential climates for the Zambezi River Valley was created for both an Unconstrained Emissions and a Level 1 Stabilization scenarios. This distribution spans both the global climate sensitivity uncertainty of the IGSM model as well as the regional climatic uncertainty (described based on the IPCC AR4 models).

Each of the 400 potential climate time series in the ensemble was used as a climate forcing for CLM-AG. Chapter 5 presents the results for the Central Province of Zambia for corn, spring wheat and cotton. The results are summarized in box diagrams in Section 5.3. These box diagrams convey visually in a simple form the relevant information related to the distribution of possible outcomes.

Maize and cotton are strongly impacted by climate change in Central Zambia while the average impact on spring wheat is minimal (and even beneficial for potential future climates). These diagrams also show how large the uncertainty associated with climate models remains. The key for policy planners whose projects depend on future climate is thus to rely on flexibility and plan contingency options in case one of the extreme scenarios happens in the future.

However, as mitigation reduces potential climate change, it also reduces the underlying uncertainty. It prevents the most extreme outcomes from happening and decreases the average change in water stress. It is thus easier to make informed decisions under a climate mitigation policy.

6.2 Future Research

CLM-AG opens new possibilities for research at the MIT Joint Program on the Science and Policy of Global Change. First, the approach used in Zambia can be repeated in any other area of the world, to differentiate the regional water impacts of climate change on the food producing system.

Second, as explained in Chapter 3, the irrigation need calculated by CLM-AG can be used in the Water Resource System framework (WRS, Strzepek *et al.* (2010)) to account for crop water need globally. Using this framework, one can identify water stressed areas in the world and study their evolution under climate change. This approach integrates economic and climatic changes to water demand and provides an integrated assessment of the resource and of its potential evolution.

Moreover, used together with the IGSM uncertainty framework, WRS could be used regionally to identify the relevant uncertainties in stream flows and the probabilities of major droughts. This approach would inform water planners on the probability of major droughts in the future, given a particular greenhouse gases emissions scenario.

Future studies coupling CLM-AG, WRS and an economic model of the agricultural sector such as IMPACT (Rosegrant *et al.*, 2008a) would create a framework to study the impacts of climate change on food prices and thus on the economy. Such a coupling would directly put a price on impacts of climate change, which would help build feedbacks in the MIT IGSM.

Bibliography

Abler, D. G., A. G. Rodríguez and J. S. Shortle, 1999: Parameter Uncertainty in CGE Modeling of the Environmental Impacts of Economic Policies. *Environmental and Resource Economics*, **14**(1): 75–94.

Adler, R. F., G. J. Huffman, A. Chang, R. Ferraro, P. P. Xie, J. Janowiak, B. Rudolf, U. Schneider, S. Curtis, D. Bolvin, A. Gruber, J. Susskind, P. Arkin and E. Nelkin, 2003: The version-2 Global Precipitation Climatology Project (GPCP) monthly precipitation analysis (1979-present). *Journal of Hydrometeorology*, **4**(6): 1147–1167.

Allen, R., L. Pereira, D. Raes and M. Smith, 1998: *Crop evapotranspiration - Guidelines for computing crop water requirements*, volume 56 of *the Irrigation and Drainage Papers Series*. FAO. (http://www.fao.org/docrep/X0490E/x0490e06.htm).

Arndt, C., 1996: An Introduction to Systematic Sensitivity Analysis via Gaussian Quadrature. Center for Global Trade Analysis, Department of Agricultural Economics, Purdue University *GTAP Technical Paper*. (http://ideas.repec.org/p/gta/techpp/305.html).

Arndt, C., J. Kozlitina and P. V. Preckel, 2006: Efficient survey sampling of households via Gaussian quadrature. *Journal of the Royal Statistical Society: Series C (Applied Statistics)*, **55**(3): 355–364.

Arndt, C., C. A. Fant, S. Robinson and K. M. Strzepek, 2012: Informed Selection of Future Climates. UNU/WIDER 19 p.

Baffles, J., 2004: The Cotton Problem. Food and Agriculture Organization (http://www.fao.org/es/ESC/common/ecg/306/en/CottonProblem_Baffes.pdf).

Banda, A. K., 2011: 2010/2011 Preliminary Crop Forecast Survey Report. Ministry of Agriculture and Co-operatives, Republic of Zambia Jun. (www.agriculture.gov.zm).

Boddiger, D., 2007: Boosting biofuel crops could threaten food security. *The Lancet*, **370**(9591): 923–924.

Bonan, G. B., K. W. Oleson, M. Vertenstein, S. Levis, X. Zeng, Y. Dai, R. E. Dickinson and Z.-L. Yang, 2002: The land surface climatology of the community land model coupled to the NCAR community climate model. *Journal of climate*, **15**(22): 3123–3149.

Brumbelow, K. and A. Georgakakos, 2001: An assessment of irrigation needs and crop yield for the United States under potential climate changes. *Journal of Geophysical Research*, **106**(D21): 27,383–27,405.

Carter, T., R. Saarikko and K. Niemi, 1996: Assessing the risks and uncertainties of regional crop potential under changing climate in Finland. *Agricultural and Food Science in Finland*, **5**(3): 329–350.

Challinor, A. J., J. M. Slingo, T. R. Wheeler, P. Q. Craufurd and D. I. F. Grimes, 2003: Toward a Combined Seasonal Weather and Crop Productivity Forecasting System: Determination of the Working Spatial Scale. *Journal of Applied Meteorology*, **42**(2): 175–192.

Christensen, J., B. Hewitson, A. Busuioc, A. Chen, X. Gao, I. Held, R. Jones, R. Kolli, W.-T. Kwon, R. Laprise, V. Magaña Rueda, L. Mearns, C. Menéndez, J. Räisänen, A. Rinke, A. Sarr and P. Whetton, 2007: Regional Climate Projections. In: *Climate Change 2007: The Physical Science Basis. Contribution of Working Group I to the Fourth Assessment Report of the Intergovernmental Panel on Climate Change*, S. Solomon, D. Qin, M. Manning, Z. Chen, M. Marquis, K. Averyt, M. Tignor and H. Miller, (eds.), Cambridge University Press: Cambridge, UK and New York, NY, USA.

Chung, S. O., 2010: Simulating Evapotranspiration and Yield Responses of Rice to Climate Change using FAO-AquaCrop. *Journal of The Korean Society of Agricultural Engineers*, **52**(3): 57–64.

Demirbas, A., 2009: Biofuels securing the planet's future energy needs. *Energy Conversion and Management*, **50**(9): 2239–2249.

Deser, C., A. Phillips, V. Bourdette and H. Teng, 2012: Uncertainty in climate change projections: the role of internal variability. *Climate Dynamics*, **38**(3): 527–546.

Döll, P., 2002: Impact of Climate Change and Variability on Irrigation Requirements: A Global Perspective. *Climatic Change*, **54**(3): 269–293.

Easterling, W., X. Chen, C. Hays, J. Brandle and H. Zhang, 1996: Improving the validation of model-simulated crop yield response to climate change: an application to the EPIC model. *Climate Research*, **06**(3): 263–273.

Easterling, W., P. Aggarwal, P. Batima, K. Brander, L. Erda, S. Howden, A. Kirilenko, J. Morton, J.-F. Soussana, J. Schmidhuber and F. N. Tubiello, 2007: Food, Fibre, and Forest Products. In: *Climate change 2007: impacts, adaptation and vulnerability. Contribution of working group II to the fourth assessment report of the intergovernmental panel on climate change*, M. Parry, O. Canziani, J. Palutikof, P. Van der Linden and C. Hanson, (eds.), Cambridge University Press: Cambridge, UK and New York, NY, USA. 273-313.

Faivre, R., D. Leenhardt, M. Voltz, M. Benoît, F. Papy, G. Dedieu and D. Wallach, 2009: Spatialising Crop Models. In: *Sustainable Agriculture*, E. Lichtfouse, M. Navarrete, P. Debaeke, S. Véronique and C. Alberola, (eds.), Springer Netherlands, pp. 687–705.

Fant, C. A., A. Gueneau, K. Strzepek, S. Awadalla, W. Farmer, E. Blanc and C. A. Schlosser, 2012: CliCrop: a Crop Water-Stress and Irrigation Demand Model for an Integrated Global Assessment Model Approach. MIT Joint Program on the Science and Policy of Global Change (http://globalchange.mit.edu/files/document/MITJPSPGC_Rpt214.pdf).

FAO, 2009: How to feed the world 2050 - High-Level Expert Forum. Food and Agriculture Organization (http://www.fao.org/fileadmin/templates/wsfs/docs/Issues_papers/HLEF2050_Global_Agriculture.pdf).

FAO, 2011: The State of Food Insecurity in the World. Food and Agriculture Organization (http://www.fao.org/docrep/014/i2330e/i2330e.pdf).

Farmer, W., K. Strzepek, C. A. Schlosser, P. Droogers and X. Gao, 2011: A Method for Calculating Reference Evapotranspiration on Daily Time Scales. MIT Joint Program on the Science and Policy of Global Change (http://globalchange.mit.edu/files/document/MITJPSPGC_Rpt195.pdf).

Fischer, G., M. Shah, F. N. Tubiello and H. Van Velhuizen, 2005: Socio-Economic and Climate Change Impacts on Agriculture: An Integrated Assessment, 1990–2080. *Philosophical Transactions of the Royal Society B: Biological Sciences*, **360**(1463): 2067–2083.

Fischer, G., F. N. Tubiello, H. van Velthuizen and D. A. Wiberg, 2007: Climate change impacts on irrigation water requirements: Effects of mitigation, 1990–2080. *Technological Forecasting and Social Change*, **74**(7): 1083–1107.

Fischer, G., F. O. Nachtergaele, S. Prieler, E. Teixeira, G. Toth, H. van Velthuizen, L. Verelst and D. A. Wiberg, 2012: Global Agro-Ecological Zones, Model Documantation. IIASA and FAO (http://www.iiasa.ac.at/Research/LUC/GAEZv3.0/docs/GAEZ_Model_Documentation.pdf).

Foley, J., 2010: The other inconvenient truth. *TEDx Twin Cities*. (http://www.ted.com/talks/jonathan_foley_the_other_inconvenient_truth.html).

Forest, C. E., M. R. Allen, P. H. Stone and A. P. Sokolov, 1999: Constraining uncertainties in climate models using climate change detection techniques. MIT Joint Program on the Science and Policy of Global Change (http://globalchange.mit.edu/files/document/MITJPSPGC_Rpt47.pdf).

Forest, C. E., P. H. Stone, A. P. Sokolov, M. R. Allen and M. D. Webster, 2002: Quantifying Uncertainties in Climate System Properties with the Use of Recent Climate Observations. *Science*, **295**(5552): 113–117.

Guereña, A., M. Ruiz-Ramos, C. H. Díaz-Ambrona, J. R. Conde and M. Mínguez, 2001: Assessment of Climate Change and Agriculture in Spain Using Climate Models. *Agronomy Journal*, **93**(1): 237.

Hack, J. J., J. M. Caron, S. G. Yeager, K. W. Oleson, M. M. Holland, J. E. Truesdale and P. J. Rasch, 2006: Simulation of the global hydrological cycle in the CCSM community atmosphere model version 3 (CAM3) : Mean features. *Journal of climate*, **19**(11): 2199–2221.

Heitholt, J. J., 1994: Canopy Characteristics Associated with Deficient and Excessive Cotton Plant Population Densities. *Crop Science*, **34**(5): 1291–1297.

Hurrell, J. W., J. J. Hack, D. Shea, J. M. Caron and J. Rosinski, 2008: A New Sea Surface Temperature and Sea Ice Boundary Dataset for the Community Atmosphere Model. *Journal of climate*, **21**(19): 5145–5153.

Iglesias, A., C. Rosenzweig and D. Pereira, 2000: Agricultural impacts of climate change in Spain: developing tools for a spatial analysis. *Global Environmental Change*, **10**(1): 69–80.

IPCC, 2007: *Climate Change 2007: Synthesis Report. Contribution of Working Groups I, II and III to the Fourth Assessment Report of the Intergovernmental Panel on Climate Change*. IPCC: Geneva, Switzerland.

IPCC, 2012: *2012: Managing the Risks of Extreme Events and Disasters to Advance Climate Change Adaptation. A Special Report of Working Groups I and II of the Intergovernmental Panel on Climate Change*. Cambridge University Press, Cambridge, UK, and New York, NY, USA.

Izaurralde, R., N. J. Rosenberg, R. A. Brown and A. M. Thomson, 2003: Integrated assessment of Hadley Center (HadCM2) climate-change impacts on agricultural productivity and irrigation water supply in the conterminous United States: Part II. Regional agricultural production in 2030 and 2095. *Agricultural and Forest Meteorology*, **117**(1–2): 97–122.

Jones, J., G. Hoogenboom, C. Porter, K. Boote, W. Batchelor, L. Hunt, P. Wilkens, U. Singh, A. Gijsman and J. Ritchie, 2003: The DSSAT cropping system model. *European Journal of Agronomy*, **18**(3–4): 235–265.

Kimball, B. A., J. R. Mauney, F. S. Nakayama and S. B. Idso, 1993: Effects of increasing atmospheric CO2 on vegetation. *Plant Ecology*, **104-105**(1): 65–75.

Kongshaug, G. and T. K. Jenssen, 2003: Energy consumption and greenhouse gas emissions in fertilizer production. *International Fertiliser Society Meeting*.

Kundzewicz, Z., L. Mata, L. Arnell, P. Döll, P. Kabat, B. Jiménez, K. Miller, T. Oki, Z. Sen and I. A. Shiklomanov, 2007: Fresh Water Resources and their Management. In: *Climate change 2007: impacts, adaptation and vulnerability. Contribution of working group II to the fourth assessment report of the intergovernmental panel on climate change*, M. Parry, O. Canziani, J. Palutikof, P. Van der Linden and C. Hanson, (eds.), Cambridge University Press: Cambridge, UK and New York, NY, USA, pp. 173–210.

Kundzewicz, Z. W., L. J. Mata, N. W. Arnell, P. Döll, B. Jimenez, K. Miller, T. Oki, Z. Şen and I. Shiklomanov, 2008: The implications of projected climate change for freshwater resources and their management. *Hydrological Sciences Journal*, **53**(1): 3–10.

Li, W., W. Li and Z. Li, 2004: Irrigation and fertilizer effects on water use and yield of spring wheat in semi-arid regions. *Agricultural Water Management*, **67**(1): 35–46.

Loladze, I., 2002: Rising atmospheric CO2 and human nutrition: toward globally imbalanced plant stoichiometry? *Trends in Ecology & Evolution*, **17**(10): 457–461.

Mearns, L. O., C. Rosenzweig and R. Goldberg, 1997: Mean and variance change in climate scenarios : Methods, agricultural applications, and measures of uncertainty. *Climatic change*, **35**(4): 367–396.

Melillo, J. M., A. C. Gurgel, D. W. Kicklighter, J. M. Reilly, T. W. Cronin, B. S. Felzer, S. Paltsev, C. A. Schlosser, A. P. Sokolov and X. Wang, 2009: Unintended Environmental Consequences of a Global Biofuels Program. MIT Joint Program on the Science and Policy of Global Change (http://globalchange.mit.edu/files/document/MITJPSPGC_Rpt168.pdf).

Mendelsohn, R., W. D. Nordhaus and D. Shaw, 1994: The Impact of Global Warming on Agriculture: A Ricardian Analysis. *The American Economic Review*, **84**(4): 753–771.

Monier, E., J. Scott, A. Sokolov, C. E. Forest and C. A. Schlosser, 2012: An Integrated Assessment Framework for Uncertainty Studies in Global and Regional Climate Change: The IGSM-CAM. MIT Joint Program on the Science and Policy of Global Change (http://globalchange.mit.edu/files/document/MITJPSPGC_Rpt223.pdf).

Monod, H., C. Naud and D. Makowski, 2006: Uncertainty and sensitivity analysis for crop models. In: *Working with Dynamic Crop Models*, D. Wallach, D. Makowski and J. Jones, (eds.), Elsevier, pp. 55 – 100.

Monteith, J. L., 1965: Evaporation and Environment. *The state and movement of water in living organisms*, **19**: 205.

Moussa, K. M. and M. Amadou, 2006: Using the CROPWAT model to analyze the effects of climate change on rainfed crops in Niger. *CEEPA DP32, University of Pretoria, South Africa.*

Nakicenovic, N., J. Alcamo and G. Davis, 2000: *IPCC Special Report on Emissions Scenarios (SRES).* Cambridge University Press.

New, M., M. Hulme and P. Jones, 1999: Representing Twentieth-Century Space–Time Climate Variability. Part I: Development of a 1961–90 Mean Monthly Terrestrial Climatology. *Journal of Climate*, **12**(3): 829–856.

Ngo-Duc, T., J. Polcher and K. Laval, 2005: A 53-year forcing data set for land surface models. *Journal of Geophysical Research*, **110**(D6): D06116.

Oleson, K. W., Y. Dai, G. B. Bonan, R. E. Dickinson, P. A. Dirmeyer, F. Hoffman, P. Houser, S. Levis, G.-Y. Niu, P. E. Thornton, M. Vertenstein, Z.-L. Yang and X. Zeng, 2004: Technical Description of the Community Land Model (CLM). National Center for Atmospheric Research May, 186 p. (http://www.cgd.ucar.edu/tss/clm/distribution/clm3.0/TechNote/CLM_Tech_Note.pdf).

Oleson, K. W., G.-Y. Niu, Z.-L. Yang, D. M. Lawrence, P. E. Thornton, P. J. Lawrence, R. Stöckli, R. E. Dickinson, G. B. Bonan, S. Levis, A. Dai and T. Qian, 2008: Improvements to the Community Land Model and their impact on the hydrological cycle. *Journal of Geophysical Research*, **113**: 26 PP.

Paltsev, S., J. Reilly, H. Jacoby, R. Eckaus, J. McFarland, M. Sarofim, M. Asadoorian and M. Babiker, 2005: The MIT emissions prediction and policy analysis (EPPA) model: version 4. MIT Joint Program on the Science and Policy of Global Change (http://globalchange.mit.edu/files/document/MITJPSPGC_Rpt125.pdf).

Parry, M., C. Rosenzweig, A. Iglesias, M. Livermore and G. Fischer, 2004: Effects of climate change on global food production under SRES emissions and socio-economic scenarios. *Global Environmental Change*, **14**(1): 53–67.

Pimentel, D., J. Houser, E. Preiss, O. White, H. Fang, L. Mesnick, T. Barsky, S. Tariche, J. Schreck and S. Alpert, 1997: Water Resources: Agriculture, the Environment, and Society. *BioScience*, **47**(2): 97–106.

Postel, S. L., G. C. Daily and P. R. Ehrlich, 1996: Human Appropriation of Renewable Fresh Water. *Science*, **271**(5250): 785–788.

Prinn, R., H. Jacoby, A. Sokolov, C. Wang, X. Xiao, Z. Yang, R. Eckhaus, P. Stone, D. Ellerman, J. Melillo, J. Fitzmaurice, D. Kicklighter, G. Holian and Y. Liu, 1999: Integrated Global System Model for Climate Policy Assessment: Feedbacks and Sensitivity Studies. *Climatic Change*, **41**(3): 469–546.

Raes, D., P. Steduto, T. C. Hsiao and E. Fereres, 2009: *AquaCrop - The FAO crop model to simulate yield response to water*. FAO, Rome.

Raes, D., P. Steduto, T. C. Hsiao and E. Fereres, 2010: *AquaCrop Reference Manual Chapter 3: Calculation Procedures*. Food and Agriculture Organization: Rome. (http://www.fao.org/nr/water/docs/aquacrop3_1/AquaCropV31Chapter3.pdf).

Ramankutty, N., A. T. Evan, C. Monfreda and J. A. Foley, 2008: Farming the planet: 1. Geographic distribution of global agricultural lands in the year 2000. *Global Biogeochemical Cycles*, **22**: 19 PP.

Randall, D., R. Wood, S. Bony, R. Colman, T. Fichefet, J. Fyfe, V. Kattsov, A. Pitman, J. Shukla, J. Srinivasan, R. Stouffer, A. Sumi and K. Taylor, 2007: Climate Models and their Evaluation. In: *Climate Change 2007: The Physical Science Basis. Contribution of Working Group I to the Fourth Assessment Report of the Intergovernmental Panel on Climate Change*, S. Solomon, D. Qin, M. Manning, Z. Chen, M. Marquis, K. Averyt,

M. Tignor and H. Miller, (eds.), Cambridge University Press: Cambridge, UK and New York, NY, USA, pp. 589–662.

Rodríguez Díaz, J., E. Weatherhead, J. Knox and E. Camacho, 2007: Climate change impacts on irrigation water requirements in the Guadalquivir river basin in Spain. *Regional Environmental Change*, **7**(3): 149–159.

Rosegrant, M. W., C. Ringler, S. Msangi, T. Sulser, T. Zhu and S. A. Cline, 2008a: International Model for Policy Analysis of Agricultural Commodities and Trade (IMPACT): Model Description. International Food Policy Research Institute (http://www.ifpri.cgiar.org/sites/default/files/publications/impactwater.pdf).

Rosegrant, M. W., T. Zhu, S. Msangi and T. Sulser, 2008b: Global Scenarios for Biofuels: Impacts and Implications. *Applied Economic Perspectives and Policy*, **30**(3): 495–505.

Rosenzweig, C., A. Iglesias and United States. Environmental Protection Agency. Climate Change Division. Adaptation Branch, 1994: *Implications of climate change for international agriculture : crop modeling study*. U.S. Environmental Protection Agency, Office of Policy, Planning, and Evaluation, Climate Change Division, Adaptation Branch: Washington, D.C.

Rosenzweig, C., A. Iglesias, X. Yang, P. R. Epstein and E. Chivian, 2001: Climate Change and Extreme Weather Events; Implications for Food Production, Plant Diseases, and Pests. *Global Change & Human Health*, **2**(2): 90–104.

Rosenzweig, C., K. M. Strzepek, D. C. Major, A. Iglesias, D. N. Yates, A. McCluskey and D. Hillel, 2004: Water resources for agriculture in a changing climate: international case studies. *Global Environmental Change*, **14**(4): 345–360.

Schlenker, W. and M. J. Roberts, 2009: Nonlinear Temperature Effects Indicate Severe Damages to U.S. Crop Yields Under Climate Change. *Proceedings of the National Academy of Sciences*, **106**(37): 15594–15598.

Schlosser, C. A., X. Gao, K. M. Strzepek, A. P. Sokolov, C. E. Forest, S. Awadalla and W. Farmer, 2011: Quantifying the Likelihood of Regional Climate Change: A Hybridized Approach. MIT Joint Program on the Science and Policy of Global Change (http://globalchange.mit.edu/files/document/MITJPSPGC_Rpt205.pdf).

Shiklomanov, I. A., 2000: Appraisal and Assessment of World Water Resources. *Water International*, **25**(1): 11–32.

Siebert, S., P. Döll, J. Hoogeveen, J.-M. Faures, K. Frenken and S. Feick, 2005: Development and validation of the global map of irrigation areas. *Hydrology and Earth System Sciences Discussions*, **2**: 1299–1327.

Smit, B. and M. W. Skinner, 2002: Adaptation options in agriculture to climate change: a typology. *Mitigation and Adaptation Strategies for Global Change*, **7**(1): 85–114.

Smith, M., 1992: *CROPWAT: A computer program for irrigation planning and management*. Food and Agriculture Organization: Rome.

Smith, P., D. Martino, Z. Cai, D. Gwary, H. Janzen, P. Kumar, B. McCarl, S. Ogle, F. O'Mara, C. Rice, B. Scholes and O. Sirotenko, 2007: Agriculture. In: *Climate Change 2007: Mitigation. Contribution of Working Group III to the Fourth Assessment Report of the Intergovernmental Panel on Climate Change*, B. Metz, O. Davidson, P. Bosch, R. Dave and L. Meyer, (eds.), Cambridge University Press: Cambridge, UK and New York, NY, USA, pp. 497–540.

Sokolov, A. P. and E. Monier, 2011: Implementation of a Cloud Radiative Adjustment Method to Change the Climate Sensitivity of CAM3. MIT Joint Program on the Science and Policy of Global Change (http://globalchange.mit.edu/files/document/MITJPSPGC_Rpt204.pdf).

Sokolov, A. P., C. A. Schlosser, S. Dutkiewicz, S. Paltsev, D. W. Kicklighter, H. D. Jacoby, R. G. Prinn, C. E. Forest, J. M. Reilly, C. Wang, B. S. Felzer, M. C. Sarofim, J. Scott, P. H. Stone, J. M. Melillo and J. B. Cohen, 2005: MIT Integrated Global System Model (IGSM) Version 2: Model Description and Baseline Evaluation. MIT Joint Program on the Science and Policy of Global Change (http://globalchange.mit.edu/files/document/MITJPSPGC_Rpt124.pdf).

Sokolov, A. P., P. H. Stone, C. E. Forest, R. Prinn, M. C. Sarofim, M. Webster, S. Paltsev, C. A. Schlosser, D. Kicklighter, S. Dutkiewicz, J. Reilly, C. Wang, B. Felzer, J. M. Melillo and H. D. Jacoby, 2009: Probabilistic Forecast for Twenty-First-Century Climate Based on Uncertainties in Emissions (Without Policy) and Climate Parameters. *Journal of Climate*, **22**(19): 5175–5204.

Steduto, P., T. C. Hsiao, D. Raes and E. Fereres, 2009: AquaCrop - The FAO Crop Model to Simulate Yield Response to Water: I. Concepts and Underlying Principles. *Agronomy Journal*, **101**(3): 426.

Stockle, C. O., J. R. Williams, N. J. Rosenberg and C. Jones, 1992: A method for estimating the direct and climatic effects of rising atmospheric carbon dioxide on growth and yield of crops: Part I—Modification of the EPIC model for climate change analysis. *Agricultural Systems*, **38**(3): 225–238.

Stott, P. A. and J. A. Kettleborough, 2002: Origins and estimates of uncertainty in predictions of twenty-first century temperature rise. *Nature*, **416**(6882): 723–726.

Strzepek, K., C. Schlosser, W. Farmer, S. Awadalla, J. Baker, M. Rosegrant and X. Gao, 2010: Modeling the Global Water Resource System in an Integrated Assessment Modeling Framework: IGSM-WRS. MIT Joint Program on the Science and Policy of Global Change (http://globalchange.mit.edu/files/document/MITJPSPGC_Rpt189.pdf).

Swanson, K. L., G. Sugihara and A. A. Tsonis, 2009: Long-term natural variability and 20th century climate change. *Proceedings of the National Academy of Sciences of the United States of America*, **106**(38): 16120–16123.

Tan, G. and R. Shibasaki, 2003: Global estimation of crop productivity and the impacts of global warming by GIS and EPIC integration. *Ecological Modelling*, **168**(3): 357–370.

Taub, D. R., B. Miller and H. Allen, 2008: Effects of elevated CO2 on the protein concentration of food crops: a meta-analysis. *Global Change Biology*, **14**(3): 565–575.

TexasET, 2012: FAO Mean Crop Coefficients, Kc, for Subhumid Climates. Texas A&M (http://texaset.tamu.edu/cropcoe.php).

UN, 2004: World Population to 2300. United Nations, Department of Economic and Social Affairs (http://www.un.org/esa/population/publications/longrange2/WorldPop2300final.pdf).

USDA, 2008: 2008 Farm and Ranch Irrigation Survey. United States Department of Agriculture, National Agricultural Statistics Service (http://www.agcensus.usda.gov/Publications/2002/FRIS/index.asp).

Vina, A., 2004: *Remote estimation of leaf area index and biomass in corn and soybean*. University of Nebraska, Lincoln. (http://digitalcommons.unl.edu/dissertations/AAI3131566).

Webster, M., M. Babiker, M. Mayer, J. Reilly, J. Harnisch, R. Hyman, M. Sarofim and C. Wang, 2002: Uncertainty in emissions projections for climate models. *Atmospheric Environment*, **36**(22): 3659–3670.

Webster, M., A. Sokolov, J. Reilly, C. Forest, S. Paltsev, A. Schlosser, C. Wang, D. Kicklighter, M. Sarofim, J. Melillo, R. Prinn and H. Jacoby, 2012: Analysis of climate policy targets under uncertainty. *Climatic Change*, **112**(3): 569–583.

Webster, M. D., S. Paltsev, J. E. Parsons, J. M. Reilly and H. D. Jacoby, 2008: Uncertainty in Greenhouse Emissions and Costs of Atmospheric Stabilization. MIT Joint Program on the Science and Policy of Global Change (http://globalchange.mit.edu/files/document/MITJPSPGC_Rpt165.pdf).

Williams, J. R. and V. P. Singh, 1995: The EPIC model. *Computer models of watershed hydrology*, pp. 909–1000.

Willmott, C. J. and J. J. Feddema, 1992: A More Rational Climatic Moisture Index. *The Professional Geographer*, **44**(1): 84–88.

Ziska, L. H., 2011: Climate change,carbon dioxide and global crop production: food security and uncertainty. In: *Handbook on Climat Change and Agriculture*, A. Dinar and R. Mendelsohn, (eds.), Edward Elgar Publishing Ltd, pp. 9–31.

Ziska, L. H. and J. A. Bunce, 2007: Predicting the impact of changing CO2 on crop yields: some thoughts on food. *New Phytologist*, **175**(4): 607–618.

Appendix A

Crop Parameters

Parameter	Maize	Spring Wheat	Cotton	Source
T_{base} (in °C)	8.0	0.0	12.0	AquaCrop
T_{upper} (in °C)	30.0	26.0	35.0	AquaCrop
CC_0 (unitless)	0.004	0.075	0.007	AquaCrop
CC_x (unitless)	0.90	0.95	0.90	AquaCrop
CGC (in GDD^{-1})	0.012	0.006	0.0065	AquaCrop
CDC (in GDD^{-1})	0.010	0.004	0.0025	AquaCrop
t_em (in GDD)	75.0	150.0	50.0	AquaCrop
t_sen (in GDD)	1400.0	1650.0	1400.0	AquaCrop
t_mat (in GDD)	250.0	500.0	200.0	AquaCrop
Kcb_x (unitless)	1.05	1.10	1.10	AquaCrop
f_{age} (in day^{-1})	0.003	0.0015	0.003	AquaCrop
h_x (in m)	2.0	1.0	1.3	TexasET (2012)
rt_{ini} (in mm)	30.0	30.0	30.0	AquaCrop
rt_{gr} (in mm/day)	20.0	15.0	20.0	AquaCrop
rt_{max} (in mm)	2500.0	2000.0	2500.0	AquaCrop
LAI_x (unitless)	6.0	3.0	5.0	See below
f_{CC} (unitless)	0.5	0.5	0.6	AquaCrop
Ky_1 (unitless)	0.4	0.2	0.2	FAO Water
Ky_2 (unitless)	0.4	0.6	0.5	FAO Water
Ky_3 (unitless)	1.3	0.8	0.5	FAO Water
Ky_4 (unitless)	0.5	0.4	0.25	FAO Water

Table A.1: Crop Parameters.

Maximum LAI values come from Vina (2004), Li *et al.* (2004) and Heitholt (1994).

Appendix B

Evaluation of CLM-AG versus GAEZ for Cotton and Spring Wheat

B.1 Cotton

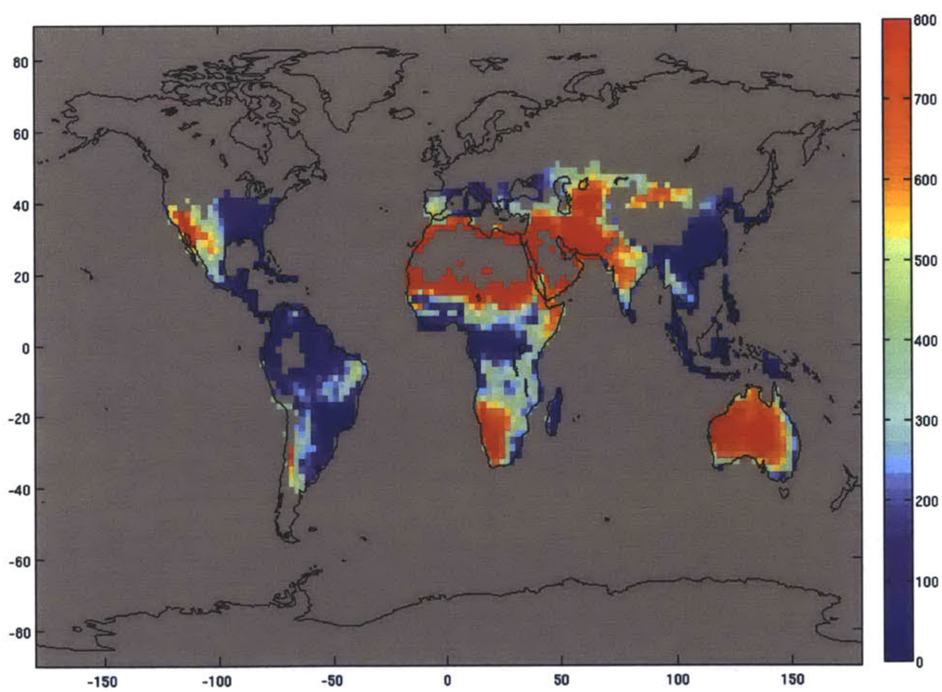

Figure B-1: CLM-AG water deficit (in mm) for irrigated cotton - NCC dataset, 1980-1999 average.

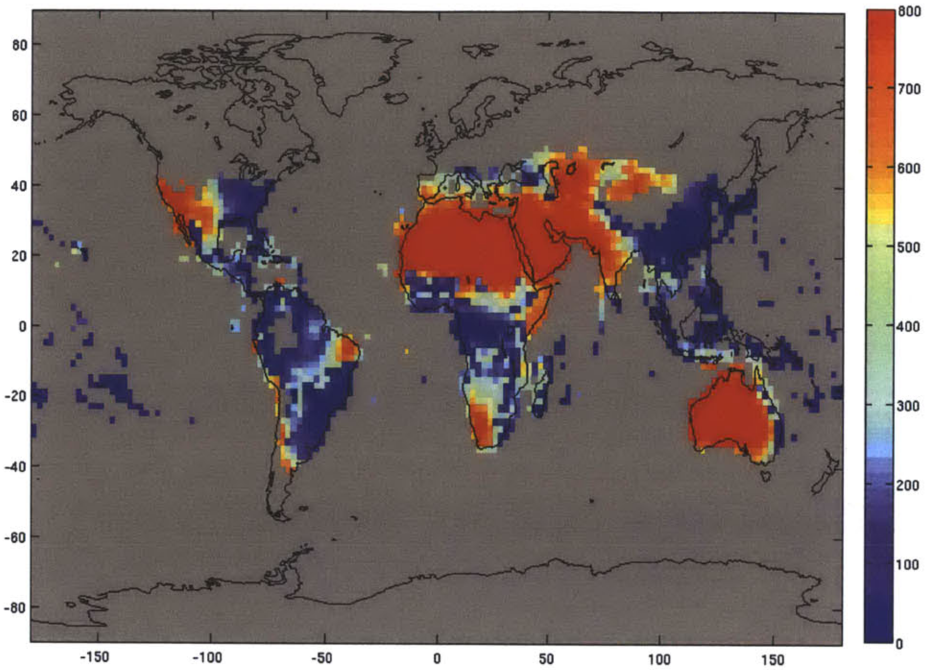

Figure B-2: GAEZ water deficit (in mm) for irrigated cotton - CRU dataset, 1961-1990 average.

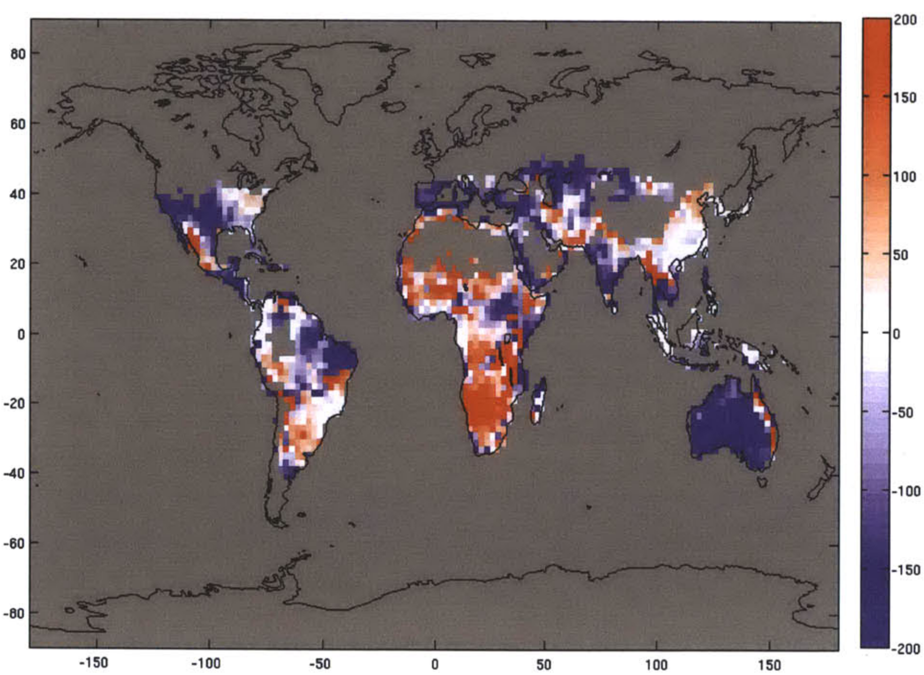

Figure B-3: Difference in water deficit estimates (in mm) for irrigated cotton between CLM-AG and GAEZ - Same specifications as the previous figures.

B.2 Spring Wheat

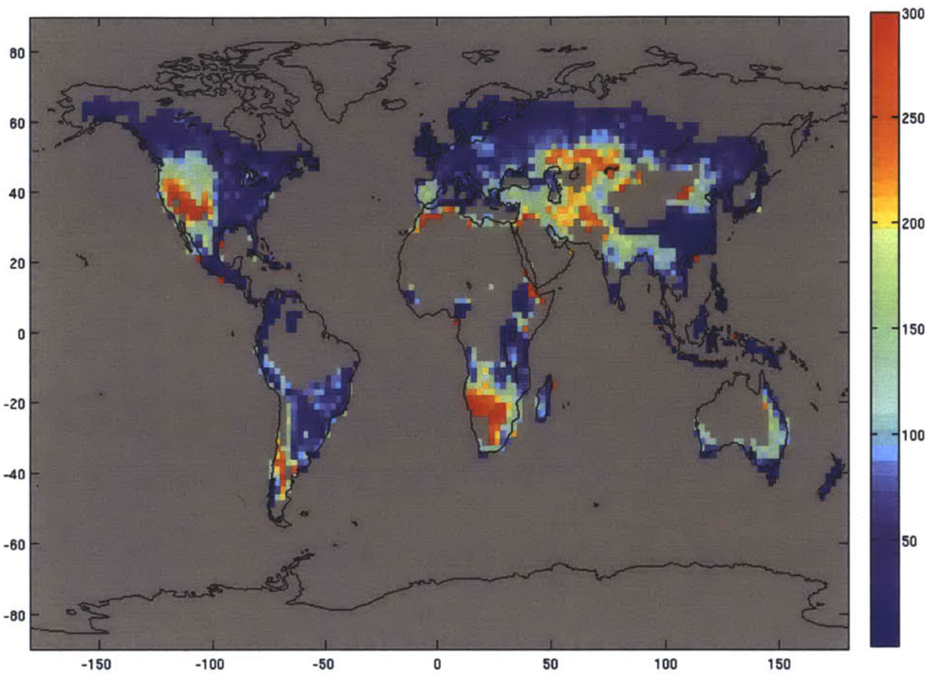

Figure B-4: CLM-AG water deficit (in mm) for rainfed spring wheat - NCC dataset, 1980-1999 average.

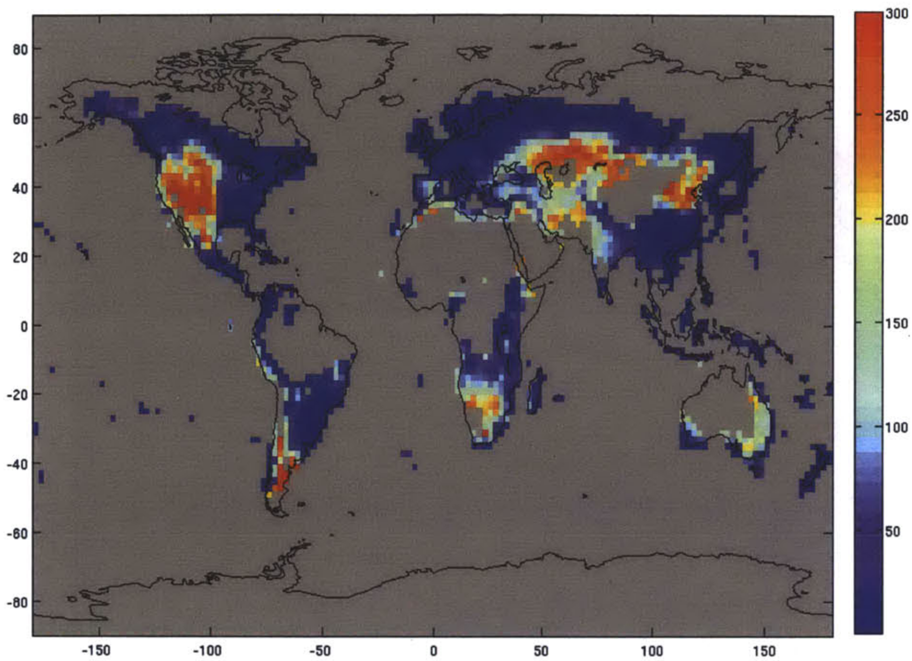

Figure B-5: GAEZ water deficit (in mm) for rainfed spring wheat - CRU dataset, 1961-1990 average.

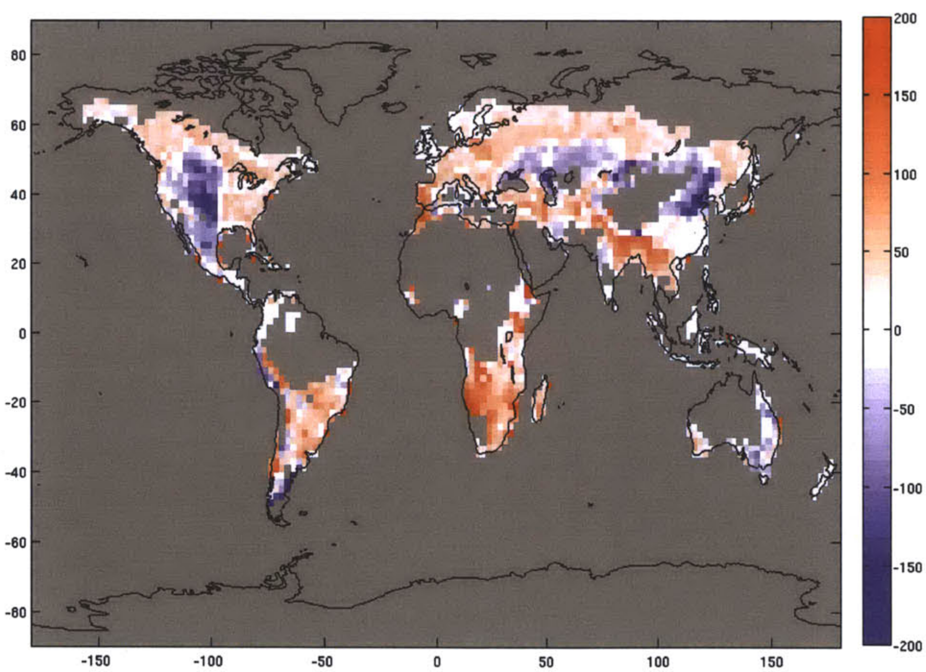

Figure B-6: Difference in water deficit estimates (in mm) for rainfed spring wheat between CLM-AG and GAEZ - Same specifications as the previous figures.